Platelet and red blood cell interaction – Unraveling of interaction molecules during cell-cell contact

Inaugural-Dissertation

zur Erlangung des Doktorgrades
der Mathematisch-Naturwissenschaftlichen Fakultät

der Heinrich-Heine-Universität Düsseldorf

vorgelegt von

Kim Jürgen Krott

aus Leverkusen

Düsseldorf, Dezember 2020

Table of Content

List of Tables

List of Figures

List of Abbreviations

A	AAA	Abdominal aortic aneurysm
	AA	Acrylamide
	AA	Aortic aneurysm
	ADP	Adenosine diphosphate
	ADAMTS	A disintegrin and metalloproteinase with thrombospondin motifs
	AMC	Age-matched control
	AMCs	Age-matched controls
	ANOVA	Analysis of variation of means
	AOD	Arterial occlusive disease
	APS	Ammonium persulfate
	ASA	Acetylsalicylic acid
	AST	Aspartate aminotransferase
B	BSA	Bovine serum albumin
C	Ca^{2+}	Calcium
	CD	Cluster of Differentiation
	CH_3OH	Methanol
	CHO	Chinese hamster ovary
	CO_2	Carbon dioxide
	COX	Cyclooxygenase
	COPD	Chronic obstructive pulmonary disease
	CRP	Collagen related peptide
	CXCL	CXC chemokine ligand
	Cy5	Cyanine5
D	DAG	Diacylglycerol
	dH_2O	Distilled water
	DIC	Differential interference contrast
	DMSO	Dimethyl sulfoxide
	DTT	Dithiothreitol
E	e.g.	Lat. *exempli gratia*, Eng. For example
	EC	Endothelial cell
	ECs	Endothelial cells
	ECL	Electrochemiluminescence
	ECM	Extracellular matrix
	EDTA	Ethylenediaminetetraacetic acid
	EGF	Epidermal growth factor
	eNOS	endothelial NO-synthase
	ER	Endoplasmic reticulum
	ERK	Extracellular signal-regulated kinase
	EtOH	Ethanol
	EVAR	Endovascular aneurysm repair
F	FACS	Fluorescence activated cell sorting
	FcR	Fc receptor
	Fig.	Figure
	FITC	Fluorescein isothiocyanate
	FSC	Forward scatter
G	g	Gramm
	G	Globular
	GAPDH	Glyceraldehyde 3-phosphate dehydrogenase
	GP	Glycoprotein
	GPCR	G-coupled protein receptor

H	h	Hours
	HCl	Hydrochloric acid
	hDcR3	Human decoy receptor 3
	HEPES	2-[4-(2-hydroxyethyl)piperazin-1-yl] ethanesulfonic acid
	HRP	Horse Radish Peroxidase
	HSC	Hematopoietic stem cells
I	IAP	Integrin-associated protein
	ICAM	Intracellular adhesion molecule
	IgG	Immunoglobulin G
	IL	Interleukin
	ILT	Intraluminal thrombus
	IP_3	Inositol-3,4,5-triphosphate
	ITAM	Immunoreceptor tyrosine-based activation motif
K	KCl	Potassium chloride
	kDa	Kilo Dalton
L	L	Liter
M	mAb	Monoclonal antibody
	MAP	Mitogen activated protein
	MCP	Monocyte chemoattractant protein
	mg	Milligram
	$MgCl_2$	Magnesium chloride
	Min	Minutes
	MK	Megakaryocytes
	mL	Milliliter
	MMP	Matrix metalloproteinase
	mol	Molarity
	MP	Microparticle
	MPs	Microparticles
N	Na_2HPO_4	Sodium phosphate dibasic
	Na_3OV_4	Sodium orthovanadate
	NaCl	Sodium chloride
	NADPH	Nicotinamide adenine dinucleotide phosphate
	NaH_2PO_4	Monosodium phosphate
	$NaHCO_3$	Sodium bicarbonate
	NaN_3	Sodium acid
	NaOH	Sodium hydrate
	NO	Nitric oxide
O	OAR	Open aneurysm repair
	OxLDL	Oxidized low-density lipoprotein
P	PAR4	Protease activated receptor 4
	PBS	Phosphate buffered saline
	PC	Procollagen
	PCR	Polymerase chain reaction
	PE	Phycoerythrin
	PFA	Paraformaldehyde
	PGE_1	Prostaglandin E_1
	PGI_2	Prostaglandin I_2
	pH	*Potentia hydrogenii*
	PKC	Protein kinase C
	PLCγ2	Phospholipase Cγ2
	Plts	Platelets
	PRP	Platelet rich plasma
	PRR	Pattern recognition receptor
	PS	Phosphatidylserine

R	RBC	Red blood cell
	RBCs	Red blood cells
	RGD	Arginine-glycerin-aspartic acid
	ROS	Reactive oxygen species
	RPE	Retinal pigment endothelium
	RT	Room temperature
S	SDS	Sodium dodecyl sulfate
	SPF	Specific pathogen free
	SSC	Sideward scatter
T	TEMED	N, N, N′, N′-Tetramethylethylendiamin
	TF	Tissue factor
	TGF	Transforming growth factor
	TIMP	Tissue inhibitor of matrix metalloproteinase
	TM	Transmembrane
	t-PA	Tissue plasminogen activator
	TPO	Thrombopoietin
	TSP	Thrombospondin
	TSR	TSP type repeats
	TxA2	Thromboxane A2
U	U/mL	Unites per milliliter
	µL	Microliter
	µM	Micromolar
V	VCAM	Vascular cell adhesion molecule
	VGEF	Vascular endothelial growth factor
	VSMC	Vascular smooth muscle cells
	vWF	Von Willebrand Factor
W	WB	Whole blood
	WBC	White blood cell
	WT	Wild type

Zusammenfassung

Die Hauptfunktion der Thrombozyten liegt in der Blutstillung, wobei bei einer intakten Barriere der Endothelzellen die Thrombozyten in einem inaktiven, diskoiden Zustand vorliegen. Wenn es zu einer Schädigung bzw. Verletzung des Gefäßwandendothels und zur Freilegung von Komponenten der subendothelialen extrazellulären Matrix (EZM) kommt, wird die primäre Thrombozyten-vermittelte Hämostase eingeleitet, welche zur Bildung eines ersten Thrombus führt. Mithilfe eines breiten Spektrums an Rezeptoren, wie Glykoprotein (GP) Ib, GPVI, Integrinen und CD36, erkennen und binden Thrombozyten die an der Gefäßschädigung exponierten Matrixproteine, wie Kollagen oder Thrombospondin-1 (TSP-1). Nachfolgend kommt es dann zur Thrombozytenaktivierung, -adhäsion, und -aggregation und schließlich zur Ausbildung eines primären Thrombus, der die Verletzung am Gefäß verschließt, um einen weiteren Blutverlust zu verhindern. Nachdem lange Zeit angenommen wurde, dass Erythrozyten eine passive Rolle bei den Prozessen der Hämostase und Thrombose spielen, zeigen aktuelle Studien, dass eine direkte Rezeptoren-vermittelte Interaktion von RBCs und Thrombozyten zur Exposition von Phosphatidylserin (PS) an der Oberfläche der RBCs führt und die Thrombingenerierung bei der Hämostase unterstützt.

In der vorliegenden Arbeit konnte nachgewiesen werden, dass eine direkte Interaktion zwischen dem Fas Liganden (FasL, CD178) der Thrombozyten und dem Fas Rezeptor (FasR, CD95) der Erythrozyten besteht. Diese Rezeptor-Ligand-Bindung induziert eine Hochregulierung von PS an der Membranoberfläche der Erythrozyten und führt somit zur Ausbildung einer prokoagulanten Oberfläche auf diesen Zellen. Über diesen Mechanismus tragen Erythrozyten aktiv zum Thrombuswachstum und zur Thrombusstabilisierung bei. Die hier gemessene PS Externalisierung auf Thrombozyten und Erythrozyten ist unabhängig von der Aktivierung intrazellulärer Caspasen. Die FasL/FasR-vermittelte Interaktion von Thrombozyten und Erythrozyten sowie deren Einfluss auf die Thrombusbildung, die Aggregation und die Kontraktilität von Thrombozyten konnte in dieser Arbeit mittels FasR knockout ($FasR^{-/-}$) und FasL knockout ($FasL^{-/-}$) Mäusen, sowie Mäusen mit einer auf Megakaryozyten und Thrombozyten beschränkten FasL-Defizienz (FasL$^{fl/fl}$;PF4-cre^{+}), nachgewiesen werden. Außerdem konnte dargelegt werden, dass die Interaktion über das Integrin $\alpha_{IIb}\beta_3$ auf Thrombozyten und dem erythrozytären FasR ebenfalls zur PS Externalisierung an der Membranoberfläche von Erythrozyten führt. Erste Analysen zur Rekrutierung von Erythrozyten an kollagen-adhärente Thrombozyten zeigen, dass es sich hier um einen aktiven Prozess handelt, welcher durch mehrere Oberflächenmoleküle auf der Thrombozyten- und der Erythrozytenmembran, einschließlich CD36, PS, FasR, FasL sowie der Freisetzung von TSP-1 aus Thrombozyten, gesteuert wird. Des Weiteren wurden neue Mechanismen der Thrombozyten-RBC-Interaktion während der Hämostase und Thrombusbildung identifiziert. Von Thrombozyten freigesetztes TSP-1 wurde als ein wichtiger Bindungspartner für CD36 nicht nur auf der Oberfläche der

Thrombozyten, sondern auch auf Erythrozyten nachgewiesen. Die Expression von CD36 auf RBCs sowie die Bindung von TSP-1 an Thrombozyten und RBCs nahm während der Inkorporation in den Thrombus signifikant zu. Nur die Inhibierung von CD36 auf Erythrozyten zeigte eine starke Reduktion der Thrombusbildung im Flusskammermodell auf verschiedenen Matrizen, nicht aber die Blockierung von CD36 auf Thrombozyten. Dieser Effekt ließ sich ebenso für die Exposition von PS auf der Erythrozytenmembran nachweisen. In statischen und dynamischen Experimenten der TSP-1 Bindung an Erythrozyten und Thrombozyten wurde gezeigt, dass TSP-1 hauptsächlich über CD36 an Erythrozyten bindet, während ein Verlust von CD36 auf der Membranoberfläche von Thrombozyten nicht zu einer reduzierten TSP-1 Bindung geführt hat. Neben CD36 wurde exponiertes PS als Interaktionspartner für TSP-1 auf Erythrozyten von Patienten mit Sichelzellanämie nachgewiesen. Diese Interaktion konnte hier jedoch weder für Thrombozyten noch für Erythrozyten aus gesunden Spendern gezeigt werden. Es ist bekannt, dass CD36 und TSP-1 in verschiedenen kardiovaskulären Erkrankungen eine wichtige regulatorische Rolle spielen.

Verschiedene entzündliche und proteolytische Prozesse begleiten die Entwicklung des Bauchaortenaneurysma (BAA) sowie die Bildung eines intraluminalen Thrombus (ILT). In der vorliegenden Arbeit wurde daher untersucht, ob die Interaktion von Thrombozyten und Erythrozyten über CD36 und TSP-1 eine Rolle in der Progression des BAA spielt. Die Externalisierung von PS auf beiden Zellarten und der thrombozytäre FasL waren stark erhöht. Des Weiteren wurde die Thrombozytenaktivierung und das Expressionsmuster von CD36 und TSP-1 analysiert. Es wurde festgestellt, dass die Thrombozyten von BAA-Patienten in einem prä-aktivierten Zustand in der Blutzirkulation vorliegen und die Proteinexpression von TSP-1 im Vergleich zu altersangepassten Kontrollen signifikant erhöht war. Die hier vorgestellten Ergebnisse zeigen erstmalig neue Mechanismen der Interaktion von Thrombozyten und Erythrozyten über FasL/FasR, $\alpha_{IIb}\beta_3$/FasR und TSP-1/CD36 während der Thrombusbildung. Des Weiteren zeigen erste Analysen, dass diese Mechanismen auch bei der Entstehung und Progression des BAA eine Rolle spielen könnten.

Abstract

Platelets play a role in many physiological and pathophysiological processes such as angiogenesis, tumor growth, inflammation, and tissue regeneration, but their main function is the regulation of hemostasis. When the barrier of endothelial cells is intact, platelets are present in an inactive, discoid state. After vascular injury, adhesive macromolecules from the extracellular matrix (ECM), e.g. collagen and thrombospondin-1 (TSP-1) are exposed to the blood flow and primary platelet-mediated hemostasis is initiated, leading to the formation of a first plug. Platelets recognize and bind the exposed matrix proteins by a broad spectrum of receptors, such as glycoprotein (GP) Ib, GPVI, integrins or CD36. These processes lead to platelet activation, adhesion, aggregation and finally the formation of a thrombus that seals the injury of the vessel and prevents further blood loss. For a long time it was assumed that red blood cells (RBCs) play a passive role in the processes of hemostasis and thrombosis. However, recent studies provide evidence for a direct receptor-mediated interaction between RBCs and platelets leading to the exposure of phosphatidylserine (PS) at the RBCs membrane followed by thrombin generation to support hemostasis.

In this thesis, a direct interaction between the Fas ligand (FasL, CD178) expressed on platelets and the Fas receptor (FasR, CD95) on RBCs was shown. This receptor-ligand binding leads to an upregulation of PS and thus contributes to the formation of a procoagulant surface on the membrane of RBCs. The direct binding of RBCs and platelets mediated via FasL/FasR provides strong evidence that RBCs are actively involved in thrombus growth and stability. Externalization of PS was independent of caspase signaling. Here, the FasL/FasR-mediated interaction of platelets and RBCs and the impact on thrombus formation, platelet aggregation and contractility was confirmed using FasR knockout ($FasR^{-/-}$) and FasL knockout ($FasL^{-/-}$) mice as well as mice with FasL deficiency restricted to megakaryocytes and platelets (FasL$^{fl/fl}$;PF4-cre$^+$). Furthermore, the interaction via integrin $\alpha_{IIb}\beta_3$ on platelets and erythroid FasR leads to PS externalization on the surface of RBCs as well. In addition, it was demonstrated that the recruitment of RBCs to collagen-adherent platelets is an active process that is mediated by several surface molecules on the platelet and RBC membrane, including CD36 and PS on both cell types, erythroid FasR, FasL on the surface of platelets and platelet-released TSP-1. Furthermore, new mechanisms of platelet-RBC interaction upon hemostasis and thrombosis have been identified. Platelet-released TSP-1 has been shown to represent an important binding partner for CD36 not only at the membrane of platelets but also of RBCs. The expression of CD36 on RBCs as well as the binding of TSP-1 to platelets and RBCs increased significantly during incorporation into the thrombus. Unexpectedly, only the inhibition of erythroid CD36 showed a strong reduction in thrombus formation in flow chamber experiments on different matrices, whereas it remained unchanged after inhibition of CD36 on platelets. This effect was also observed when the exposure of PS at the RBC membrane was measured. Moreover, TSP-1 binds to RBCs mainly via CD36, while a

loss of CD36 on the platelet membrane did not affect TSP-1 binding as shown in static and dynamic experiments. Besides CD36, exposed PS acts as interaction partner for TSP-1 on RBCs from patients with sickle cell anemia. However, this interaction was not observed using platelets or RBCs from healthy donors. It is known that both CD36 and TSP-1 play an important regulatory role in cardiovascular diseases. Various inflammatory and proteolytic processes accompany the development of an abdominal aortic aneurysm (AAA) as well as the formation of an intraluminal thrombus (ILT). Therefore, the interaction of platelets and RBCs via CD36 and TSP-1 was analyzed to proof if this mechanism plays a role in the progression of AAA. The exposure of PS at the membrane of both cell types and FasL on the surface of platelets were increased. Furthermore, platelet activation and the expression of CD36 and TSP-1 were analyzed. It was found that platelets from patients with AAA are in a preactivated state in the circulation and protein expression of TSP-1 was increased compared to age-matched controls (AMCs). The results presented here show new mechanisms of platelets-RBC interaction via FasL/FasR, $\alpha_{IIb}\beta_3$/FasR and TSP-1/CD36 upon thrombus formation. Furthermore, the experiments provide first evidence that these mechanisms might play a role in the development and progression of AAA.

1. Introduction

1.1 Platelets in hemostasis and thrombosis

Physiological processes in the human body are directed by the vascular system to distribute oxygen and nutrients to all tissues. Besides erythrocytes (red blood cells, RBCs) and leukocytes (white blood cells, WBCs), thrombocytes (platelets) are the major component of human blood [1, 2]. RBCs are responsible for oxygen supply, WBCs are important for the immune response and platelets are essential for hemostasis after vascular injury. Apart from the unique role in primary hemostasis, platelets are also important in other physiological and pathophysiological processes such as angiogenesis, tumor growth, inflammation, and tissue regeneration [3]. Platelets are relevant in the pathology of atherosclerosis, inducing chronic inflammatory processes at the vascular wall and thus platelets contribute to the formation of atherosclerotic plaques [4]. The release of proinflammatory mediators by platelets can affect the inflammatory process of other cells like ECs, smooth muscle cells (SMCs) and leukocytes [3]. In addition, uncontrolled three-dimensional thrombus formation may lead to thrombotic vessel occlusion, loss of oxygen supply accompanied by tissue injury, and myocardial infarction such as ischemic stroke [5, 6]. Furthermore, platelets are able to recruit leukocytes to the damaged endothelium [6] and influence the progression of abdominal aortic aneurysm (AAA) [7, 8] (further described in 1.4).

1.1.1 Platelet physiology

Platelets are small discoid anucleate cells that circulate in the blood stream in a nonstimulated condition (resting) and contain granules (α, dense, lysosomes), mitochondria, and endoplasmatic reticulum [9]. Platelets are derived from megakaryocytes (MKs) that are located in the bone marrow. Thereby, the maturation of megakaryocytes (megakaryopoiesis) is strictly controlled by thrombopoietin (TPO signaling) [10, 11]. In rodents, platelets are additionally formed in the spleen [10] and in 2017, Lefrançais and colleagues provided first evidence for platelet production in the lung [12]. In humans, platelets have a diameter of 3.6 ± 0.7 μm in size and have a lifespan of 8 – 10 days [13]. However, in the murine system, platelets are 2 μm in size and have a lifespan of 3 – 4 days [10]. A normal platelet count in humans is maintained in a range of $1.5 – 4 \times 10^6$ platelets per μL blood, ensured by a constant balance of platelet production and clearance [14]. In mice, 1.1×10^6 platelets per μL blood are present [15]. During maturation, platelets lose their RNA content and are only moderately active regarding biosynthesis [16, 17]. Aged, dysfunctional or preactivated

platelets are cleared from the circulation by macrophages and neutrophils in the liver and spleen through scavenger receptors [9, 12, 14].

In a healthy vessel, which includes an intact barrier of endothelial cells (ECs), two major physiological inhibitors, namely prostaglandin I_2 [or prostacyclin (PGI_2)] and nitric oxide (NO) are important to keep platelets in a resting state. PGI_2 is synthesized from its progenitor prostaglandin H_2 in the endoplasmic reticulum (ER) of ECs through the prostacyclin synthase [18] and NO is produced in platelets and the endothelium by (endothelial NO-synthase (eNOS) [5, 19]. During vascular injury, platelets are able to bind to the extracellular matrix (ECM) and become activated accompanied by a shape change and the subsequent release of their granules [20]. This is followed by the synthesis of a fibrin network, which is generated by the cleavage of fibrinogen by thrombin [21] (further described in 1.1.2).

1.1.2 Primary and secondary hemostasis

Hemostasis includes platelet adhesion to exposed ECM, platelet activation and aggregation accompanied by the formation and stability of a thrombus. In primary hemostasis, platelet adhesion and activation is essential to form a hemostatic plug. This hemostatic plug seals the injured vessel wall and interacts with components of the ECM such as collagen, von Willebrand factor (vWF), fibronectin, laminin and thrombospondin to facilitate stable platelet adhesion by activation of integrins at the site of injury [22-24]. In the event of vascular injury, the initial binding of the membrane bound glycoprotein-Ib-V-IX-complex (GPIb-V-IX) of platelets to collagen immobilized plasmatic vWF leads to an unstable transient adhesion (tethering) of the platelets at the vessel wall, where platelets are stopped in the blood stream and thus "roll" on the injured tissue. GPIb binding to vWF facilitates GPVI binding to exposed collagen, to induce platelet activation (Fig. 1) [24]. GPVI is associated with the Fc receptor (FcR) γ-chain, which directly phosphorylates the immunoreceptor tyrosine-based activation motif (ITAM), followed by binding of tyrosine kinase Syk upon its SH2-domane, which leads to phosphorylation of phospholipase Cγ2 (PLCγ2). PLCγ2 induces the generation of 1,2-diacylglycerin (DAG) and inositol-1,4,5-Trisphosphat (IP3), important for activation of protein kinase C (PKC) and the release of intracellular calcium, respectively (Fig. 2). GPVI activation induces several intracellular signaling pathways including integrin activation, degranulation of α- and δ-granules and the reorganization of the cytoskeleton (shape change) to facilitate stable platelet adhesion and the recruitment of platelets from the blood stream to the growing thrombus (Fig. 1) [24-26].
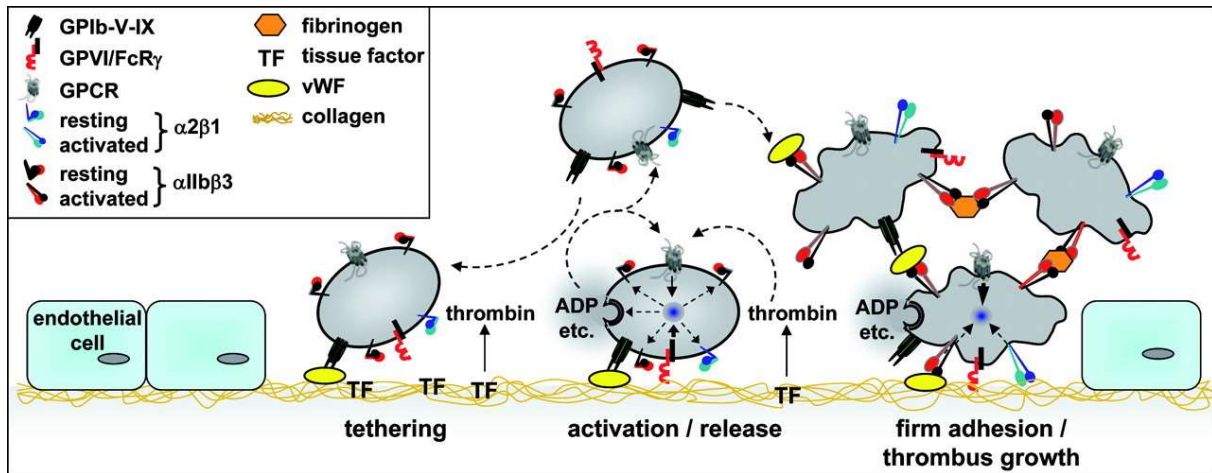
Figure 1: The role of platelets in primary hemostasis after vessel injury. The initial interaction of glycoprotein-Ib-V-IX-complexes (GPIb-V-IX) of platelets to von Willebrand factor (vWF) is triggered by exposed subendotheliale matrix (ECM) and enables the platelet tethering to ECM associated proteins. In addition, GPVI-mediated signaling induces several intracellular signaling pathway including integrin activation, degranulation of α- and δ-granules and the reorganization of the cytoskeleton (shape change), followed by further recruitment of platelets to the growing thrombus, platelet aggregation and thrombus formation. Taken from: Varga-Szabo, 2008 [24].

The fusion of α- and δ-granules to the outer membrane of platelets leads to the release of second wave mediators such as adenosine diphosphate (ADP) and thromboxane A2 (TxA$_2$) and to the release of fibrinogen, accompanied by the local generation of thrombin which reinforces platelet activation due to the stimulation of G protein-coupled receptors (GPCR) (Fig. 2) [24]. The second wave mediator ADP binds to the platelet receptors P_2Y_1 that contributes to calcium mobilization, shape change and aggregation of platelets and to P_2Y_{12}, which inhibits the adenylyl cyclase thereby leading to integrin $\alpha_{IIb}\beta_3$ activation and platelet aggregation [27-29]. TxA$_2$ is generated by cyclooxygenase 1/2 (COX 1/2) from its progenitor arachidonic acid and stored in platelet granules. Released TxA$_2$ binds to the specific G protein-coupled thromboxane A$_2$ receptors, TPα and TPβ (T-prostanoid receptor; TP-Receptor) to induce platelet shape change, calcium mobilization and integrin $\alpha_{IIb}\beta_3$ activation (Fig. 2) [24, 30, 31]. Besides the release of second wave mediators, additional adhesion proteins can be released by platelets such as fibronectin or vWF that contribute to the recruitment of further platelets to the growing thrombus. Activation of integrin $\alpha_{IIb}\beta_3$ leads to fibrinogen binding resulting in cross linkage of platelets to each other [32]. However, platelets are only weakly connected via protein bridges between cross-linked $\alpha_{IIb}\beta_3$ integrins. Thus, the initial thrombus is unstable and has to be stabilized due to the incorporation of fibrin during the phase of the secondary hemostasis [33].
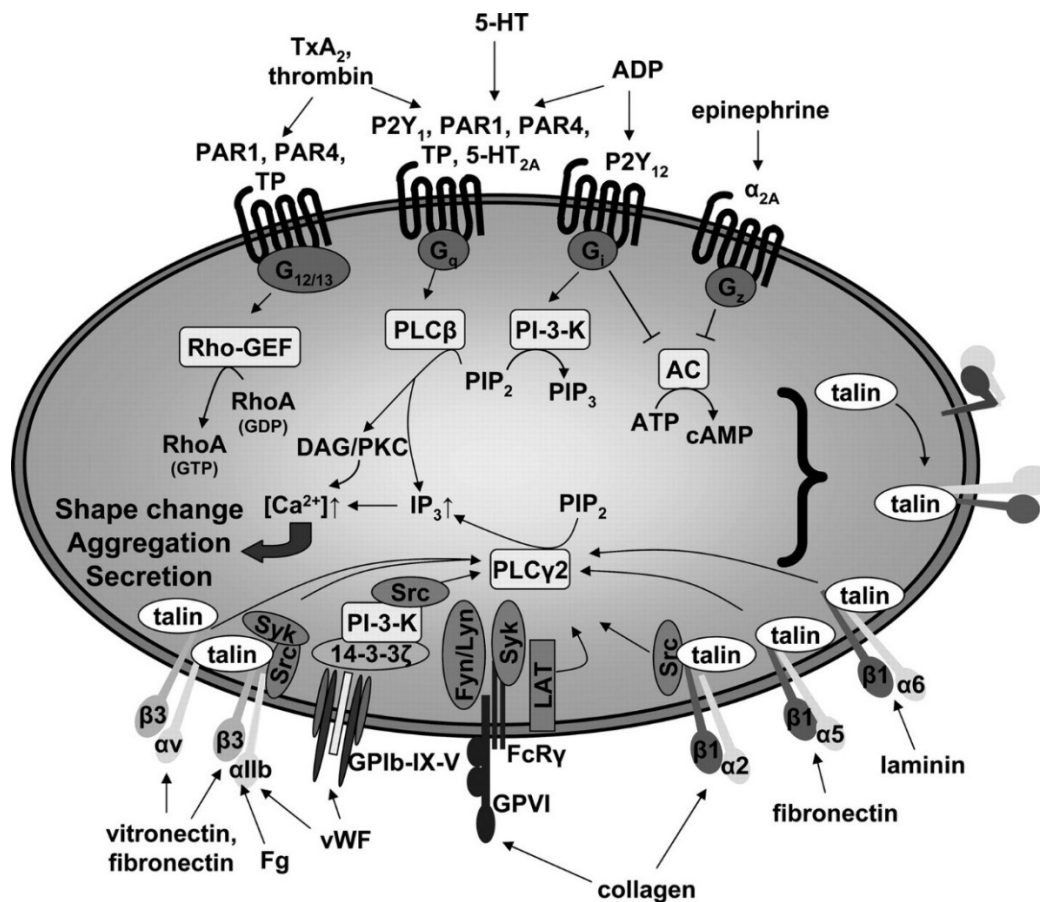
Figure 2: Platelet signaling pathways induced by binding of soluble and immobilized ligands to the respective receptors. Soluble agonists such as adenosine diphosphate (ADP), thromboxane A2 (TxA$_2$) mediate signaling via G protein-coupled receptors coupled to different G proteins (G$_q$, G$_{12/13}$, G$_i$) and activate downstream effectors. GPVI and integrins bind to immobilized ligands and induce PLCγ2 activation followed by integrin activation, cytoskeleton reorganization (shape change), degranulation and aggregation of platelets. TxA2 = thromboxane A2; TP = TxA2 receptor; PAR = protease-activated receptor; Rho-GEF = Rho-specific guanine nucleotide exchange factor; PI-3-K = phosphoinositide-3 kinase; AC = adenylyl cyclase; PIP2 = phosphatidylinositol-4,5 bisphosphate; PIP3 = phosphatidylinositol-3,4,5 trisphosphate; IP3 = inositol-1,4,5-trisphosphate; DAG = diacylglycerol; PKC = protein kinase C; Fg = fibrinogen. Taken from: Varga-Szabo, 2008 [24].

In the secondary hemostasis, prothrombin is cleaved to thrombin by different coagulation factors [34], followed by thrombin-mediated cleavage of fibrinogen to fibrin. Thus, thrombin is involved in primary hemostasis by binding to the protease-activated receptors (PAR), PAR1 and PAR4 (Fig. 2) of human platelets and PAR3 and PAR4 of murine platelets but also in secondary hemostasis by generating fibrin [30, 35]. The cross-linkage of fibrin leads to a fibrin network and stabilizes the platelet plug that is formed upon vascular injury accompanied by incorporation of other blood components such as RBCs and further platelets [36]. Furthermore, platelet activation leads to the formation of a procoagulant surface by the exposure of anionic phospholipid phosphatidylserine (PS) on the surface of activated platelets [37]. This is necessary for the generation of thrombin and mediated by the intrinsic prothrombinase complex. In addition, PS can generate the coating of platelets with several

proteins from α-granules such as fibrinogen, fibronectin, thrombospondin, and vWF [38]. This process and PS on the surface of platelets is important for the stability of the thrombus. Vascular regeneration and prevention of an occlusive event is important after the formation of a stable thrombus due to primary and secondary hemostasis. Therefore, the stable thrombus has to be removed. Accordingly, plasminogen is proteolytically converted to plasmin by tissue plasminogen activator (t-PA), which is generated and released from the endothelium. Plasmin is essential for the cleavage of cross-linked fibrin, thus necessary for thrombi lysis [39].

1.1.3 Integrins

Platelets have a high number of various integrin receptors on their surface that become activated under physiological and pathophysiological conditions. Therefore, different signaling pathways of platelet integrins are activated due to different ligands that bind to specific integrins. Moreover, they can be upregulated at the platelet membrane following platelet activation. Activated integrins mediate platelet adhesion, aggregation and thrombus formation after vascular injury. The bidirectional signal transduction of integrins include integrin activation by different platelet agonists (inside-out signaling) and ligand binding to activated integrins (outside-in signaling) that enables a dynamic adjustment of platelets to their environment [40].

1.1.3.1 Integrin $\alpha_{IIb}\beta_3$

The transmembrane heterodimeric receptor $\alpha_{IIb}\beta_3$ (fibrinogen receptor) belongs to the β-integrins and is only expressed on the surface of platelets and megakaryocytes [41]. This integrin is the most abundant platelet receptor with approximately ~ 80,000 copies per cell [42]. It is composed of a 95 kDa heavy β_3-subunit and α-subunit of 142 kDa in size (under non-reducing conditions) [43]. Both subunits are located in the membrane and specific contacts between the ectodomains, the transmembrane (TM), and the cytoplasmic domains keep the integrin in its bent conformation (Fig. 3). During integrin activation, these two cytoplasmic tails form a functional unit supported by the binding of talin-1 and kindlin-3 to the β-integrin tail [44, 45]. Integrins are responsible for cell-cell interactions and stable platelet adhesion to the ECM [46]. The integrin $\alpha_{IIb}\beta_3$ receptor binds a various number of ligands, which causes the activation of the integrin, e.g. fibrinogen (highest affinity), fibronectin and vWF that all contain an arginine-glycine-aspartic acid (RGD) sequence [47-49]. In the resting state of platelets, integrin $\alpha_{IIb}\beta_3$ has a low affinity to bind its respective ligands; therefore, the

binding domain is inaccessible for the RDG-sequence of different ligands [32]. After activation of platelets a conformational change of integrin $\alpha_{IIb}\beta_3$ leads to a high affinity state accompanied by the accessibility of the RGD-sequence (Fig. 3) (integrin inside-out signaling). Furthermore, ligand binding promotes an additional conformational change as well as a clustering of integrin $\alpha_{IIb}\beta_3$, which leads to transphosphorylation of the cytoplasmic tails of the receptor and to a downstream signaling cascade (outside-in signaling) [32]. Outside-in signaling leads to strong platelet activation and is important for the activation of numerous kinases and phosphatases, e.g. the tyrosine kinase Src and the tyrosine phosphatases SHP-1 and SHP-2. This culminates in the reorganization of the cytoskeleton (filopodia and lamellipodia formation), whereby platelet spreading on different surfaces can be induced [41, 50, 51]. Loss or dysfunction of integrin $\alpha_{IIb}\beta_3$ is manifested in the bleeding disorder Glanzmann thrombasthenia (GT). Patients with GT suffer from severe and uncontrollable bleeding events such as menstrual, gastrointestinal or increased postoperative bleeding [52].
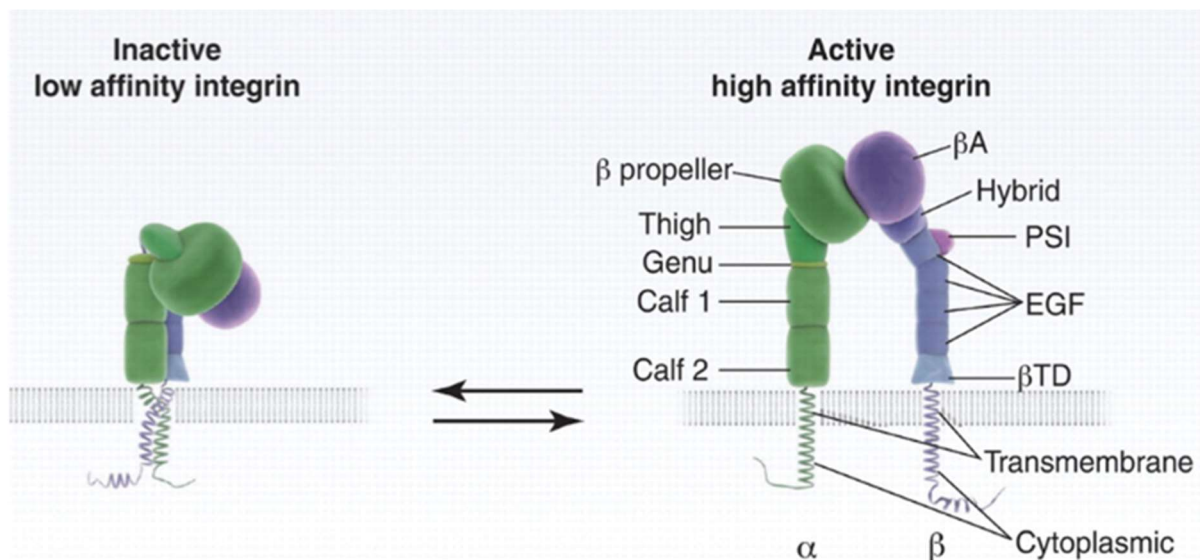
Figure 3: Structure of integrin $\alpha_{IIb}\beta_3$ and the change from low affinity to high affinity state upon platelet activation. Specific contacts between the ectodomains, the transmembrane (TM), and the cytoplasmic domains keep the integrin in its bent conformation. Separation of the components occurs during integrin activation, resulting in an extended integrin conformation. The α-subunit is shown in green and the β-subunit in violet. Taken from: Moser 2009 [44].

1.2 Red blood cells

RBCs are the most abundant cell type in human blood with a cell count that ranges from 4.7×10^6 to 6.1×10^6 cells/µL in men, from 4.2×10^6 to 5.4×10^6 cells/µL in woman and from 4.0×10^6 to 5.5×10^6 cells/µL in children [53]. RBCs are anucleated cells with a diameter of 6.2 – 8.2 µm and a lifespan of 120 days under physiological conditions. These deformable

6

biconcave discs descend from hematopoietic stem cells (HSC) located in the bone marrow and result from a tightly regulated process called erythropoiesis. During maturation, RBCs lose their mitochondria, nucleus, Golgi apparatus, endoplasmic reticulum (ER) and ribosomes [54]. In human adults, two million RBCs are formed and enter the circulation every second and at the same time the same number of RBCs are cleared from the circulation [55]. Since their main function is the supply of oxygen throughout the whole body and the removal of carbon dioxide (CO_2), RBCs have a relatively large surface area and a very thin lipid membrane, making them competent for optimal gas exchange [53]. The Embden-Meyerhof pathway (glycolysis) is the only metabolic pathway for energy production in these cells. In addition, RBCs can interact with several peripheral blood components such as ECs, monocytes, lymphocytes, other RBCs, platelets, bacteria, plasma proteins and the ECM following vessel injury [56].

1.2.1 Red blood cells in hemostasis and thrombosis

At first, researchers believed that only platelets, ECs and soluble coagulation factors are the important players enabling hemostasis and thrombosis; however, RBCs were described as unimportant and only influence these procedures in a passive manner [57]. Over the years, it became apparent that RBCs play an important, clinically significant role in blood clotting, hemostasis and thrombosis. It is known for decades that RBCs influence rheology in a passive manner and a low hematocrit is associated with prolonged bleeding times independent of the platelet count [58]. However, an abnormally high hematocrit leads to enhanced blood viscosity and thrombotic events, e.g. in polycythemia vera [59, 60]. This abnormal high hematocrit leads to axial accumulation of RBCs accompanied by alterations of blood viscosity, decreased blood flow, and decreased wall shear stress. Furthermore, the rheological effect of RBCs displaces platelets to the vessel wall. In addition, the decrease in wall shear stress attenuates the release of NO from the endothelium and promotes cell activation [61, 62]. Besides rheology, RBCs can directly interact with other cells to modulate hemostasis and thrombosis. Recent studies of Klatt *et al*. demonstrate that RBCs are essential for thrombus formation *in vitro* and *in vivo*, because the reduction of RBCs results in attenuated hemostasis and prolonged occlusion times in anemic mice. Furthermore, it was shown that platelet-RBC interactions include Fas ligand (FasL, CD178)/ Fas receptor (FasR, CD95)-mediated signaling, which is important for the externalization of PS at the RBC membrane, and this points to a direct role of RBCs in thrombin generation, thrombus formation and –stabilization in hemostasis and thrombosis [63]. High FasL and PS exposure of platelets and RBCs in arterial thrombi of patients provide evidence

that FasL/FasR-mediated cell contact between platelets and RBCs represents a pathophysiological mechanism as well. In addition, the PS exposing RBCs in turn bind to platelets via the receptors CXC chemokine ligand 16 (CXCL16) and CD36 [64]. PS positive RBCs facilitate the formation of the prothrombinase complex, thereby increasing thrombin generation [65]. Furthermore, the interaction of RBCs with ECs under physiological conditions is limited, but increased under certain pathophysiological conditions. For example, adhesion of RBCs to ECs is mediated by intercellular adhesion molecule 4 (ICAM-4), vascular cell adhesion molecule 1 (VCAM-1), and other adhesion molecules [66]. In addition, RBCs can bind to the subendothelial matrix if the endothelium is damaged. Under venous shear rates, RBCs are able to directly bind to platelets [67]. The incorporation of RBCs into a thrombus leads to structural alterations, which affect the stabilization and the character of the thrombus [68] accompanied by fibrinolytic resistance [69]. However, the role of RBCs in hemostasis and the underlying mechanisms how RBCs contribute to thrombosis is still not clear.

1.3 The scavenger receptor CD36 and the natural ligand TSP-1

1.3.1 The scavenger receptor CD36

Glycoprotein IV (CD36) belongs to the class B scavenger receptor family and is one of the most abundant GP on the surface of human and murine platelets with 10,000 – 25,000 copies per cell and additional copies present in platelet α-granules [70]. To date, the copy number of CD36 on RBCs has not been determined. This double membrane-spanning GP has a molecular weight of 80 – 90 kDa, two short N- and C-terminal cytoplasmic domains, and a highly glycosylated extracellular domain (Fig. 4) which can bind several ligands, e.g. thrombospondin-1 (TSP-1), oxidized low-density lipoprotein (oxLDL), long chain fatty acids, oxidized forms of phospholipids and collagen [71, 72]. CD36 was first discovered in 1973 in mammary epithelial cells and then verified on various other cell types, including monocytes, macrophages, microvascular ECs, platelets and RBCs [73, 74]. In the beginning, CD36 was defined as collagen receptor [75], but CD36-deficient patients showed an unaltered response to collagen [76, 77]. So far, two major deficiencies in humans are known, the type I deficiency that lacks CD36 on monocytes and platelets, while in patients with type II deficiency the protein is absent only on the platelet surface [78, 79]. CD36 deficiency appears more often in the African and Japanese populations [79, 80]. If CD36 deficiency is restricted to monocytes and platelets or if RBCs lack CD36 as well is not described yet. However, it is known that normal, mature RBCs possess CD36 on their surface [81]. CD36

functions as an adhesion molecule and is upregulated under different stress situations [73, 82].
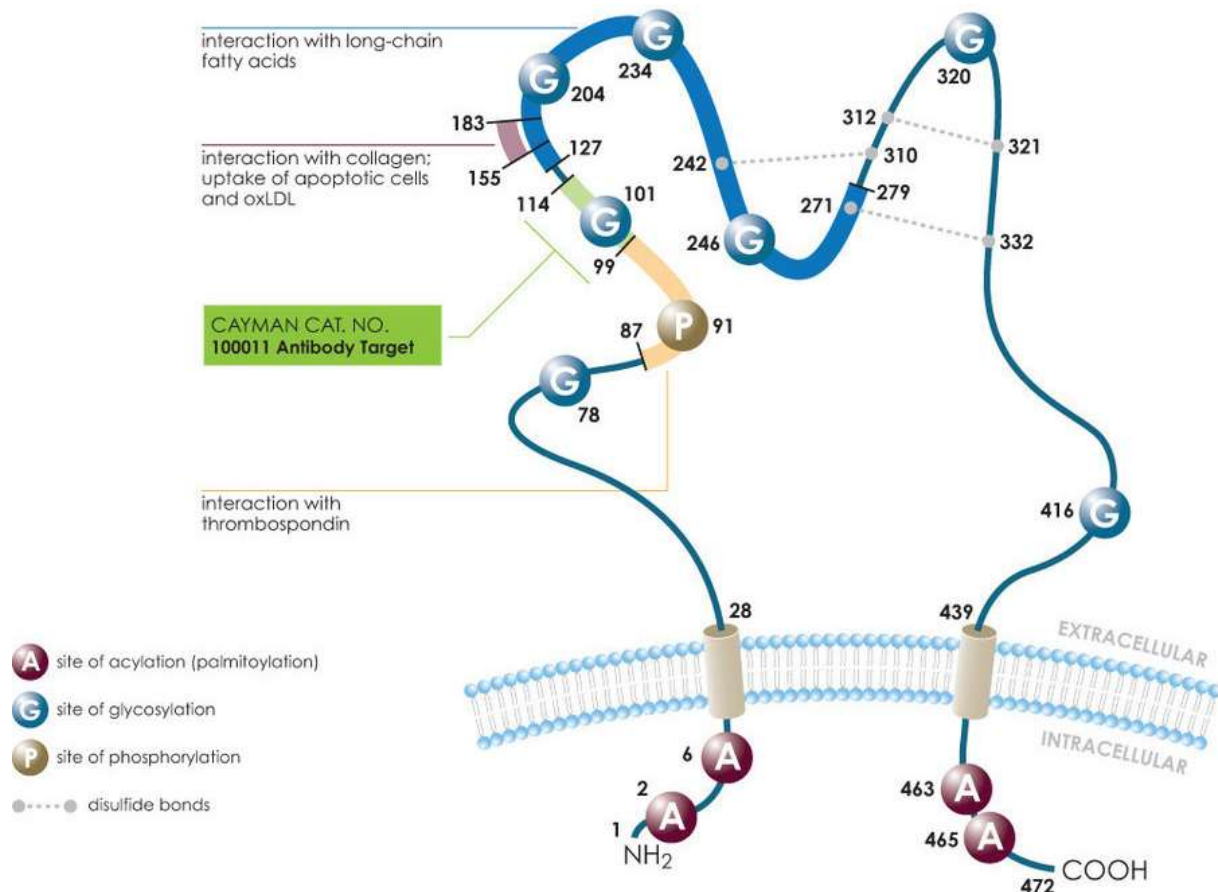
Figure 4: Predicted structure and binding sites of CD36. CD36 is a double membrane-spanning glycoprotein with several binding sites. The two short N- and C-terminal cytoplasmic domains and the highly glycosylated extracellular domain, which can bind several ligands, e.g. thrombospondin-1 (TSP-1), oxidized low-density lipoprotein (oxLDL), long chain fatty acids, PS of apoptotic cells and collagen are shown. Additionally, the binding site for the Cayman blocking antibody 100011 is marked. Taken from: Tom Brock [82].

Due to the expression on many cell types and the variety of binding partners, CD36 plays an important role in multiple cellular functions, under physiological as well as under pathophysiological conditions. Silverstein and colleagues demonstrated that CD36 is essential for the progression of atherosclerosis by the uptake of oxLDL to macrophages followed by the formation of foam cells. CD36-defiecient mice revealed a dramatic decrease of atherosclerotic plaque formation. Furthermore, CD36 recognizes PS on senescent and apoptotic cells, consequently leading to the removal of these cells [83].

CD36 is a highly evolutionary conserved protein with an essential role as pattern recognition receptor (PRR) and in the immune response. The receptor can recognize lipid and

lipoprotein components of cell walls from bacteria such as staphylococcus and mycobacterium shown in drosophila [84]. In humans and mice, the recognition of *Plasmodium falciparum* infected RBCs via CD36 on the surface of macrophages leads to phagocytosis of these RBCs [85]. In addition, CD36 that is located at the surface of vascular ECs or uninfected RBCs mediates the adherence to *Plasmodium falciparum* infected RBCs [85]. The rosetting of infected RBCs with uninfected RBCs is accompanied by alterations of rheology and accumulation of RBCs within the spleen and microvasculature, leading to life-threatening complications [86].

Silverstein and colleagues describe CD36 as a linker molecule between inflammation, oxidative stress, hyperlipidemia and thrombosis [83]. This was further supported by the fact that oxLDL binding to CD36 leads to direct platelet activation accompanied by the activation of Src family kinases (Fyn and Lyn), Syk tyrosine kinases, the generation of reactive oxygen species (ROS) and subsequent calcium influx into platelets [87-89]. The calcium influx enables the activation of the redox sensitive MAP kinase, extracellular signal-regulated kinase 5 (ERK5), followed by caspase cleavage and integrin activation [90, 91]. Caspase signaling results in PS exposure on the outer membrane of platelets, enabling the formation of the prothrombinase complex, which facilitates thrombin generation, followed by fibrin turnover and thrombus formation [90, 91]. Furthermore, studies with CD36-deficient mice suggest an additional autocrine feed-forward loop by the interaction of CD36 and platelet-released TSP-1 that supports the formation of a stable collagen-dependent thrombus [92]. However, CD36-deficient mice and humans show no bleeding diathesis.

1.3.2 The multifunctional glycoprotein TSP-1

In 1970, thrombospondin was first discovered on the surface of thrombin-stimulated platelets and termed as "thrombin-sensitive protein" [93]. TSP-1 is a multidomain non-structural glycoprotein within the ECM and is one of the most abundant proteins in platelet α-granules with 101,000 copies per cell. TSP-1 appears in blood vessels likely after deposition of Weibel-Palade bodies from ECs and platelets [94, 95]. Furthermore, monocytes, macrophages, SMCs, the retinal pigment endothelium (RPE), adipocytes and fibroblasts secrete TSP-1 [96]. TSP-1 is a homotrimeric glycoprotein that has a molecular weight of 420 – 450 kDa under non-reduced conditions [97, 98]. The homotrimeric structure is composed of three identical subunits with a molecular weight of 185 kDa each [99]. Under physiological conditions the concentration of TSP-1 in human plasma is 20 – 40 ng/mL [100]. Of note, TSP-1 levels can increase rapidly after tissue injury as observed in cardiovascular diseases [101]. Furthermore, the structure of TSP-1 is well known: Each TSP-1 monomer is

composed of an N-terminal (globular, G) heparin-binding domain, a linker strand including the two cysteine residues essential for trimerization, a procollagen (PC) homology domain, three type I repeats (TSR1, propadine-like), three epidermal growth factor (EGF) type II repeats (TSP2), seven calcium-binding type III repeats (TSR3) and a globular C-terminal domain with structural homology to L-lectin domains (Fig. 5) [102]. Moreover, the last type III repeat has a RGD-motif that allows the binding of integrins and the second and third type I repeat mediates the binding of TSP-1 to CD36 (CSVTCG-motif) (Fig. 5). The PC domain exhibits the cleavage site for several proteases including thrombin, plasmin, cathepsins, leucocyte elastases and a disintegrin and metalloproteinase with thrombospondin motifs (ADAMTS1). The proteolytic cleavage of TSP-1 by thrombin results in two fragments with a molecular weight of 25 kDa (N-terminal fragment) and 160 kDa (C-terminal fragment). In contrast, cleavage by ADAMTS1 leads to the formation of two fragments with a molecular weight of 36 kDa (N-terminal fragment) and 110 kDa or 140 kDa (C-terminal fragment) [103-105]. TSP-1 fragments of 110 kDa and 140 kDa in size enhance anti-angiogenic properties and the 160 kDa fragments is able to promote platelet adhesion and string formation under flow [99, 106, 107]. The cleavage of TSP-1 by plasmin and elastase leads to full degradation of TSP-1.
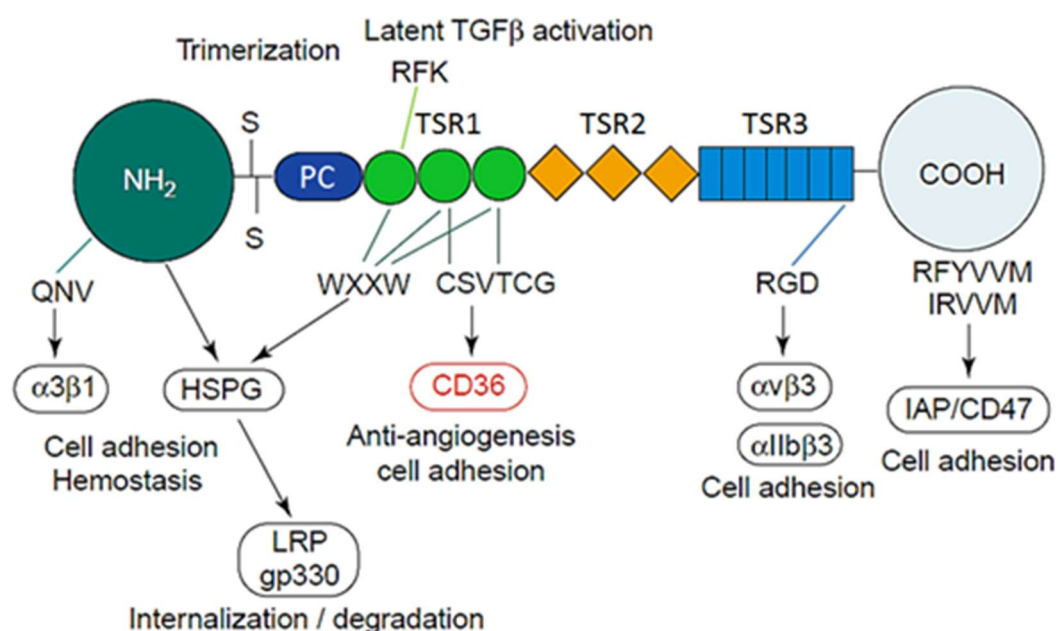
Figure 5: TSP-1 monomeric structure and multiple receptor binding sites. Each monomer is composed of an N-terminal (globular, G, -NH2), followed by the oligomerization domain, the procollagen (PC) region, the linker strand with central repeats (TSR1 – TSR3) and the C-terminal (globular, G, -COOH) domain. Each domain of the TSP-1 molecule binds to a specific receptor, which modulates different signaling pathways. Additionally, the TSR2 and TSR3 domains are capable to bind several Ca^{2+} ions, enabling further interactions and modulations. The biological function of receptor-TSP-1 interaction are indicated. IAP = integrin-associated protein; LRP = low-density lipoprotein receptor-related protein; TGFβ = transforming growth factor β. Modified and taken from: de Fraipont, 2001 [102].

TSP-1 participates in various biological processes, sometimes with even opposing effects. One explanation of these findings is the ability of TSP-1 to bind an immense number of different ligands, its expression in different cell types and altered function through proteolytic cleavage [101, 104]. One specific role of TSP-1 is the regulation (as inhibitor) of angiogenesis through the binding of CD36 on ECs accompanied by cell apoptotic signaling including FasR and the blockage of vascular endothelial growth factor (VEGF) under physiological conditions [108]. These processes play a significant role in EC death which are essential for maintaining the normal structure of the vascular system under physiological conditions [108]. Furthermore, the binding to the integrin-associated protein (IAP, CD47) regulates nitric oxide (NO) signaling that is important under physiological and pathophysiological conditions, e.g. in vasodilation [109, 110]. The interaction of the C-terminal domain of TSP-1 with CD47 and other integrins leads to cell adhesion and spreading [102, 111]. Moreover, TSP-1 activates transforming growth factor-β1 (TGFβ1), which mediates wound healing, cell proliferation, extra cellular matrix formation and the immune response [112]. In addition, CD36/TSP-1 interaction can also activate the NFkB pathway in macrophages and ECs leading to proinflammatory signaling [113].

Besides the role of TSP-1 in angiogenesis, platelet-released TSP-1 is known to be important for thrombus formation and –stabilization [92, 114]. During thrombus formation, TSP-1 protects vWF from cleavage through ADAMTS13, thus enabling the recruitment of flowing platelets to the growing thrombus by GPIb binding [115, 116]. This TSP-1/GPIb binding is an alternative mechanism to vWF binding to GPIb that is important for platelet adhesion under pathophysiological high shear rates [117]. In addition, binding of TSP-1 to platelets via several receptors such as CD36, CD47, integrin $\alpha_v\beta_3$ and integrin $\alpha_{IIb}\beta_3$ leads to direct platelet activation [118]. The secretion of TSP-1 from platelet α-granules and the interaction to its counter-receptor CD36, induces an additional autocrine feed-forward loop that enforces the interaction of platelets in a growing thrombus [92]. In addition, Bonnefoy and colleagues demonstrated that TSP-1 is able to link fibrinogen and its receptor leading to macromolecular aggregates of TSP-1/fibrinogen/integrin $\alpha_{IIb}\beta_3$ under flow conditions [118]. These macromolecular aggregates were also found on the surface of activated platelets as shown by microscopic studies [119].

1.4 Abdominal aortic aneurysm

An abdominal aortic aneurysm (AAA) develops when the abdominal aortic wall becomes permanently weakened, resulting in a dilatation of all three layers of the vascular tunica (the intima, media and adventitia, Fig. 6). An AAA is defined as a 1.5-fold enlargement of the

aorta compared to the normal aortic diameter or when the diameter is larger than 3 cm in the maximum transverse dimension. Most common, the AAAs are located in an infrarenal position (> 80%), while thoracic, juxtarenal and suprarenal aneurysms are rare [120, 121]. Several risk factors support the development of this multifactorial disease such as smoking, a positive family history, hypertension, chronic obstructive pulmonary disease (COPD), hyperlipidemia, aging (> 65 years) and male gender. However, this tendency might decrease in future, as the smoking prevalence trends towards equality between the genders [122]. In several industrial countries such as the U.S. or Europe, the AAA is the 12th to 15th leading cause of death in elderly society and the 10th leading cause of death in men older than 55 (U.S.). Because most AAA are asymptomatic, it is difficult to estimate their prevalence but screening studies reported a prevalence between 1 – 3% in men and 0.5 – 1% in women over 65 years of age [123, 124]. Most AAAs have a non-specific character without any kind of consequences due to a specific cause, e.g. trauma, inflammatory diseases or acute or chronic infection.
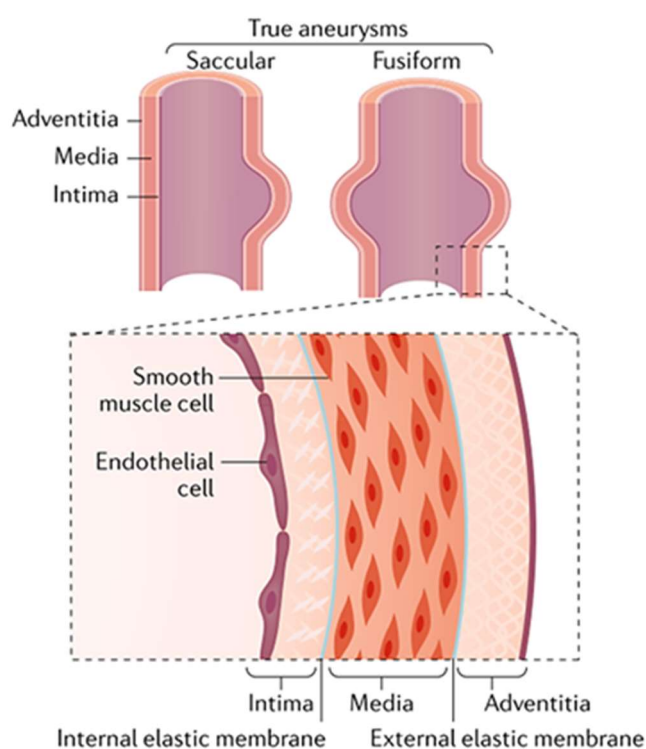
Figure 6: Morphological classification of an AAA and architecture of the aortic wall. A true aneurysm can be either saccular, or fusiform. Saccular describes a one-sided dilatation, fusiform a both-sided. The vessel wall consists of three layers: intima, media and adventitia. The intima consists of ECs and is the border between ECM and the blood circulation, the media contains VSMCs, elastic tissue and collagen. Besides the wide array of cell types, the adventitia also contains nerves, blood– and lymph vessels. Modified and taken from: Sakalihasan 2018 [122].

Conventionally, the AAA was assessed as a consequence of atherosclerosis; however nowadays, the pathogenesis of an aneurysm and an arterial occlusive disease (AOD) is different, e.g. a loss of vascular smooth muscle cells (VSMCs) is described in AAA while an accumulation of VSMCs occurs in AOD [125, 126]. Furthermore, the proteolysis based process in AAA is higher than in AOD demonstrated by decreased expression of plasminogen activator inhibitor 1 (PAI-1) and tissue inhibitor of metalloproteinase 2 (TIMP-2), the physiological inhibitors of proteases [126]. Additionally, a life-time smoker has a 4-fold

13

increased risk to develop AAA compared to a non-smoker [127] and a more than 10% higher dilatational growth rate [128]. Mechanistically, smoking stimulates elastase activity due to the inhibition of α1-antitrypsin and reinforces the secretion of elastase by neutrophils, resulting in the degradation of the elastic tissue in the aorta [129].

As mentioned above the pathology of this disease is characterized by irreversible dilatation of the abdominal aortic wall, which can rupture, when there is a loss of wall strength in combination with the high pressure in the aorta. This rupture leads to a massive intraabdominal hemorrhage and, in 80% of the patients, to death. Rarely, it is possible that the intraluminal thrombus (ILT, further described in 1.4.3) covers the damaged vessel wall and the patients have more time to undergo surgical intervention. Diagnosed aneurysms should be treated by inserting a vascular graft when the diameter of the abdominal aorta exceeds 5.5 cm, if the thoracic aorta exceeds 6.0 cm or if an increase of the aortic diameter with 0.5 cm in the past six months is observed. The repair of a smaller aneurysm was shown to be unbeneficial [122]. Commonly, patients underwent either an open aneurysm repair (OAR) or an endovascular aneurysm repair (EVAR). Without surgery, it was demonstrated that the 5-year survival rate of patients with an aneurysm larger than five centimeter is approximately 20% [130]. Based on their shape, either "true" aneurysms are classified as "fusiform", where the whole vessel is dilated or "saccular" with only one side being affected (Fig. 6). In contrast, a "false" aneurysm (pseudoaneurysm) is a dissection after a vessel wall injury accompanied by a separate blood flow besides the aortic vessel, in between the media and adventitia [122].

1.4.1 Pathology of AAA disease

The pathophysiology of AAA is characterized by several inflammatory and proteolytic events, including the degradation of the ECM, oxidative stress at the aortic wall, immune cell infiltration, death of VSMCs and the development of an ILT [122]. Inflammation is prominent in AAA disease and characterized by infiltration of inflammatory cells such as lymphocytes and macrophages into the aortic wall [131, 132]. On the one hand, the infiltration of immune cells induces oxidative stress and on the other hand, leukocytes are the main source of matrix metalloproteinases (MMPs) and serine proteases, known for their property to degrade structural proteins [122]. These immune cells are either transported to the media through the ILT or via neoangiogenesis in the media which is normally devoid of blood vessels [133]. Oxidative stress is a metabolic state, which exceeds the accumulation of oxidant substances, such as free radicals like O_2^-, and causes cell death by damaging DNA and protein oxidation. In AAA progression, RBCs, infiltrating macrophages and leucocytes are the main source of

reactive oxygen species (ROS) inducing oxidative stress [122, 134, 135]. ROS contributes to AAA pathogenesis by modulating the expression of chemotactic cytokines and adhesion molecules thus inducing leukocyte recruitment to the vascular wall [136]. For example, ROS influences the expression of monocyte chemoattractant protein 1 (MCP-1), interleukin 8 (IL-8), ICAM-1 and P-selectin (GMP-140) on ECs [137-139]. Mechanical stretch was shown to upregulate ROS production via the vascular NADPH-oxidase of VSMCs, leading to MMP-2 expression [140]. Furthermore, ROS activates MMPs and induces VSMC apoptosis, resulting in an irreversible degradation of the ECM [141, 142]. Several MMPs participate in aneurysmal growth, including MMP-2, MMP-9 and MMP-12 [143-145]. Furthermore, MMP-9 is of the utmost interest because it is highly upregulated and therefore the most abundant elastolytic protease in AAA tissue whereas TIMP-1 and TIMP-2 get downregulated simultaneously (Fig. 7) [122, 144, 146]. This imbalance between MMPs and TIMPs when accompanied by elastin fragmentation and aortic dilatation leads to the rupture of the aneurysm [147, 148].
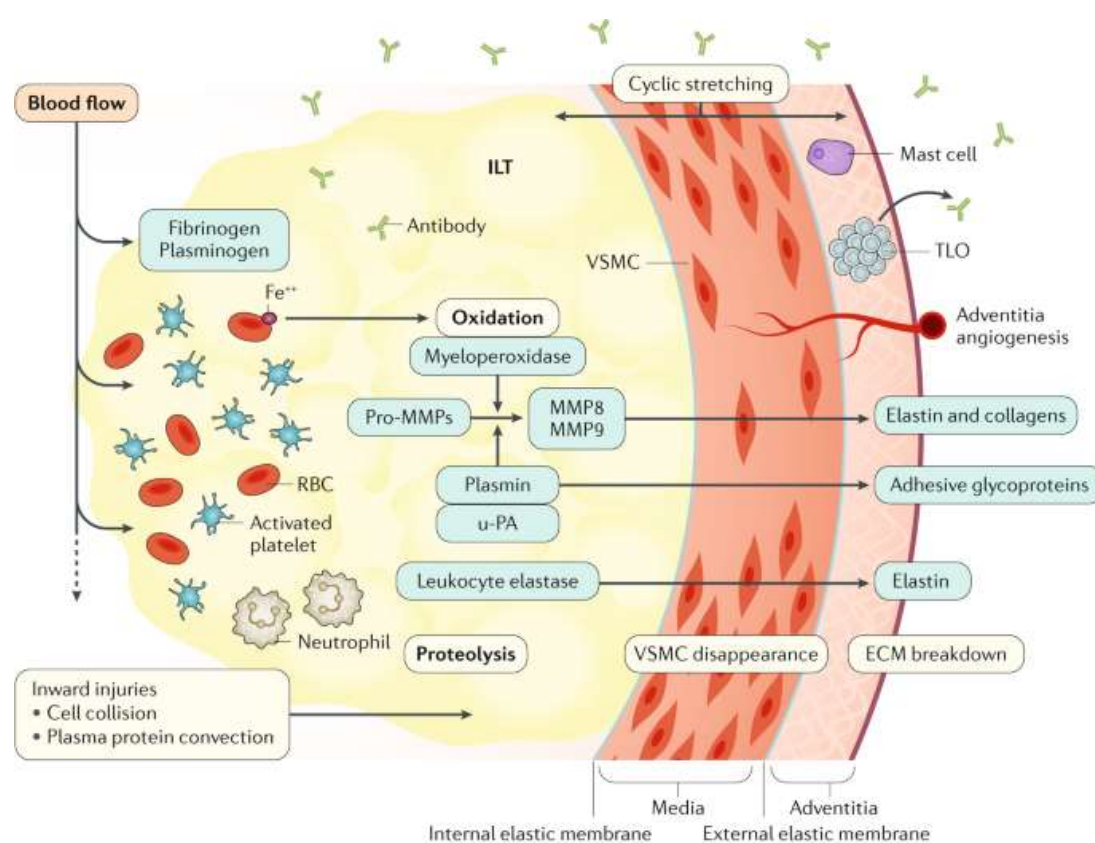
Figure 7: Different mechanisms lead to progression of AAA. ILT formation is a typical characteristic of AAA pathology and provides a constant interface with the blood circulation accompanied by platelet activation the release of proinflammatory cytokines and the recruitment of immune cells. These immune cells release proteases such as leukocyte elastases and MMPs that degrade elastin and collagens, or plasmin that degrade adhesive glycoproteins. Furthermore, the infiltrating immune cells, alongside with redox active iron from RBCs, are the main source of oxidative stress. ROS production, active MMPs and cyclic stretching lead to VSMCs detachment and apoptosis. AAA progression is also associated with neoangiogenesis into the media, which is normally devoid of blood vessels. Modified and taken from: Sakalihasan 2018 [122].

The expression of MMP-9 correlates with the AAA diameter and is elevated in the plasma of AAA patients [149]. Besides the elastin fragmentation, the turnover of collagen, mainly type III, is increased in AAA patients [150]. The fragmentation of elastin is associated with the dilatation of the aorta, while collagen degradation is the ultimate cause of rupture [151]. In contrast, the serine proteases plasmin and elastase are associated with the death of VSMCs. Plasmin, activated at the luminal site of the ILT, degrades adhesive glycoproteins, while elastase induces elastin degradation, both leading to VSMC detachment and apoptosis (Fig. 7) [152, 153]. To date, the involvement of VSMCs in AAA pathology, the main cell type in the elastic media, is not fully understood. It was demonstrated that this cell type is significantly decreased in AAA specimens [142], leading to a decrease in elastin and collagen levels, which are the main products of VSMCs. In addition, aneurysm formation and apoptosis of VSMCs were suppressed by inhibiting caspases, indicating a protective effect of VSMCs in AAA progression [154]. In contrast, they are also capable to contribute to inflammation and MMP production thus exhibiting a unique proelastolytic phenotype [146, 155, 156].

1.4.2 Platelets and RBCs in the pathology of AAA

RBCs are thought to play a prominent role in the pathogenesis of AAA. RBCs are incorporated into the mural thrombus and due to hemagglutination at the ILT ROS is generated through increased oxidative stress and the participation of released hemoglobin in chemical reactions [122]. Furthermore, iron deposition in the aneurysmal wall, originated from the ILT which potentially promotes the recruitment of monocytes to the highly vascularized adventitia [157]. It was demonstrated that RBC-borne iron retention might obstruct iron recycling leading to reduced circulating hemoglobin levels in AAA patients. In addition, AAA patients with anemia have an increased mortality risk as compared to AAA subjects without anemia [158]. Furthermore, the membrane composition of RBCs is altered in AAA patients [159]. Platelets are assumed to play an essential role in the pathogenesis of AAA as well because they are a main component of the ILT [160] and support inflammatory processes due to the release of proinflammatory cytokines [161]. Furthermore, platelet activation and aggregation is important for ILT formation and expansion of the aneurysm in rats [160]. The experimental aortic aneurysms in rats were induced by implantation of a segment (1.5 cm) of sodium dodecyl sulfate-decellularized guinea-pig aorta (xenogenic matrix), which leads to an intraluminal thrombus. In addition, platelets were also shown to contribute to AAA progression by stimulating macrophage recruitment, ROS production and MMP activity [161, 162]. Moreover, in a mouse model of angiotensin II (AngII)-induced AAA

formation, the change of aortic expansion and aneurysm formation was reduced (by 47%) due to the treatment of mice with clopidogrel, a well-known inhibitor of the ADP receptor P_2Y_{12} [163]. However, the benefit of acetylsalicylic acid (ASA) to reduce AAA progression and patient's mortality is highly debated and might depend on the progression state of the disease [8]. The release of TSP-1 from activated platelets induce various signaling pathways (described in chapter 1.3.2), but this protein is also involved in AAA in rodents. In detail, TSP-1 is of the utmost interest because it promotes AAA in the absence of an atherosclerotic background in mice by modulating macrophage recruitment, adhesion and migration into the inflamed area [164]. In contrast, in the presence of an arteriosclerotic background, TSP-1 slows down the progression of AAA [162]. Because of comorbidities including atherosclerosis in AAA patients, TSP-1 could act as a protective protein [165]. Moreover, TSP-1 deficiency leads to a two-fold higher macrophage infiltration and enhanced MMP-9 accumulation resulting in a 30-fold elevated incidence of elastic lamina degradation [166]. This indicates a protective role of TSP-1 in mice and can be explained by the ability to modulate TIMP-2 expression, the physiological inhibitor of MMP-9 [167]. In summary, TSP-1 has strong modulating but context dependent effect on the development of AAA in mice. However, the role of TSP-1 in patients with AAA remains to be determined.

1.4.3 The intraluminal thrombus

AAA is often accompanied by the formation of an ILT, a multi-layered, biological active neo-tissue with its own microenvironment, which occurs in 70 – 80% of AAA patients [168]. The underlying mechanism of ILT formation is poorly understood. The ILT in its complexity has a luminal layer, full of undegraded cross-linked fibrin and aggregated RBCs (hemagglutination), and a medial/abluminal layer, full of nucleated, cell-rich fibrin which is the proteolysed layer (Fig. 8) [133, 169].
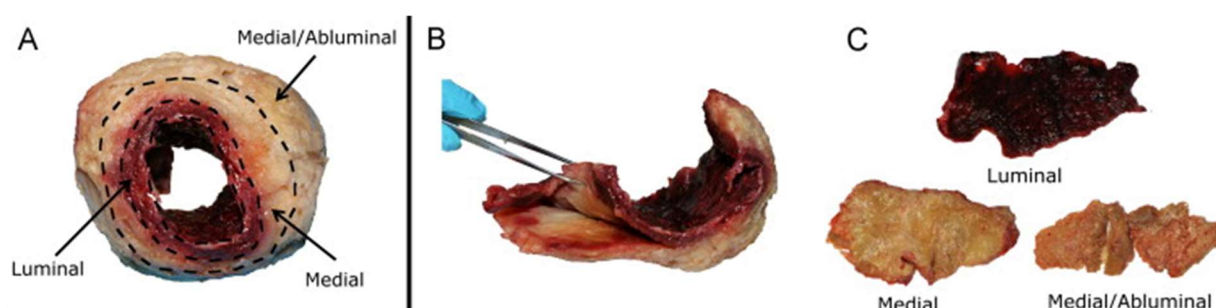
Figure 8: Architecture of the intraluminal thrombus. (A – C) Macroscopic view showing the red, luminal layer of the ILT and the medial/abluminal proteolysed layer. Taken from: O'Leary 2014 [169].

The ILT is pervaded with a continuous network of canaliculi, allowing unrestricted macromolecular penetration [170]. The luminal layer is highly biologically active due to the deposition of PS and tissue factor (TF) in this layer (unknown origin) and the accumulation of activated platelets in the interface of the ILT. This reinforces the thrombogenicity which is further supported by the released of high concentrations of platelet activation markers that could easily be detected in plasma of AAA patients. Furthermore, the release of microparticles from platelets and neutrophils are supporting these biological processes on the surface of ILT [133, 160]. This is followed by the formation of fibrin with increased levels of activated thrombin. Regardless of their localization, abdominal [171], thoracic [172] or intracranial [173] the ILT was shown to affect AAA pathogenesis, contributing to a thinner arterial wall and a higher level of vascular inflammation. Furthermore, clinical studies reported a direct correlation between ILT thickness, AAA diameter, MMP levels, elastin degradation and SMC apoptosis [174, 175]. As mentioned above, RBCs are incorporated into the mural thrombus and due to hemagglutination at the ILT, oxidative stress is increased [122]. In addition, fibrinolysis is spatially and temporarily delayed and the release of fibrin degradation products increases from the inner to the outer layers of the ILT [176]. Moreover, the luminal layer is spiked with neutrophils associated with increased levels of MMP-9 [177]. The thickness of the ILT is related to local hypoxia and leads to increased, mural neovascularization and inflammation [178]. Despite the negative effects described above, the ILT can protect the aneurysm from rupture by altering wall stress distribution [179].

1.5 Aim of the study

The role of platelets in hemostasis as well as in thrombotic disorders has been demonstrated. Furthermore, patients with high RBC counts as well as patients with inherited RBC abnormalities suffer from thrombotic complications and exhibit cardiac and cerebral thrombosis. However, the influence and participation of platelet-RBC interaction and the underlying mechanism are poorly understood. Further understanding is essential in order to identify new targets for antithrombotic therapy. Recently, our working group described a completely new mechanism of platelet-RBC interaction that is mediated by binding of platelet FasL to the FasR on the RBC membrane leading to the externalization of PS on the RBC membrane. This attributes a direct role for RBCs to thrombin generation, which on the one hand activates platelets and on the other hand stabilizes the growing thrombus by the inclusion of fibrin [63]. The first aim of this study was to provide further evidence for the impact of the FasL/FasR signaling pathway in platelet-RBC interactions. Therefore, analysis of thrombus formation and platelet aggregation of FasR-deficient, FasL-deficient and platelet-

specific FasL KO mice was performed. FasR mediating effects in thrombus formation exceeds the effects of FasL [63]. This suggested that other interaction partners on platelets are present, which induces FasR activation on RBCs besides FasL. Therefore, the second aim of this study was to identify new mechanisms of platelet-RBC interaction that play a role in hemostasis and thrombosis.

Platelet-released TSP-1 was proposed as an important binding partner for CD36 on the surface of platelets, and this mechanism reinforces stable thrombus formation and stability [92, 114]. However, the binding of TSP-1 to CD36 on the RBC membrane and further effects on thrombus growth and formation have not yet been investigated.

To date, the initial contact of RBCs with platelets and the mechanism how RBCs are incorporated into the thrombus are not understood and should be investigated as well.

The impact of platelets in cardiovascular diseases such as myocardial infarction, stroke and thrombosis has been analyzed in detail. However, platelet-RBC interaction and the impact of these interactions in cardiovascular diseases are poorly understood. We hypothesized that platelet-RBC interaction could be important for the development and progression of cardiovascular diseases such as AAA. Thus, as a first translational approach, the analysis of platelets and RBCs in AAA pathology was investigated. Accordingly, procoagulant surface, FasL/FasR externalization and CD36/TSP-1 expression was analyzed. In addition, the migration and deposition of platelets and RBCs into the aortic wall and into the ILT of AAA patients was investigated.

Overall, the aim of this thesis was to elucidate the mechanisms of platelet-RBC interaction in hemostasis and thrombosis, the recruitment of RBCs to the growing thrombus and the impact of these mechanisms for AAA progression to identify new targets for diagnosis and therapy of patients.

2. Material

2.1 General devices and equipment

If not mentioned otherwise, general material like tubes, falcons, pipette tips, syringes, etc. were purchased from ErgoOne, Starlab, Sarstedt, Kindler, BD Bioscience and Braun.

2.1.1 Equipment

Table 1: Laboratory equipment

Equipment	Model	Company
Benchtop, pH-Meter	WTW pH526	Xylem Inc.
Bench scale	AE166	Mettler -Toledo
Bench scale	Practum®	Sartorius
Bench scale	Secura®	Sartorius
Centrifuge, cooling	5424-R	Eppendorf
Centrifuge, cooling	5804-R	Eppendorf
Centrifuge, Mini	D-6020	neoLab
Centrifuge, tabletop	5415-C	Eppendorf
Centrifuge, tabletop	2-16	Sigma-Aldrich
Flow chamber system		Maastrich Instruments
Flow cytometer	FACS Calibur	BD Biosciences
Hematologic analyzer	KX-21N	Sysmex
Magnetic stirrer	RET basic	IKA laboratory technology
Micropipettes	Research plus	Starlab & Eppendorf
Microwave	NN-E201WM	Panasonic
Multichannel pipette	Peqpette	Peqlab
Multipipette	Multipette® plus	Eppendorf
Parafilm	PM-996	Bemis®
PCR cycler	Mastercycler nexus gradient	Eppendorf
Pipettor	Pipetboy acu	Integra Biosciences
Roll mixer	RM5	CAR
Syringe pump	KDS100	KD Scientific Inc.
Thermo shaker	TS-100C	Biosan

2.1.2 Equipment for tissue preparation and histology

Table 2: Equipment for tissue preparation and histology

Equipment	Model	Company
Automatic microtome	Microm HM355	Thermo Fisher Scientific
Humidity chamber		Simpore Inc.
Paraffin dispenser	Round model	Medax
Paraffin section flotation bath	MH8517	Electrothermal

2.1.3 Equipment for electrophoresis, Western blot and imaging

Table 3: Equipment for electrophoresis, Western blot and imaging

Equipment	Model	Company
Chemiluminsence Imager	Vilber Fusion-FX6	Vilber Lourmat
Double gel system	PerfectBlue™	Peqlab
Horizontal agarosegel system	PerfectBlue™ Wide Format Gel System	Peqlab
Filter paper		Whatman
Microscope, inverse	AX10 Observer.D1 HAL 100	Zeiss
Microscope color camera	Axiocam 503 color	Zeiss
Microscope color camera	Axiocam 105 color	Zeiss
Microscope laser	HXP 120C	Zeiss
Nitrocellulose membrane		GE Healthcare
Semi-Dry blot system	PerfectBlue™	Peqlab
Universal power supply	PowerPac™	BioRad Laboratories

2.2 Chemicals and buffers

2.2.1 Chemicals

Table 4: Reagents

Reagent	Catalogue number	Company
0.9% NaCl solution		Fresenius Kabi
2-[4-(2-hydroxyethyl)piperazin-1-yl]ethanesulfonic acid	9105	Carl ROTH GmbH
4′,6-diamidino-2-phenylindole (DAPI)	10236276001	Roche
Abciximab (ReoPro®)		Janssen Biologics B. V.
AccuStart™ II	95136-500	Quantabio
Accutase®	L11-007	PAA Laboratories
Acrylamide	3029	Carl ROTH GmbH

Adenosine diphosphate (ADP)	A2754	Sigma-Aldrich
Agarose	A9539	Sigma-Aldrich
Ammonium persulfate (APS)	9592	Sigma-Aldrich
Apyrase	A7646	Sigma-Aldrich
Bovine serum albumin (BSA)	A7906	Sigma-Aldrich
Brompehnol blue	115-39-9	Merck Millipore
Calcium chloride (CaCl$_2$)	C5080	Sigma-Aldrich
Citric acid (C$_6$H$_8$O$_7$)	6490	Sigma-Aldrich
Collagen (Horm®)	1130630	Takeda
Collagen related peptide (CRP)	XL1	University of Cambridge, UK
Dithiothreitol (DTT)	D0632	Sigma-Aldrich
DMSO (dimethyl sulfoxide)	D8418	Sigma-Aldrich
Ethylenediaminetetraacetate (EDTA) solution (0.5 M)	03690	Sigma-Aldrich
Ethanole 100% (EtOH)		Merck Millipore
Fibrinogen	F3879	Sigma-Aldrich
Fluoromount™ Aqueous Mounting Medium	F4680	Sigma-Aldrich
Glucose	HN06	Carl ROTH GmbH
Glycine	3908	Carl ROTH GmbH
Goat serum	ZIE.SE.0100	Bio & Sell
Heparin-Sodium-25000	15782698	B Braun
Human decoy receptor 3 (hDcR3)	142-DC	R&D Systems
IGEPAL® CA-630	I8896	Sigma-Aldrich
Isoflurane		Piramal critical care
Ketamin (Ketaset)		Zoetis
Magnesium chloride (MgCl$_2$)	KK36	Carl ROTH GmbH
Mepacrine	Q3251	Sigma-Aldrich
Methanol (CH$_3$OH)	20847.320	VWR
Molecular weight marker	161-0374	BioRad
Pan caspase inhibitor	551476	Merck Millipore
PAR4 peptide		JPT Peptide Technologies
Paraffin wax		Carl ROTH GmbH
Paraformaldehyde 4%		Carl ROTH GmbH
Phosphate buffered saline (PBS)	D8537	Sigma-Aldrich
Ponceau S solution	P7170	Sigma-Aldrich
Potassium chloride (KCl)	9023717	Merck Millipore
Potassium permanganate (KMnO$_4$)	8004	Carl ROTH GmbH
Powdered skim milk	Instant powdered skim milk	Frema Reform
Prostaglandin I$_2$ (PGI$_2$)	538925	Merck Millipore
Prostaglandin E$_1$ (PGE$_1$)	538903	Merck Millipore
Precision Plus Protein Dual Color Standards	1610374	BioRad Laboratories

Proteinase-inhibitor (cOmplete Tablets Mini Easypack)	04693124001	Roche
Roti®Histol	6640	Carl ROTH GmbH
Sodium dodecyl sulfate (SDS)	2326	Carl ROTH GmbH
Sodium chloride (NaCl)	3014	Sigma-Aldrich
Sodium orthovanadate (Na_3VO_4)	S6508	Sigma-Aldrich
Sodium phosphate, dibasic (Na_2HPO_4)	4984	Carl ROTH GmbH
Sodium dihydrogen phosphate (NaH_2PO_4)	6345	Merck Millipore
Sodium acid (NaN_3)	S2002	Sigma-Aldrich
Sodium hydrogen carbonate ($NaHCO_3$)	6885	Carl ROTH GmbH
Tetramethylethylenediamine (TEMED)	T9281	Sigma-Aldrich
Thrombin 20U		Roche
Tirofiban (Aggrastat®)		Correvio
Trisodium citrate	3580	Carl ROTH GmbH
Triton™ X-100	T8787	Sigma-Aldrich
Trizma®-base	T6066	Sigma-Aldrich
Trizma® hydrochlorid	T5941	Sigma-Aldrich
Tween® 20	822184	Merck Millipore
Xylazine (Xylazinhydrochlorid)		Serumwerk Bernburg
β-mercaptoethanole	4227	Carl ROTH GmbH
ε-aminocaproic acid ($C_6H_{13}NO_2$)	A2504	Sigma-Aldrich

2.2.2 Buffers and solutions

Table 5: Recipes of buffers and solutions

Buffer/Solution	Recipe
Acid-citrate-dextrose (ACD) buffer	2.5 g trisodium citrate dihydrate 1.36 g citric acid 2 g glucose *ad* 100 mL adjust pH to 4.69
ADP solution	0.1 g ADP 11.7 mL PBS Adjust pH to 7.4
Binding buffer	0.477 g HEPES 1.636 g NaCl 0.0735 g $CaCl_2$ adjust pH to 7.4 and fill up to 20 mL
Blot buffer A	36.3 g Trizma®-Base

	200 mL MeOH 800 mL dH$_2$O adjust pH to 10.4
Blot buffer B	3.03 g Trizma$^®$-Base 200 mL MeOH 800 mL dH$_2$O adjust pH to 10.4
Blot buffer C	5.2 g ε-aminocaproic acid 200 mL MeOH 800 mL dH$_2$O
Citrate buffer	41 mL 0.1 M trisodium citrate dihydrate 9 mL 0.1 M citrate acid 450 mL dH$_2$O adjust pH to 6.4
Heparin-solution (20 U/mL)	40 µL Heparin-Natrium 5000 I.E 10 mL PBS
Human Tyrode's buffer	137 mM NaCl 12 mM NaHCO$_3$ 2.8 mM KCl 0.4 mM NaH$_2$PO$_4$ 5.5 mM glucose adjust pH to 7.4
IP-buffer (stock solution 5x)	15 mM Tris-HCl 155 mM NaCl 1 mM EDTA 0.005% NaN$_3$ 1 L dH$_2$O
Laemmli (6x)	0.93 g DTT 1 g SDS 7 mL Tris HCl/SDS pH 6.8 (4x stacking gel buffer) 3 mL glycerin 1.2 g Bromophenol blue 0.02%
Lysis buffer (5x stock solution)	100 mM Tris HCL 725 mM NaCl 20 mM EDTA Triton 2.5 mL 50 mL dH$_2$O pH 7.40
Murine Tyrode's buffer	134 mM NaCl 12 mM NaHCO$_3$ 2.9 mM KCl 0.34 mM Na$_2$HPO$_4$ 20 mM HEPES 10 mM MgCl$_2$ 5 mM glucose 0.2 mM CaCl$_2$

	adjust pH to 7.35
Murine Ca^{2+} Tyrode's buffer	2 mL Murine Tyrode's buffer 40 µL CaCl$_2$
Resolving gel 8%	3.75 mL Resolving gel buffer (4x) 7.25 mL dH$_2$O 4 mL Acrylamide (30%) 150 µL APS (10%) 15 µL TEMED
Resolving gel 12%	3.75 mL Resolving gel buffer (4x) 5.25 mL dH$_2$O 6 mL Acrylamide (30%) 150 µL APS (10%) 15 µL TEMED
SDS-PAGE running buffer (5x stock solution)	15.1 g Trizma®-Base 72 g glycine 5 g SDS or 25 mL SDS (20%) *ad* 1 L dH$_2$O adjust pH to 8.3
SDS-PAGE stacking gel buffer (4x stock solution)	6.05 g Trizma®-Base 80 mL dH$_2$O adjust pH to 6.8 *ad* 100 mL dH$_2$O Filter the solution and add 0.4 g SDS
SDS-PAGE running gel buffer (4x stock solution)	91 g Trizma-Base 400 mL dH$_2$O Adjust pH to 8.8 *ad* 500 mL dH$_2$O Filter the solution and add 2 g SDS
Stacking gel	1.25 mL Stacking gel buffer (4x) 3.05 mL dH$_2$O 650 µL Acrylamide (30%) 25 µL APS (10%) 5 µL TEMED
TBS-T	100 mL 5x TBS-Puffer 500 µL Tween 400 mL dH$_2$O
Tris buffered saline (TBS, 5x stock solution))	15.8 g Trizma-HCl 45 g NaCl *ad* 1 L dH$_2$O adjust pH to 7.6
Tris acetate EDTA (TAE)-buffer	242 g Trisma-base 57.1 ml acetic acid 100 ml 0.5% EDTA adjust pH to 8.0

2.3 Antibodies and peptides

2.3.1 Primary antibodies

Table 6: Commercially purchased primary antibodies

Antibodies	Host species	Clonality	Use	Company
Anti-GAPDH 14C10, #2118	rabbit	monoclonal	WB	Cell Signaling
Anti-CD235a #NBP2-45024	mouse	monoclonal	IF	Novus Biologicals
Anti-GPIX #orb167288	rabbit	monoclonal	IF	Biorbyt
Anti-GPIbβ (DyLight488®) #X488	rat	monoclonal	flow chamber	Emfret Analytics
Anti-CD36 #10009893	mouse	monoclonal	Blocking	Cayman Chemical
Anti-CD36 #PA1-16813	rabbit	polyclonal	WB	Thermo Fisher Scientific
Anti-FasR #GTX13549			Blocking (B)	GenTex
Anti-TSP-1 #ab85762	rabbit	polyclonal	IF	Abcam
Anti-TSP-1 #NB100-2059	mouse	monoclonal	Flow cytometry/B/WB	Novus Biologicals
Anti-TER119 #550565	rat	monoclonal	IF	BD Biosciences
Anti-mouse/human IgG$_1$ κ #554121	mouse		IF, flow cytometry	BD Biosciences
Anti-mouse/human IgG$_1$ #ab27478	rabbit		IF	Abcam
Anti-mouse IgG$_{2b}$, κ #559478	rat		IF	BD Biosciences

2.3.2 Secondary antibodies

Table 7: Commercially purchased secondary antibodies

Antibodies	Host species	Clonality	Conjugated	Company
Anti-rabbit #NA934	goat	polyclonal	horseradish-peroxidase	GE Healthcare
Anti-mouse #NA931	goat	polyclonal	horseradish-peroxidase	GE Healthcare
Anti-mouse #A11001	goat	polyclonal	Alexa-Fluor™488	Invitrogen
Anti-rabbit #A11008	goat	polyclonal	Alexa-Fluor™488	Invitrogen
Anti-rabbit #A21428	goat	polyclonal	Alexa-Fluor™555	Invitrogen
Anti-rat #A32740	goat	polyclonal	Alexa-Fluor™594	Invitrogen

2.3.3 Antibodies for flow cytometry

All Antibodies used for flow cytometric analysis were monoclonal [1:10 dilution in respective Tyrode's buffer].

Table 8: Commercially purchased antibodies for flow cytometry

Antibodies	Host species	Conjugated	Company
Anti-human CD235a #IM2212U	mouse	FITC	Beckman Coulter
Anti-human CD36 #A15793	mouse	PE	Invitrogen
Anti-human FasL #306407	mouse	PE	BioLegend
Anti-human FasR #305608	mouse	PE	BioLegend
Anti-human CD61 #555754	mouse	PE	BD Biosciences
Anti-human CD42a #348083	mouse	FITC	BD Biosciences
Anti-human CD42a #558819	mouse	PE	BD Biosciences
Anti-human CD62P #348107	mouse	PE	BD Biosciences
Anti-human PAC-1 #340507	mouse	FITC	BD Biosciences
Anti-mouse CD61 #M031-1	rat	FITC	Emfret Analytics
Anti-mouse CD42b #M040-1	rat	FITC	Emfret Analytics
Anti-human IgM #314507	mouse	PE	BioLegend
Mouse IgG$_1$ κ #345815	mouse	FITC	BD Biosciences
Mouse IgG$_1$ κ #345816	mouse	PE	BD Biosciences

2.3.4 Peptides and dyes

Table 9: Commercially purchased peptides and dyes

Peptide/ Dye	Conjugated	Dilution/ Concentration	Company
Annexin V #559934	Cy5	1:10	BD Biosciences
FasR protein #10217-H08H		50 µg/mL	Sino Biological
Native human TSP-1 #605225-25UG		100 µg/mL	Merck Millipore
Recombinant Annexin V #556416		5 µg/mL	BD Biosciences

2.4 Oligonucleotides

All Oligonucleotides used in this study were synthesized and purchased from Eurofins Scientific.

Table 10: Oligonucleotides for genotyping

Target gene	Direction	Primer sequence
FasL	forward	5-'GAACACAGACCTACACAGAAGTCACATC-3'
	reverse	5-'GTACTTCTTCTGATAAGGACC-3'
PF4-cre	forward	5-'CCCATACAGCACACCTTTTG-3'
	reverse	5-'TGCACAGTCAGCAGGTT-3'
CD36	forward	5-'CAGCTCATACATTGCTGTTTATGCATG-3'
	NEO forward	5-'GGTACAATCACAGTGTTTTCTACGTGG-3'
	reverse	5-'CCGCTTCCTCGTGCTTTACGGTATC-3'

2.5 Kits

Table 11: Kits

Kit	Catalogue number	Company
Clarity Western ECL Substrate	EK07000	Boster Biological Technology

2.6 Software

Table 12: Software

Software	Company
GraphPad Prism 7.02	GraphPad Software
Fiji Is Just ImageJ	NIH Image
FlowJo Single Cell Analysis v10	FlowJo LLC
Microsoft Office 2016	Microsoft Corporation
ViiA™ 7 Software	Thermo Fisher Scientific
ZEN 2012 (blue)	Zeiss

2.7 Animals

All mice used for animal experiments were either obtained from commercial animal suppliers or were generated in the animal facility of the Heinrich Heine University of Düsseldorf

(ZETT). The mice were kept under standard laboratory specific pathogen free (SPF) conditions according to the guidelines of FELASA (Federation of European Laboratory Animal Science Association). Mice were kept in groups in plastic cages (GMOs) with a standardized 12 h day/night rhythm. They were fed with standard rodent chow and water *ad libitum*.

Specific pathogen-free C57BL/6J mice were obtained from Janvier Labs. Gene-targeted mice lacking FasR (C57BL/6J.MRL-FAS^{lpr}) were obtained from The Jackson Laboratory. *Cd36*$^{-/-}$ were obtained from Prof. Hadi Al-Hasani (German Diabetes Center), originally from Prof. Maria Febbraio. FasL$^{fl/fl}$ mice were provided by Prof. Ana Martin-Villalba (University of Heidelberg, Heidelberg, Germany) and crossed to PF4-Cre mice, which were purchased from The Jackson Laboratory (C57BL/6-Tg [PF4-cre] Q3Rsko/J). FasL$^{fl/fl}$ mice were originally from Saoussen Karray (Inserm, Institute human immunology, physiopathology and & immune therapy) and a valid MTA is present. Experiments carried out in this work were performed with male and female mice in the age of 8-16 weeks. All animal experiments were conducted according to the Declaration of Helsinki and the guidelines from Directive 2010/63/EU of the European Parliament on the protection of animals. The protocol was approved by the Heinrich-Heine-University Animal Care Committee and by the State Agency for Nature, Environment and Consumer Protection of North Rhine-Westphalia (LANUV: 84-02.05.40.16.073).

2.8 Human blood samples

2.8.1 Ethics vote

Fresh citrate-anticoagulated blood (BD-Vacutainer®; Becton, Dickinson and Company) was obtained from healthy volunteers aged between 18 and 70 years and AAA patients. AAA patients were compared to age-matched controls (AMCs, older than 60 years). Participants provided their written informed consent to participate in this study according to the Ethics Committee of the University Clinic of Düsseldorf, Germany (2018-140-kFogU, study number: 2018064710; biobank study number: 2018-222_1 and MELENA study: 2018-248-FmB, study number: 2018114854). The Ethics Committee of the University Clinic of Düsseldorf, Germany approved the consent procedure and specifically this study according to the Declaration of Helsinki.

3. Methods

3.1 Cell biological methods

3.1.1 Human platelet preparation

Fresh citrate-anticoagulated blood (BD-Vacutainer®; Becton, Dickinson and Company) was obtained from healthy volunteers aged between 18 and 70 years and AAA patients. Human blood was collected into Vacutainer® sodium citrate tubes [105 mM Na_3-citrate] and centrifuged at 231 x g for 10 min without brake. The upper phase consisting of the platelet rich plasma (PRP) was carefully transferred into phosphate buffered saline (PBS) pH 6.5 containing apyrase [2.5 U/mL] and 1 μM PGE_1. The tubes are centrifuged at 1000 x g for 6 min without brake and the obtained pellet was resuspended in Tyrode's buffer [137 mM NaCl, 2.8 mM KCl, 12 mM $NaHCO_3$, 0.4 mM NaH_2PO_4, 5.5 mM glucose, pH 6.5]. The final cell count was determined in a 1:10 dilution in PBS using hematology analyzer (Sysmex - KX21N, Norderstedt, Germany) and adjusted according to the requirements of each experiment. For additional plasma collection, after the second centrifugation step and the extraction of the PRP the tubes were centrifuged at 1500 x g for 10 min and at 4 °C. The platelet free plasma (PFP) was collected and either stored on ice for immediate usage or stored at –70 °C for later experiments.

3.1.2 Isolation of human red blood cells

Human blood was collected into Vacutainer® sodium citrate tubes [105 mM Na_3-citrate] and centrifuged at 231 x g for 10 min without brake. The platelet-rich plasma was separated. The remaining blood was centrifuged at 800 x g for 15 min in a closed syringe. The plasma was removed and used to prepare cell-free plasma. To separate RBCs from leukocytes the syringe was opened and the red blood cells were collected in a new container. The intermediate leukocyte layer (buffy coat) – a white cell layer on top of the red blood cells – were left in the syringe. Red blood cells were washed with the fivefold volume of saline solution [154 mM] three times by centrifugation at 300 x g for 10 min. RBCs were directly used. The final cell count was measured by a hematology analyzer (Sysmex, Norderstedt, Germany) and adjusted according to the requirements of the experiment.

3.1.3 Human platelet and RBC lysates and supernatants

Platelets and RBCs were isolated following the standard protocols (methods 3.1.1 and 3.1.2). Cell counts were adjusted according to the needs of the following experiment as indicated. For the experiments, five different samples were prepared. Resting and CRP-stimulated [5 µg/mL] platelets in the absence or presence of RBCs and RBCs alone. All samples were filled up with Tyrode's buffer to a final volume of 100 µL. The samples were incubated for 5 min at 37 °C and then centrifuged at 800 x g for 10 min. The supernatants were collected and stored at –20 °C for further experiments. The pellets were washed with 500 µL of HEPES or PBS and were centrifuged at 21,000 x g for 20 min at 4 °C. The supernatants were discarded and 30 µL lysis buffer was added to the pellets. After incubating for 15 min on ice, the samples were centrifuged at 10,000 x g for 5 min at 4 °C. The lysate were prepared with 6 µL reducing sample buffer (6x Laemmli buffer) and stored at –20 °C for further experiments.

3.1.4 Murine platelet preparation

Mice were anesthetized in a chamber with isoflurane (3% isoflurane and 1.0 L/min oxygen-flow). As soon as the mouse had reached an adequate anesthesia depth, blood was collected by puncturing the retrobulbar venous plexus with a microcapillary (VWR). Murine blood from retro-orbital plexus was collected in 300 µL heparin solution [20 U/mL in PBS] in a 1.5 mL reaction tube and platelets were isolated through centrifugation. To avoid platelet preactivation, all centrifugation steps were performed without a break. First, the heparinized whole blood was centrifuged at 250 x g for 5 min at room temperature (RT) to separate the individual blood components. The upper phase and the whole interphase were transferred into a new reaction tube, following centrifugation at 50 x g for 5 min at RT. The resulting platelet rich plasma (upper phase) was transferred into a new reaction tube. After discarding the buffy coat (intermediate phase), the remaining RBCs (bottom phase) were taken for further experiments. The remaining pellet was resuspended in 200 µL Tyrode´s buffer [136 mM NaCl, 0.4 mM Na_2HPO_4, 2.7 mM KCl, 12 mM $NaHCO_3$, 0.1% glucose, 0.35% bovine serum albumin (BSA), pH 7.4], centrifuged at 50 x g for 5 min at RT. The newly formed supernatant was added to the previously taken PRP. To avoid preactivation of platelets, apyrase [0.02 U/mL] and PGI_2 [0.5 µM] were added to the cell suspension. The PRP is subsequently centrifuged at 650 x g for 5 min, washed two times with Tyrode´s buffer supplemented with PGI_2 and apyrase and finally resuspended in 200 µL Tyrode´s buffer using calcium chloride [0.2 mM] to guarantee a proper platelet activation.

The platelet count was determined in a 1:10 dilution in PBS using a hematology analyzer (Sysmex KX21N, Sysmex Corporation) and the platelet count was adjusted as required for the applied functional assays.

3.1.5 Mouse plasma preparation

Mice were anesthetized as described above and the blood was collected in a 1.5 mL reaction tube containing 300 µL anticoagulant heparin buffer. After blood collection, the sample was centrifuged at 8,500 x g for 10 min at RT to sediment all cellular blood components. The upper aqueous phase, the blood plasma, was transferred into a clean reaction tubes and either stored on ice for immediate usage or stored at –80 °C for further analysis.

3.1.6 Adhesion experiments

To study cell adhesion on different proteins, adhesion experiments on FasR protein and fibrinogen were performed with isolated human platelets and Chinese hamster ovary cells (CHO cells) as well as integrin $\alpha_{IIb}\beta_3$ transfected into Chinese hamster ovary cells (A5 CHO cells). Glass coverslips (24 x 60 mm) were either coated with FasR protein [50 µg/mL] or fibrinogen [100 µg/mL] at a defined area (10 x 10 mm); incubated in humidity chambers overnight (O/N) at 4 °C and afterwards blocked with 1% BSA for at least 1 h at RT. After blocking with BSA (1%), the coverslips were mounted in humidity chambers. Resting or ADP [10 µM]-stimulated platelets (4 x 10^3/µL) in Tyrode's buffer were pretreated with the inhibitors hDcR3 (human decoy receptor 3) [10 µg/mL], tirofiban [1 µg/mL] and abciximab [10 µg/2 million platelets] for 10 min and then allowed to adhere to the coated coverslips for 60 min at RT. IgG-FC [10 µg/mL] peptide served as control. CHO and A5 CHO cells were allowed to adhere to the coated coverslips for 30 min. Afterwards, cover slips were rinsed two times with PBS to wash off unbound platelets and CHO cells. Adherent platelets or CHO cells where fixated immediately with 4% paraformaldehyde (PFA), covered with the mounting medium Aquatex® and monitored by microscopic DIC images. Five pictures from different areas were taken (platelets: 400x total magnification; CHO cells: 100x total magnification; Axio Observer.D1, Carl Zeiss). The total number of adherent platelets was counted using ImageJ-win64 software.

3.1.7 Aggregometry experiments

Impedance in aggregometry studies was determined upon the change in electrical impedance between two electrodes when an agonist induces platelet aggregation. Impedance measurement of platelets in the absence or presence of RBCs as well as whole blood of human or mice was performed compared to NaCl (0.9% saline) buffer using Chrono-Log dual channel lumi-aggregometer® (model 700) at 37 °C stirring at 1,000 rpm. Human blood was collected into Vacutainer® sodium citrate tubes [105 mM Na_3-citrate] and murine blood in ACD buffer. Suspensions of murine platelets or PRP in the absence or presence of RBCs as well as whole blood of knockout mice were stimulated with collagen [whole blood: 10 µg/mL collagen and platelets in the absence and presence of RBCs: 20 µg/mL collagen] or PAR4 peptide [200 µM] in the presence of fibrinogen [70 µg/mL]. Respective human samples were stimulated with collagen [10 µg/mL] without fibrinogen. Isolated human and murine platelets and RBCs were reconstituted with plasma (human: 4 x 10^6 RBCs/µL and 2 x 10^5 platelets/µL; mouse: 4 x 10^6 RBCs/µL and 3 x 10^5 platelets/µL).

3.1.8 Clot retraction

To determine the clot retraction, wild type (WT), FasL$^{fl/fl}$;PF4-cre and *FasR$^{-/-}$* PRP in the absence or presence of WT RBCs and WT PRP in the absence or presence *FasR$^{-/-}$* RBCs were prepared and treated with thrombin [5 U/mL] in the presence of $CaCl_2$ [20 mmol/L]. The reaction mixtures were left unstirred for a total duration of 5 h at 37 °C, and clot retraction was measured by taking photographic pictures at indicated time points. The remaining supernatant fluid was removed and measured after 5 h.

3.1.9 Thrombus formation assay

Glass coverslips (24 x 60 mm) were coated with collagen [200 µg/mL] (Horm®, Takeda Pharmaceutical), TSP-1 [100 µg/mL] (#605225-25UG) or collagen/TSP-1 incubated O/N at 4 °C. On the next day, the spare collagen was removed and the coverslips were blocked with 1% BSA for at least 1 hour at RT. Whole blood or recomposed blood was perfused through the chamber (50 µm x 5 mm). Human or murine platelets, plasma and RBCs were isolated according to the standard protocols (methods 3.1.1, 3.1.2, 3.1.4 and 3.1.5). The cell counts were adjusted to 2 x 10^5 platelets/µL and 4 x 10^6 RBCs/µL for human samples or 3 x 10^5 platelets/µL and 5 x 10^6 RBCs /µL for mouse samples using plasma. Murine blood components were recomposed as indicated in the individual experiment. Blocking studies in

human whole blood were performed using a TSP-1 [2 µg/mL] (#NB100-2059), a CD36 mAb [2 µg/mL] (#10009893) and pan caspase inhibitor [10 µM] (#551476) for 10 min, following flow chamber experiments. For single blood component blocking experiments, either RBCs or platelets were incubated with a CD36 mAb [2 µg/mL] (#10009893), TSP-1 mAb [2 µg/mL] (#NB100-2059) or respective IgG control [2 µg/mL] (#554121) for 10 min. For PS exposure blocking experiments whole blood of $Cd36^{-/-}$ mice was incubated for 10 min with or without recombinant Annexin V inhibiting protein [5 µg/mL] (#556416). In every experiment, Mepacrine [10 µM] (human system) or DyLight 488-conjugated anti-mouse (GP) Ibβ antibody [2 µg/mL] (murine system) was added and incubated for 10 min. After incubation, the blood was perfused over a collagen-coated surface at a shear rate of 1,700 s^{-1} using a pulse-free electric pump. After a predefined timespan (3 min), the blood perfusion was stopped and the flow chamber was perfused with Tyrode's buffer at a shear rate of 1,000 s^{-1}. Five pictures from different areas were taken (400x total magnification; Axio Observer.D1, Carl Zeiss). The surface coverage was analyzed using the Zen 2012 software (Carl Zeiss). Cells from thrombi were resolved by Accutase® treatment for 15 min (120 µL per coverslip; solution with protease and collagenolytic activity) to detach and solve adherent and aggregated cells and analyzed by flow cytometry. Suspensions of one condition were pooled and centrifuged at 650 g for 7 min. The pellet was resuspended in either 100 µL binding buffer [10 mM HEPES, 140 mM NaCl, 2.5 mM $CaCl_2$, pH 7.4] following PS exposure measurement or 100 µL Tyrode's buffer for analysis of TSP-1 (shown in further detail in 3.1.11) and CD36 (CD36-PE) binding to RBCs and platelets. The cell suspension for Annexin V binding was incubated in the dark for 15 min with an antibody mix containing CD42a-PE (#558819), CD235a-FITC (#B49206) and AnnexinV-Cy5. In mice, isolated platelets were incubated with AnnexinV-Cy5 alone. The cell suspension for TSP-1 binding was incubated with a TSP-1 mAb (#NB100-2059) in the dark for 30 min and subsequently incubated with Alexa Fluor™ 488 goat anti-mouse IgG (#A11001). The cell suspension for CD36 binding was incubated with an antibody mix containing CD235-FITC and CD36-PE (#A15793) in the dark for 15 min. The incubation was stopped by adding 300 µL binding buffer or PBS and the samples were analyzed using a FACSCalibur™ (BD Bioscience). For immunofluorescence staining of thrombi which were generated under flow conditions (1,700 s^{-1}) using WT, FasR and FasL-deficient mice, the unconjugated rat anti-mouse TER-119 antibody [3 µg/mL] against mouse RBCs (#557909) and the unconjugated polyclonal rabbit anti-mouse/human GPIX antibody [10 µg/ml] (#orb167288) against platelets as primary antibodies. Secondary antibodies were used as follows; goat anti-rabbit Alexa Fluor™ 488 [20 µg/mL] and goat anti-rat Alexa Fluor™ 594 [20 µg/mL] (Invitrogen). Samples were analyzed using confocal microcopy (Leica TCS SP8 STED 3x, 63x objective, Wetzlar, Germany).

3.1.10 Red blood cell recruitment assay

Coverslips (24 x 60 mm) were coated with collagen [200 µg/mL] (Horm®, from Takeda Pharmaceutical), incubated O/N at 4 °C. On the next day, the spare collagen was removed and the coverslips were blocked with 1% BSA for at least 1 h at RT. Human platelets, plasma and RBCs were isolated according to the standard protocols (methods 3.1.1 and 3.1.2). ADP [10 µM]-stimulated platelets were spread on collagen for 10 minutes, mounted in the flow chamber system and 4×10^6 RBCs/µL were perfused through the flow chamber at a shear rate of $1,700\ s^{-1}$ using a pulse-free electric pump. Tethering RBCs on collagen-adherent platelets were measured during a 3 min video. Cells (collagen-adherent platelets or isolated RBCs) were treated with several Inhibitors. The FasL inhibitor (hDcR3) was added to platelets and was used at final concentration of 10 µg/mL. IgG-Fc [10 µg/mL] served as control. A FasR mAb from GenTex (GTX13549) was used at a final concentration of 10 µg/mL. RBCs were preincubated with FasR antibody for 15 min. IgG$_1$ antibody (#554121) served as control. Platelets were incubated with a TSP-1 mAb (#NB100-2059) at a concentration of 2 µg/mL for 10 min. Independent incubation of platelets and RBCs with a CD36 mAb (#10009893) at a concentration of 2 µg/mL for 10 min were performed. Respective IgG was used. Platelets were incubated with abciximab at a concentration 10 µg/2 million cells for 10 min. All inhibitory experiments were performed at RT.

3.1.11 Flow cytometry

The fluorescence-activated cell scanning (FACS) is based on discriminating cells regarding their size (forward scatter, FSC) and their granularity (side or sideward scatter, SSC). Cells in suspension are passed through a flow cell and irradiated with a laser. Depending on the size and granularity of the cells, a cell-specific scattered light is generated. Using this scattered light, a dot plot is calculated displaying the FSC and the SSC for each single cell passed through the flow cell. Besides the FSC and SSC profile of each cell, fluorescence labeled dyes or antibodies can be used to further distinguish between different cell types and subpopulations. Flow cytometry analysis of platelets and RBCs were performed and cells were gated towards their SSC and FSC profile. Isolated cells or PRP were adjusted to a final concentration of 1×10^5 platelets/µL and/or 1×10^5 RBCs/µL (mouse and human) for flow cytometric analysis. Human whole blood (fresh citrate-anticoagulated blood) was diluted 1:10 in Tyrode's buffer. In mice, heparinized blood was diluted with 500 µL of Tyrode's buffer and centrifuged at 250 x g for 5 min. The supernatant was discarded and the pellet resuspended in 800 µL Tyrode's buffer. After centrifugation at 250 x g for 5 min, the supernatant is discarded again and the pellet is resuspended in 500 µL Ca^{2+} Tyrode's buffer. Respective

samples were mixed with antibodies after addition of 2 mM $CaCl_2$. Human and murine samples were stimulated with indicated agonists for 15 min at RT and all antibodies used in this study were diluted 1:10 in a total reaction volume of 50 µL and incubated for 15 minutes in the dark at RT. Staining was stopped by addition of 300 µL PBS and subsequently analyzed on a FACSCalibur™ (BD Bioscience). Activation of human platelets was determined using the fluorophore-labeled antibodies for P-selectin expression (P-selectin-FITC) and the active form of integrin $\alpha_{IIb}\beta_3$ (PAC-1-PE) as well as inactive form of integrin $\alpha_{IIb}\beta_3$ (CD61-PE; β3 integrin subunit, #555754, BD Bioscience). In mice, the inactive form of integrin $\alpha_{IIb}\beta_3$ was stained with CD61-FITC (#M031-1, Emfret Analytics). For AnnexinV-Cy5 staining, binding buffer [10 mM HEPES, 140 mM NaCl, 2.5 mM $CaCl_2$, pH 7.4] was used instead of PBS and only 4 µL AnnexinV-Cy5 were necessary. CD42-PE served as platelet specific marker, while CD235a-FITC was used as specific cell marker for human RBC. For TSP-1 binding to human or murine platelets and RBCs, a TSP-1 mAb was preincubated with the respective samples for 30 min in the dark at RT and subsequently incubated with Alexa Fluor™ 488 goat anti-mouse IgG (# A11001) for further 30 min. Externalization of FasL (FasL-PE), PS exposure, CD36 (CD36-PE) and FasR (FasR-PE) on activated and nonstimulated platelets was determined by flow cytometry. If a cell specific inhibition was necessary, cells were pretreated with abciximab [10 µg/2 million cells], tirofiban [1 µg/mL], anti-FasR mAb [10 µg/ml], hDcR3 [10 µg/mL], anti-TSP-1 mAb [2 µg/mL], pan caspase inhibitor [10 µM], anti-CD36 mAb [2 µg/mL] or recombinant Annexin V inhibiting protein [5 µg/mL] for 15 minutes at RT. Subsequently, platelets were activated with indicated agonist following coincubation with RBCs for 10 min.

3.2 Protein biochemical methods

3.2.1 SDS-PAGE

Sodium dodecyl sulfate polyacrylamide gel electrophoresis (SDS-PAGE) is an analytical method for the separation of proteins based on their molecular weight and charge in an electrical field. By using SDS, which binds to the hydrophobic areas of a protein, the proteins are denatured, and negative charges are introduced into the denatured polypeptide chains. As a result, the proteins migrate towards the anode in an electrical field. Additionally, β-mercaptoethanol is used to cleave disulfide bridges in order to obtain a primary, linear protein structure. First, a separating gel was poured, which was overlaid with the stacking gel after polymerization. The stacking gel [4% acrylamide (AA)] is used to concentrate the samples. The separating gel (10% AA) forms a small-pored structure which exhibits a sieving

effect to separate the net negatively charged proteins according to their molecular weight in an electrical field. The Precision Plus Protein™ Dual Color Standards (#1610374EDU) marker was used to estimate the size of the proteins of interest. The electrophoresis was typically carried out for 180 – 210 minutes in 1x Laemmli running buffer at 25 mA per gel. The gel was then directly used for a Western blot in order to transfer the size-separated proteins onto suitable membranes.

3.2.2 Western Blot

The proteins separated by gel electrophoresis were transferred onto a nitrocellulose membrane using the semi-dry Western blot method. For this purpose, buffer systems with varying ions and methanol concentrations were used to equilibrate filter paper (Whatman), the nitrocellulose membrane and the gel in a specific arrangement. The bubble-free construction of the blotting chamber was assembled according to the following scheme: cathode, six filter papers moistened with buffer C, activated nitrocellulose membrane soaked in buffer B, polyacrylamide gel, six filter papers immersed in buffer A, anode plates. The transfer was conducted for 1 h at 0.75 mA/cm^2 gel. After blotting, the membrane was first stained with a 0.1% Ponceau S solution to verify a successful protein transfer and the several times washed in TBS-T (TBS buffer supplemented with 0.1% Tween 20) to decolorize the membrane. Subsequently, the membrane was blocked with 5% BSA or 5% (w/v) powdered skim milk in TBS-T for 60 min and probed with a TSP-1 mAb (#NB100-2059, 1:1000) and a CD36 mAb (#PA1-16813, 1:1000). The antibody incubations were performed at 4 °C O/N. On the next day, the membrane was washed three times with TBS-T, and incubated with the corresponding horseradish peroxidase (HRP)-conjugated secondary anti-rabbit and anti-mouse IgG antibodies in 5% powdered skim milk in TBS-T (1:2500, #NA931 and #NA934) for 1 h at RT. For visualizing protein bands, the membrane was washed three times with TBS-T and incubated for 1 – 2 min with Immobilon™ Western Chemiluminescent HRP substrate solution resulting in a chemiluminescence signal that was recorded with a Vilber Fusion-FX6-EDGE V.070 imaging system. GAPDH served as housekeeping protein. The membranes were washed and incubated for 30 – 60 min with the primary antibody (GAPDH 14C10, #2118, 1:2000). The remaining, unbound antibody was washed away and the membranes were incubated for 1 h with the respective secondary antibody (1:1500). Proteins were detected as described above. Proteins were quantified based on a densitometric analysis of the chemiluminescent signals using Evolution-Capt EDGE software (Version 18, 02). Relative protein amounts were normalized to GAPDH.

3.3 Immunohistological methods

For the analysis of platelets, RBCs and TSP-1 in samples of aortic walls and ILT of AAA patients as well as occluding thrombi of patients undergoing thrombectomy (peripheral thrombi), 5 micron sections of paraffin-embedded tissue were prepared. For the preparation of tissue slides, 5 µm sections were cut from the tissue paraffin block at a microtome, transferred in a 37 °C preheated water bath and pulled up on microscope slides. Before using the sections, they were additionally heat-fixed on the slides at 37 °C O/N. Prior staining tissue sections, they were deparaffinized in a descending ethanol concentration (table 13), washed in PBS and used for following staining. For the embedding of the ILT and the aortic wall the ascending ethanol series was performed.

Table 13: Steps to exchange hydrophilic and hydrophobic state of the paraffin-embedded tissue before and after histological procedure

Ascending ethanol series		Descending ethanol series	
time (min)	reagent	Time (min)	reagent
10	Roti Histol	2	70% EtOH
2	100% EtOH	2	80% EtOH
2	96% EtOH	2	90% EtOH
2	80% EtOH	2	100% EtOH
2	70% EtOH	10	Roti Histol

3.3.1 Immunofluorescence staining

For visualization of platelets, RBCs and TSP-1 located in the ILT and the aortic wall of AAA as well as thrombi form patients who underwent thrombectomy, a fluorescence staining for the platelet specific GPIX and RBC specific glycophorin A was performed. For this purpose, after deparaffinization the tissue sections were transferred into citrate buffer (pH 6.0) and boiled in the microwave with 300 W for 15 min. This step is required for a proper demasking of antigens that could be blocked due to the fixation in paraffin. The boiled sections were allowed to cool down to RT for approximately 30 min in the citrate buffer and washed in PBS. The following steps were all performed in a humidity chamber to prevent dehydration of the tissue sections. The slides were positioned in the chamber and the tissue was circled with a grease pencil. Then, the tissue slides were blocked for 1 h at RT with blocking solution (5% BSA in PBS) washed with PBS and incubated with the primary antibody at 4 °C O/N

using a GPIX mAb (#orb167288, 1:100), for RBC staining a CD235 mAb (#NBP2-45024, 1:200) and for TSP-1 staining a TSP-1 mAb (#NB100-2059, 1:100) were used. On the next day, unbound primary antibody was removed by washing with PBS. The tissue was incubated with fluorescence-labeled secondary antibody for 1.5 h at RT. As control staining, either specific IgG primary antibodies or no antibody (only PBS) were applied on the tissue sections. For counterstaining of cell nuclei, the sections were stained with the auto-fluorescent dye DAPI for 5 min at RT. After rinsing the slides with PBS, the tissue sections were mounted with mounting medium and let dry at 4 °C in the dark.

3.4 Molecular biological methods

3.4.1 Animal genotyping

In the present work, the genotyping of the FasL$^{fl/fl}$;PF4-cre mice was carried out following the protocol of the "AccuStart™ II - Mouse - Genotyping Hot Start Kit" obtained from Quantabio. *Cd36$^{-/-}$* were genotyped by the staff of Hadi Al-Hasani (German Diabetes Center). All mice were identified by ear punches resulting in biopsies used for genotyping. For the DNA extraction, the ear punches were lysed by heating to 95 °C in a buffer/enzyme mixture for 30 min.

Table 14: Composition of the PCR reaction mixture using the AccuStart™ II - Mouse - Genotyping Hot Start Kit

Mastermix – genotyping	Volume
KAPA Mix	6.25 µL
Primer forward	0.625 µL
Primer reverse	0.625 µL
dH$_2$0	4.5 µL
DNA	1.5 µL

For the following PCR, all required reagents, and their corresponding volumes for are listed in table 14.

Table 15: Reaction steps of the PCR for murine genotyping

	Temperature (°C)	Time (s)	Cycles
Initial denaturation	95	180	1
Denaturation	95	15	
Annealing	56	30	35
Elongation	72	30	
Final elongation	72	240	1

After PCR protocol samples were stored at 4°C. The PCR products were subjected to agarose gel electrophoresis on a 2% agarose gel supplemented with Midori Green (Biozym)/ Tris acetate EDTA (TAE) buffer and recorded with the Vilber Fusion-FX6-EDGE V.070 system.

3.5 Statistical analysis

The number of analyzed individuals is indicates as *n*. All diagrams depict the mean value (MW) for the parameter of the ordinate (Y axis) with the standard error of mean (SEM). Statistical analysis regarding a systemic difference in two or more matrices within different groups was calculated using the software GraphPad Prism 7.02. Throughout this work, ANOVA or student´s t-test were applied as appropriate and as stated in the respective figure legends. Significant differences were indicated with an asterisk in all diagrams and divided into the following categories: $p \leq 0.05 = *$, $p \leq 0.01 = **$, $p \leq 0.001 = ***$.

4. Results

4.1 Platelet-RBC interaction via FasL/FasR mediates PS exposure and causes thrombus formation and aggregation

RBCs influence hemostasis by altering rheology as well as by the release of mediators such as ADP, ATP and NO [180, 181]. Recently, a direct interaction of platelets and RBCs via FasL/FasR was found to be important for the externalization of PS at the RBC membrane that attributes a direct role for RBCs in thrombin generation, thrombus formation, and stability upon hemostasis and thrombosis [63]. To study FasL/FasR interaction of platelets and RBCs in further detail, aggregation experiments, analysis of procoagulant surface and thrombus formation *ex vivo* were performed using FasR knockout (*FasR*$^{-/-}$), and FasL knockout (*FasL*$^{-/-}$) mice as well as mice with FasL deficiency restricted to megakaryocytes and platelets (FasL$^{fl/fl}$;PF4-cre$^+$). In all experiments platelets from either wild type (WT) or *FasL*$^{-/-}$ mice were incubated with WT RBCs, and WT platelets with *FasR*$^{-/-}$ RBCs were used. Furthermore, intracellular caspase signaling of platelets and RBCs was investigated by flow cytometric analysis and flow chamber experiments using blood from healthy human volunteers.

4.1.1 Genetic deletion of FasR and FasL reduces thrombus formation under arterial shear rates

Thrombus formation at sites of vascular damage requires stable shear-resistant platelet adhesion to the extracellular matrix and platelet activation by locally released secondary mediators [21]. Three-dimensional thrombus formation on a collagen matrix was significantly reduced when fluorescently labeled *FasL*$^{-/-}$ platelets and WT RBCs or WT platelets and *FasR*$^{-/-}$ RBCs were perfused through the chamber at a shear rate of 1,700 s^{-1}. Surface coverages were significantly reduced when coincubating *FasR*$^{-/-}$ RBCs with WT platelets ($p < 0.001$) and *FasL*$^{-/-}$ platelets with WT RBCs ($p < 0.001$) compared to WT platelets with RBCs (Fig. 9A, B). In addition, thrombus formation with whole blood from FasL$^{fl/fl}$;PF4-cre$^+$ mice was significantly decreased, resulting in a marked reduction of surface coverage compared to whole blood of FasL$^{fl/fl}$;PF4-cre$^-$ mice ($p < 0.001$) (Fig. 9C, D). These results demonstrate that FasL/FasR interaction of RBCs and platelets is crucial for thrombus formation under arterial shear rates *ex vivo*.
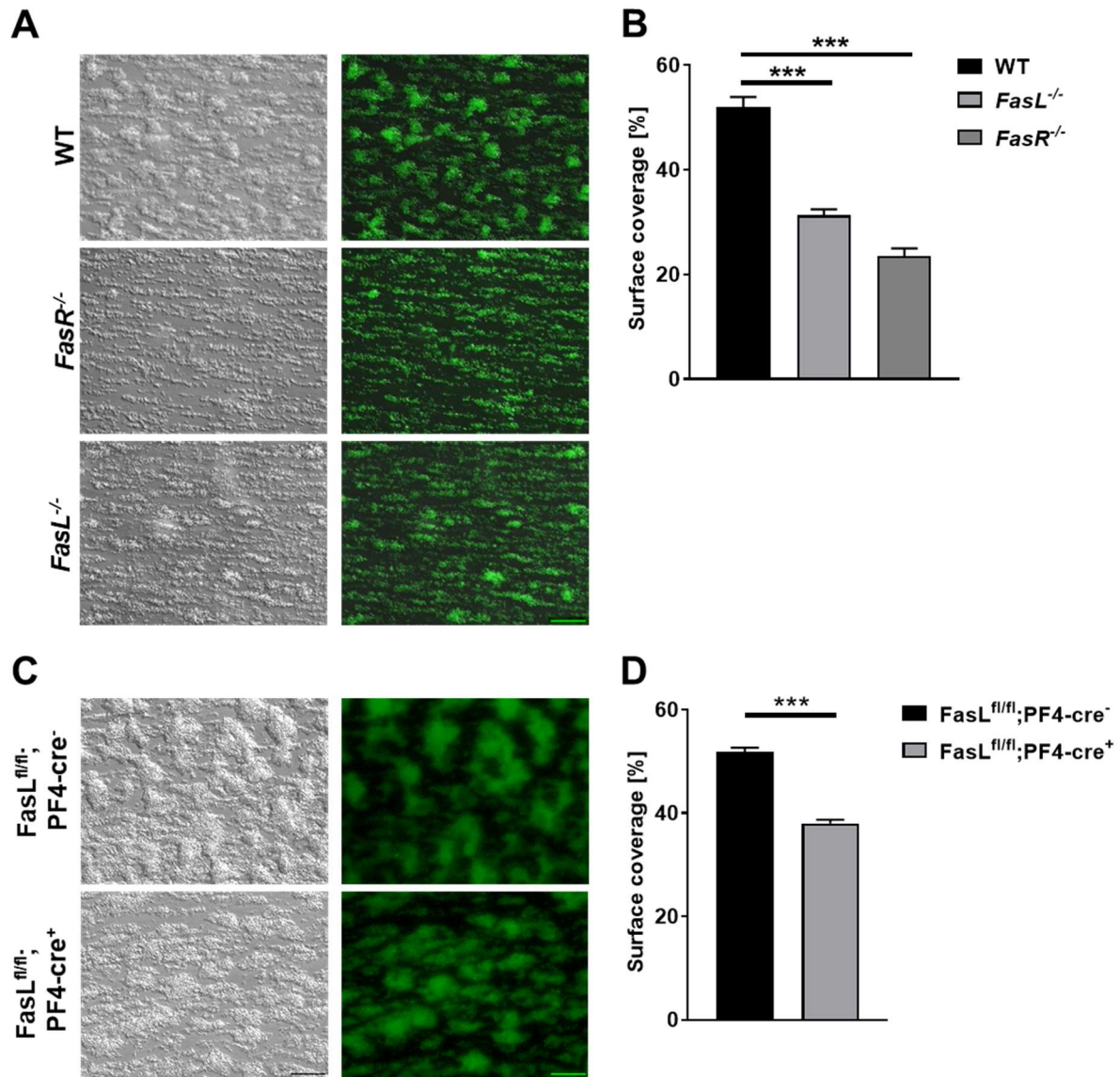
Figure 9: Genetic deletion of FasR or FasL and platelet specific FasL knockout leads to reduced thrombus formation _ex vivo_. (A, C) Thrombus formation and (B, D) surface coverage of fluorescently labeled platelets on collagen [200 µg/mL] was assessed in flow chamber experiments at a shear rate of 1,700 s^{-1}. (A, B) Platelets from either WT or _FasL$^{-/-}$_ mice were incubated with WT RBCs, and WT platelets with _FasR$^{-/-}$_ RBCs were used (n = 4 – 6). (C, D) Whole blood from FasL$^{fl/fl}$;PF4-cre mice was used (n = 5). (A, C) Representative Differential Interference Contrast (DIC) and fluorescent images of thrombus formation are shown. Scale bar: 50 µm. Results represent mean values ± SEM. ***p < 0.001 tested by ordinary One-Way ANOVA with Sidak's multiple comparison post-hoc test. (B) and unpaired student's t-test (D). WT = wild type. (A) Already published in JCI [63].

In addition, the number of RBCs in thrombi after three-dimensional thrombus formation on a collagen matrix were investigated using the RBC specific marker TER-119 (red) and the platelet specific marker GPIX (green) (Fig. 10B). The number of RBCs in thrombi was significantly decreased after the perfusion of whole blood from _FasL$^{-/-}$_ (_p = 0.0063_) and _FasR $^{-/-}$_ mice (_p = 0.0165_) through the chamber compared to WT (Fig. 10C).
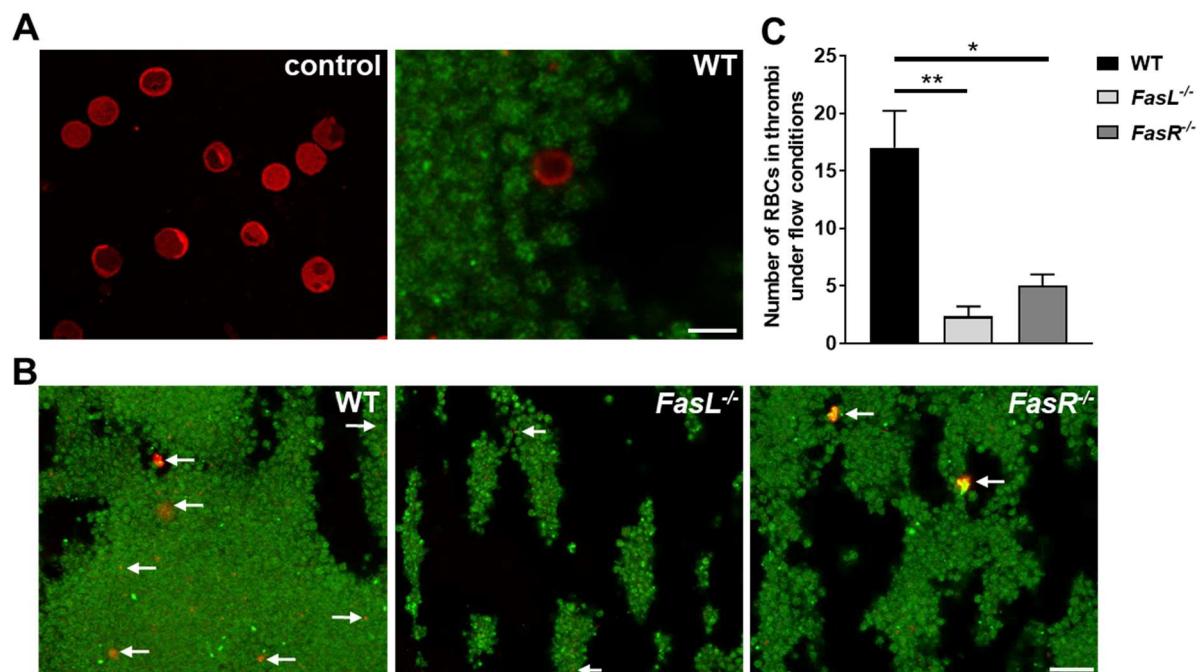
Figure 10: Genetic deletion of FasR and FasL leads to reduced incorporation of RBCs into the thrombus under dynamic conditions. (A) Staining of isolated RBCs (TER-119 antibody, red; left panel) and of RBCs and platelets in thrombi (RBCs: TER-119 antibody, red; platelets: GPIX antibody, green; right panel). Scale bars: 10 µm. (B) Representative fluorescent images of RBCs in thrombi after flow chamber experiments on a collagen matrix [200 µg/mL, 1,700 s^{-1}] with whole blood from WT, FasR$^{-/-}$, or FasL$^{-/-}$ mice. Arrows indicate RBCs. Scale bars: 20 µm. (C) Quantification of the number of RBCs in thrombi after flow chamber experiments (n = 3). Results represent mean values $\pm$ SEM. *p < 0.05; **p < 0.01 tested by ordinary One-Way ANOVA with Sidak's multiple comparison post-hoc test. WT = wild type; RBCs = red blood cells. (A - C) Already published in JCI [63].

4.1.2 Genetic deletion of FasR and FasL reduces PS exposure under static and dynamic conditions *in vitro*

Activated platelets and RBCs expose negatively charged PS, thereby providing high affinity binding sites for specific coagulation factors that promote thrombin generation [182]. In the presence of WT RBCs, resting (*p < 0.05*) and ADP [10 µM]-stimulated platelets (*p < 0.01*) from FasL$^{-/-}$mice displayed notably decreased PS exposure compared to WT platelets and RBCs, as determined by flow cytometric analysis of Annexin V binding (Fig. 11A). In the absence of RBCs, reduced PS exposure of FasL$^{-/-}$ platelets was already detected in the resting state (*p < 0.05*). In the presence of FasR$^{-/-}$ RBCs, PS exposure of WT platelets was decreased after stimulation with ADP (Fig. 11A). In addition, Annexin V binding to WT RBCs incubated with ADP-stimulated FasL$^{-/-}$ platelets as well as PS exposure of FasR$^{-/-}$ RBCs incubated with ADP-stimulated WT platelets was significantly reduced (Fig. 11B). Similarly, Annexin V binding to platelets (Fig. 11C) and RBCs (Fig. 11D) that were isolated from thrombi after flow chamber experiments was significantly reduced when either FasR$^{-/-}$RBCs and WT platelets or FasL$^{-/-}$ platelets and WT RBCs were perfused through the chamber using

a shear rate of 1,700 s^{-1}. These results provide strong evidence for FasL/FasR-mediated PS exposure on platelets and RBCs under static and dynamic conditions, supporting recent results obtained from inhibitory experiments with human blood cells [63].
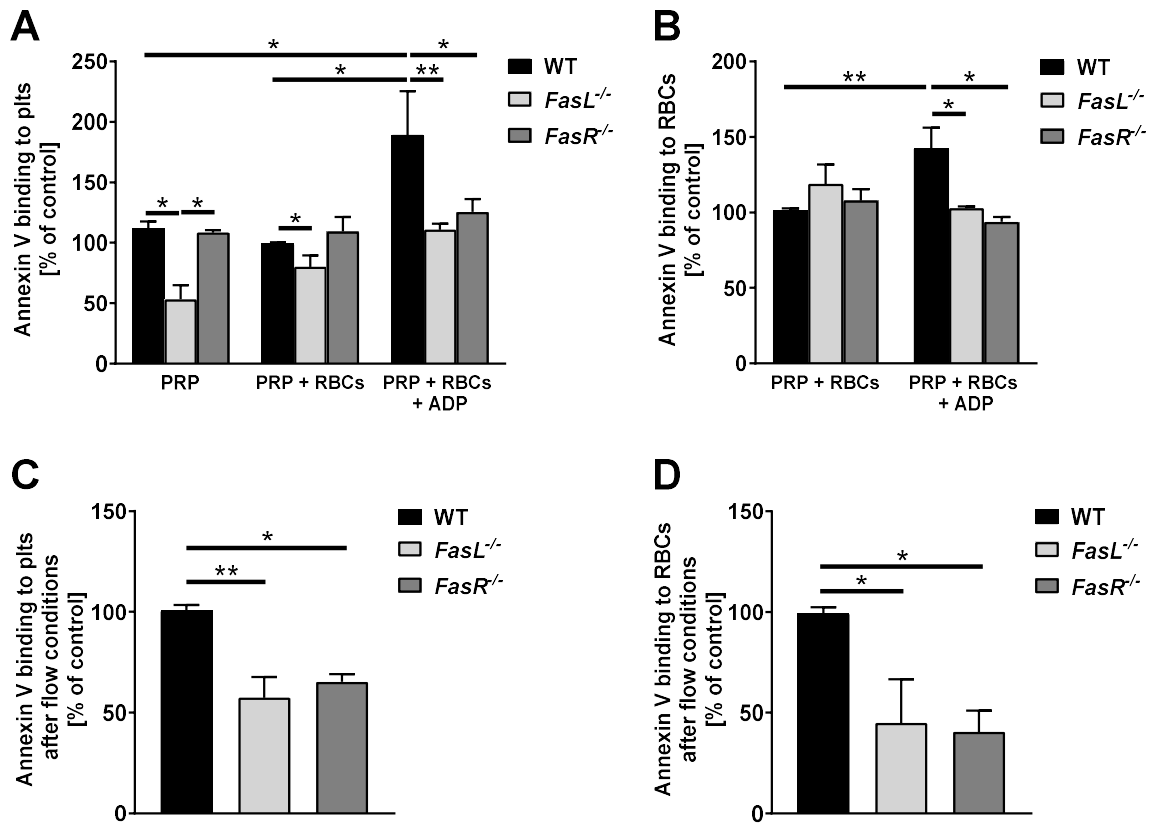
Figure 11: Genetic deletion of FasR and FasL reduces PS exposure *in vitro*. (A – D) Murine platelets were analyzed by flow cytometric analysis regarding their specific side scatter (SSC) and forward scatter (FSC) profile. (A, B) Effects of *FasL$^{-/-}$* platelets and *FasR$^{-/-}$* RBCs on PS exposure of platelets (A) and RBCs (B) *in vitro* (n = 4). PRP from either WT or *FasL$^{-/-}$* mice was incubated with WT RBCs. Additionally, WT PRP was incubated with *FasR$^{-/-}$* RBCs. (C, D) Annexin V binding to platelets (C) and RBCs (D) isolated from thrombi (dissolved with Accutase$^{®}$) after flow chamber experiments (n = 4). Platelets from either WT or *FasL$^{-/-}$* mice were incubated with WT RBCs, and WT platelets with *FasR$^{-/-}$* RBCs were used. Thrombus formation was analyzed on a collagen matrix [200 µg/mL] using a shear rate of 1,700 s^{-1}. Results represent mean values $\pm$ SEM. *p < 0.05; **p < 0.01 tested by Two-Way ANOVA (A, B) and by ordinary One-Way ANOVA (C, D) with Sidak's multiple comparison post-hoc test. WT = wild type; plts = platelets; PRP = platelet rich plasma; RBCs = red blood cells. (A - D) Already published in JCI [63].

4.1.3 Genetic deletion of FasR and platelet specific FasL knockout reduces platelet aggregation

To elucidate weather RBCs are necessary for platelet aggregation, aggregometry analysis of either human or murine whole blood and platelets in the absence or presence of RBCs were investigated (Fig. 12A, B).
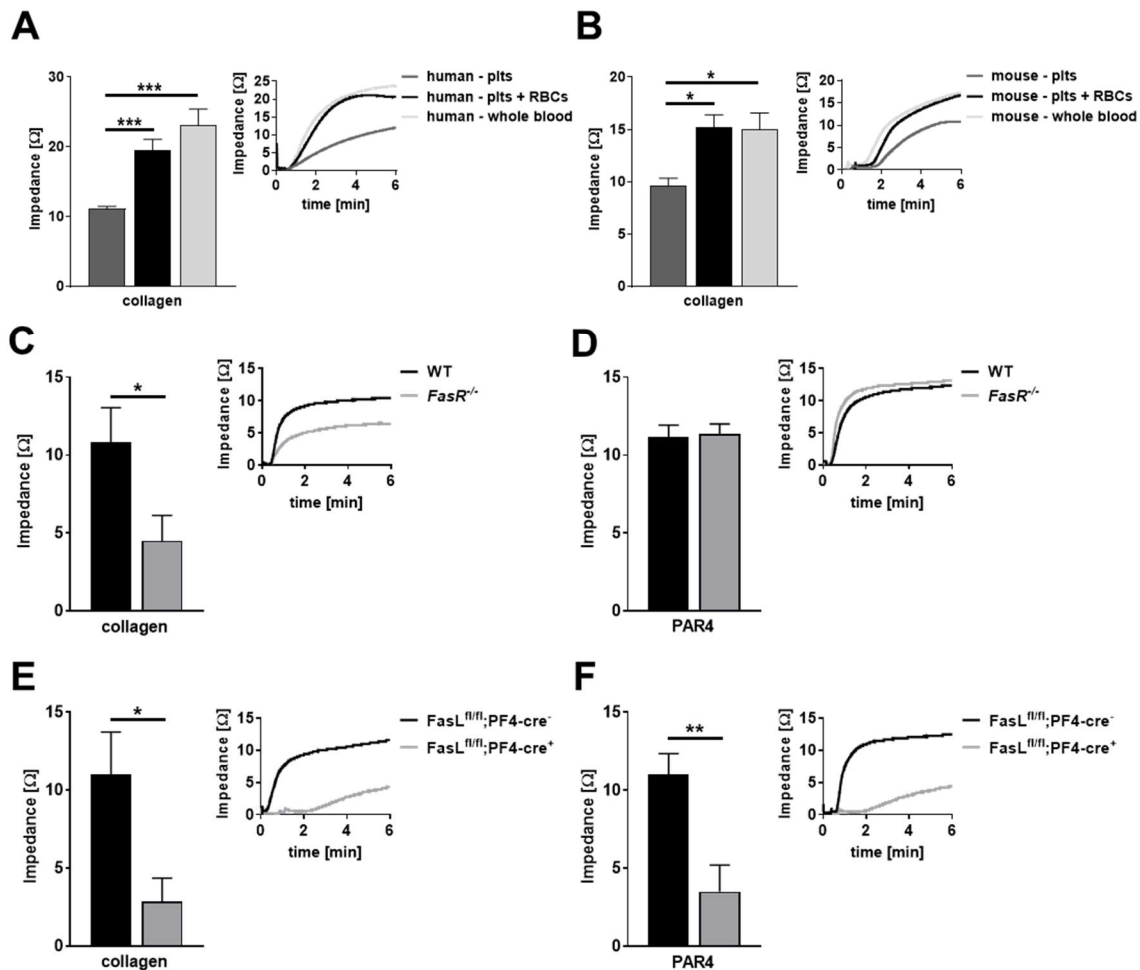
Figure 12: RBCs support platelet clotting and genetic deletion of FasR or platelet specific knockout of FasL alters platelet aggregation. (A, B) Impedance measurements were performed to analyze platelet aggregation using human and murine platelets in the absence or presence of RBCs and whole blood that was stimulated with collagen [human: 10 µg/mL collagen, n = 6; mouse: 10 µg/mL collagen (whole blood) and 20 µg/mL collagen (platelets in the absence or presence of RBCs), n = 4]. (A) Isolated human platelets and RBCs were recomposed to a concentration of 4×10^6 RBCs/µL and 2×10^5 platelets/µL. (B) Isolated murine platelets and RBCs were recomposed to a concentration of 4×10^6 RBCs/µL and 3×10^5 platelets/µL. (C – F) Impedance measurements were performed to analyze platelet aggregation using whole blood from $FasR^{-/-}$ and FasL$^{fl/fl}$;PF4-cre mice that was stimulated with collagen [10 µg/mL] (C, E) and PAR4 peptide [200 µM] (D, F). Representative aggregation curves are shown (n = 6). Results represent mean values $\pm$ SEM. *p < 0.05; **p < 0.01; ***p < 0.001 tested by ordinary One-Way ANOVA with Sidak's multiple comparison post-hoc test (A, B) and unpaired student's t-test (C – F). WT = wild type; plts = platelets; RBCs = red blood cells; PAR4 = protease-activated receptor 4 (PAR4) activating peptide.

While PRP in the presence of RBCs showed aggregation comparable to whole blood, samples of PRP without RBCs revealed decreased aggregation in humans and mice (Fig. 12A, B). To elucidate the impact of FasR and FasL on platelet aggregation and clotting, aggregometry with whole blood and clot retraction experiments were performed. In aggregometry, whole blood of indicated knockout and WT mice was used, whereas in clot retraction experiments, platelet rich plasma (PRP) in the absence and presence of RBCs were analyzed. Aggregometry with whole blood of $FasR^{-/-}$ mice revealed a severe reduction of collagen-mediated platelet aggregation over time (*p = 0.0452*) (Fig. 12C), whereas protease-activated receptor 4 (PAR4) peptide stimulation [200 µM] displayed normal aggregation compared to WT controls (Fig. 12D). In contrast, aggregation responses of whole blood from FasL-deficient mice was impaired for both, collagen (*p = 0.0262*) and PAR4-mediated (*p = 0.0063*) platelet aggregation compared to whole blood of WT mice (Fig. 12E, F).

Besides the aggregation studies, clot retraction experiments with thrombin-stimulated PRP in the absence or presence of RBCs from indicated mice strains were performed. During the clot retraction experiments (over a 300 min time period) images were taken (Fig. 13A). After clot retraction, the remaining fluid of the sample was determined. Samples with PRP alone showed a significant higher volume of the remaining fluid (contraction-dependent) after clot retraction compared to samples with PRP in the presence of RBCs, indicating a higher contractility of platelets alone (Fig. 13D). In the presence of RBCs, a markedly reduced volume of remaining fluid was detected in FasL-deficient PRP coincubated with WT RBCs compared to PRP from FasL$^{fl/fl}$;PF4-cre^{-} mice in the presence of WT RBCs (*p < 0.001*) (Fig. 13D). In addition, clot retraction experiments with FasL-deficient PRP in the presence of WT RBCs revealed significantly decreased contractility compared to WT RBCs and platelets (*p < 0.001*) (Fig. 13D). Furthermore, the remaining fluid after clot retraction experiments in samples of FasL-deficient PRP in the presence of WT RBCs was significantly reduced compared to $FasR^{-/-}$ RBCs coincubated with WT platelets (*p = 0.0195*) (Fig. 13D). After clot retraction, the morphology of clots derived from PRP and RBCs (Fig. 13C, right image) were three-dimensional and cylindrical compared to the clots that only contain PRP (Fig. 13C, left image), which were flat and had a gel-like consistency.
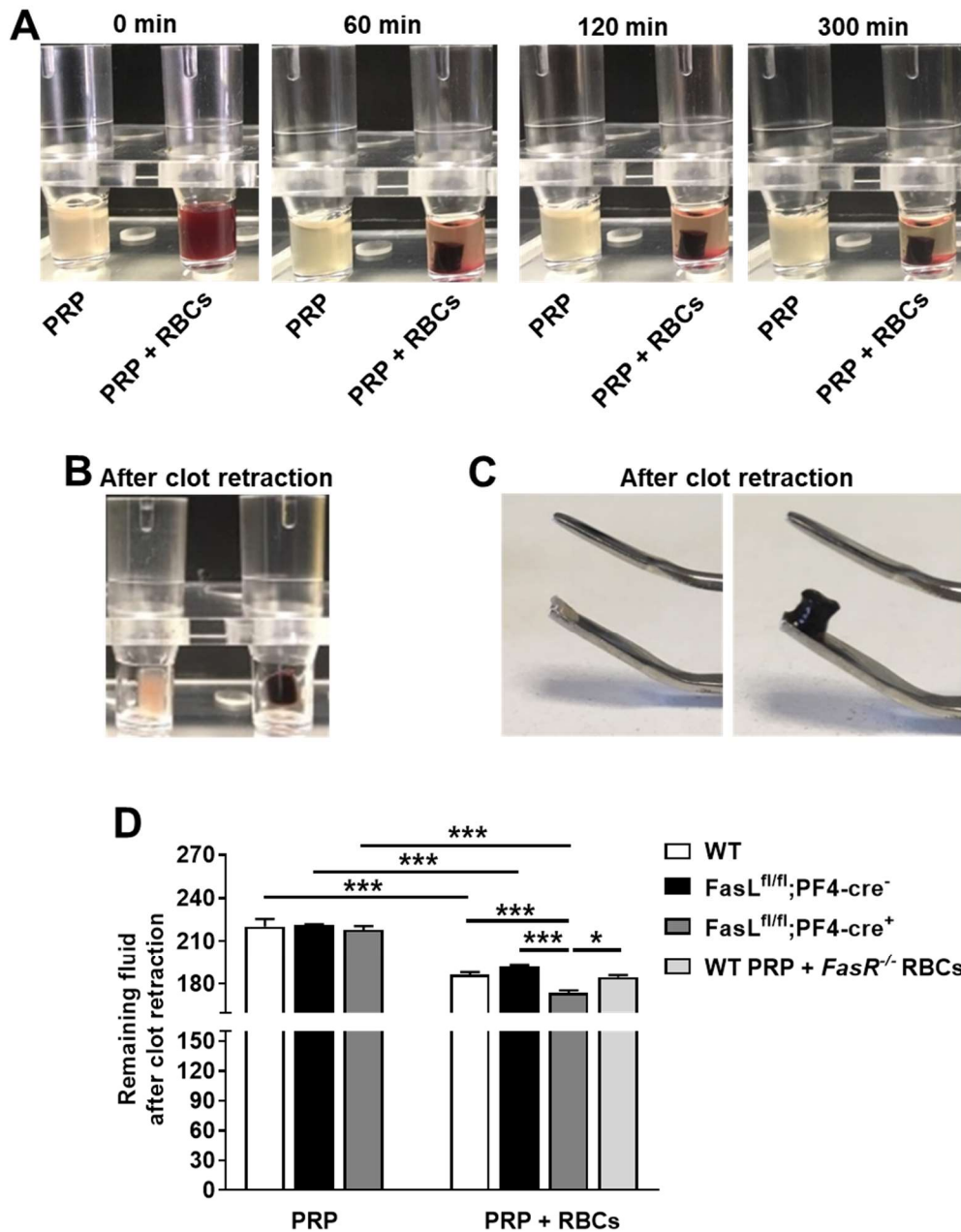
Figure 13: Platelet specific deletion of FasL alters clot retraction of platelets. (A) Representative images of clot retraction with PRP in the absence and presence of RBCs at the beginning (0 min), intermediately (60 min and 120 min) and in the end (300 min) of the experiment. (B) Representative images of clot retraction after the removal of remaining fluid. (C) Morphology of clots derived from PRP in the absence (left image) and presence (right image) of RBCs. (D) Clot retraction experiments with thrombin-stimulated PRP (5×10^5 platelets/µL) isolated from indicated mouse lines in the absence or presence of RBCs (2×10^6 RBCs/µL; WT and $FasR^{-/-}$). Results represent mean values $\pm$ SEM. *p < 0.05; ***p < 0.001 tested by Two-Way ANOVA with Sidak's multiple comparison post-hoc test (A). WT = wild type; PRP = platelet rich plasma; RBCs = red blood cells.

4.1.4 Impact of caspase signaling on PS exposure of RBCs and thrombus formation

FasL binding to FasR has been shown to reflect a general mechanism to induce apoptosis in target cells [183, 184]. Furthermore, RBCs are known to have caspase-3 and caspase-8 which may be involved in the exposure of PS at the surface of RBCs [185, 186]. Therefore, flow chamber experiments and flow cytometric analysis of PS exposure of human platelets and RBCs were performed.
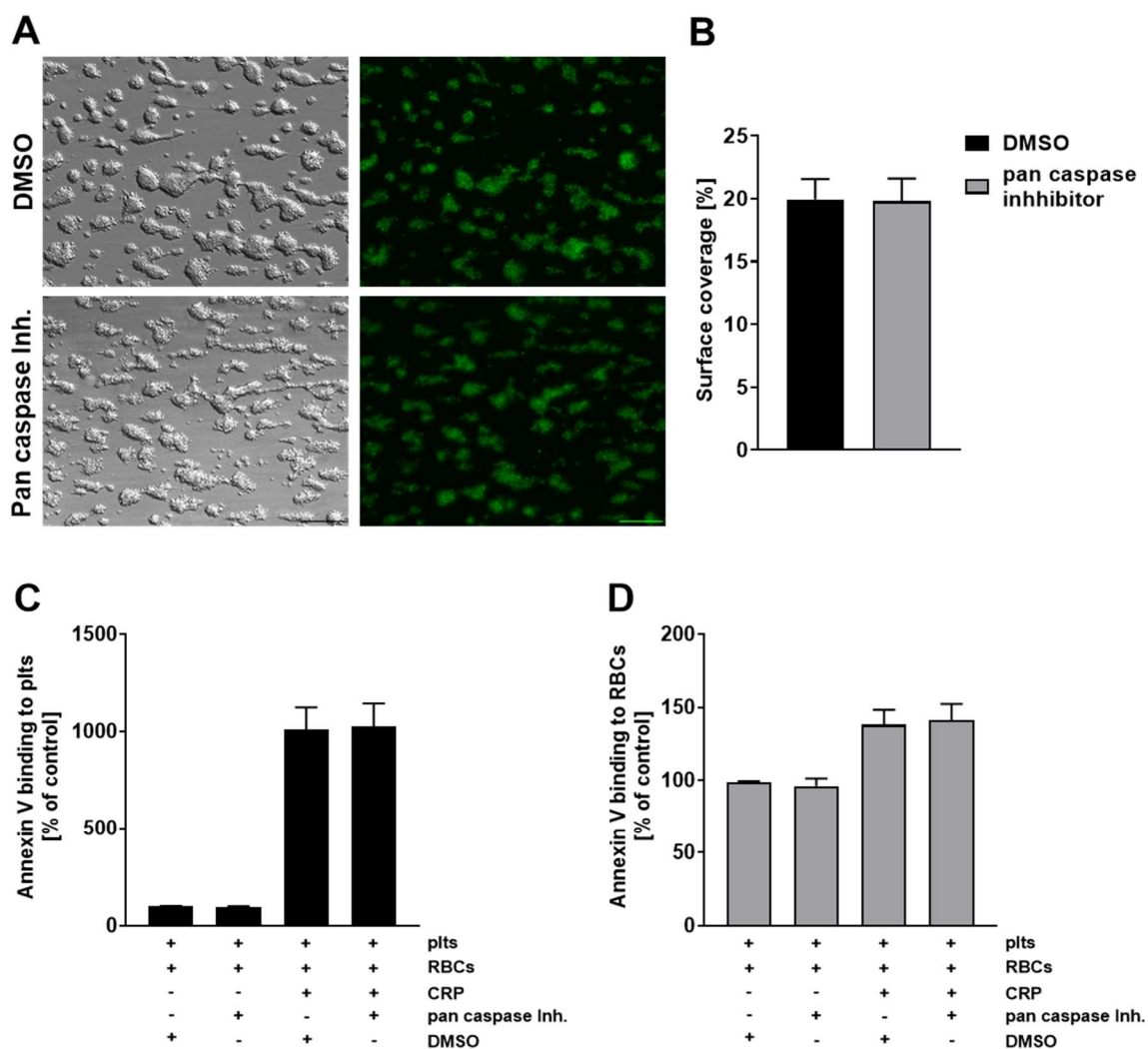
Figure 14: Caspase inhibition leads to unaltered thrombus formation and PS exposure of RBCs and platelets *ex vivo*. (A) Representative images of thrombus formation on collagen [200 µg/mL] at a shear rate of 1,700 s^{-1} and (B) determination of surface coverage of thrombi in the absence and presence of a pan caspase inhibitor using human whole blood (n = 6). Platelets were fluorescently labeled. (A) Representative DIC and fluorescent images are shown. Scale bar: 50 µm. (C, D) Annexin V binding to platelets (C) and RBCs (D) in the absence and presence of a pan caspase inhibitor was determined by flow cytometric analysis with the cell specific marker CD235-FITC (RBCs) and CD42-PE (platelets) (n = 6). DMSO served as control. Results represent mean values ± SEM. Plts = platelets; RBCs = red blood cells; CRP = collagen related peptide; pan caspase inh. = inhibitor of caspase-1,-3,-8 and -9; DMSO = dimethyl sulfoxide.

Thrombus formation on a collagen matrix [200 µg/mL] at arterial shear rates of 1,700 s^{-1} and Annexin V binding to platelets and RBCs under static conditions were unaltered after caspase inhibition compared to control experiments with dimethyl sulfoxide (DMSO) (Fig. 14A – D). These results suggest that thrombus formation and PS exposure are independent of caspase signaling of platelets and RBCs.

4.2 Integrin α$_{IIb}$β$_3$ serves as another ligand on the platelet membrane important for FasR activation on RBCs

The direct interaction of platelets and RBCs via FasL/FasR is crucial for PS exposure on the surface of RBCs. This leads to local thrombin generation which is essential for platelet adhesion, thrombus formation and aggregation as described before. However, FasR inhibitory studies provided first evidence that FasR-mediated effects in PS exposure and thrombus formation exceed the effects of FasL [63]. This led to the hypothesis that platelet-RBC interaction is also triggered by other signaling pathways and suggests the existence of another ligand on the platelet surface that is able to activate the FasR on RBCs. Accordingly, further experiments were performed. In a first approach, platelet activation in the absence or presence of RBCs was analyzed. Secondly, adhesion studies of platelets on immobilized FasR protein and the inhibition of FasL and integrin α$_{IIb}$β$_3$ (fibrinogen receptor) were established. In addition, adhesion of CHO cells and A5 CHO cells to immobilized fibrinogen and FasR protein were performed. In a third approach, flow cytometric analysis of PS exposure on human platelets and RBCs after inhibition of FasL and integrin α$_{IIb}$β$_3$ was determined. To support the results of human platelets, PS exposure on murine platelets and RBCs isolated from FasL-deficient and *FasR$^{-/-}$* mice were analyzed in the absence and presence of an integrin α$_{IIb}$β$_3$ inhibitor.

4.2.1 Upregulation of β$_3$ integrin on the platelet surface after coincubation with RBCs

To identify the effects of RBCs on platelet activation, flow cytometric analysis of platelets in the absence or presence of RBCs was performed. In detail, activation of platelet integrin α$_{IIb}$β$_3$, the upregulation of the β$_3$ integrin subunit at the platelet surface and the exposure of P-selectin as marker for platelet degranulation in response to different agonists were analyzed. As shown in figure 15A, externalization of β$_3$ integrin subunit was significantly increased in the presence of RBCs under resting conditions (*p = 0.0044*) and following

platelet activation with indicated agonists compared to platelets alone (ADP [10 µM]: *p = 0.038*; collagen related peptide (CRP) [5 µg/mL]: *p = 0.0064*; PAR4 [200 µM]: *p = 0.005*). However, platelet activation, which was measured by active integrin $\alpha_{IIb}\beta_3$ and exposure of P-selectin at the platelet surface, revealed no alterations in the absence or presence of RBCs (Fig. 15B, C). These results indicate that RBCs might play a role in the upregulation of the platelet β_3 integrin subunit at the platelet membrane.
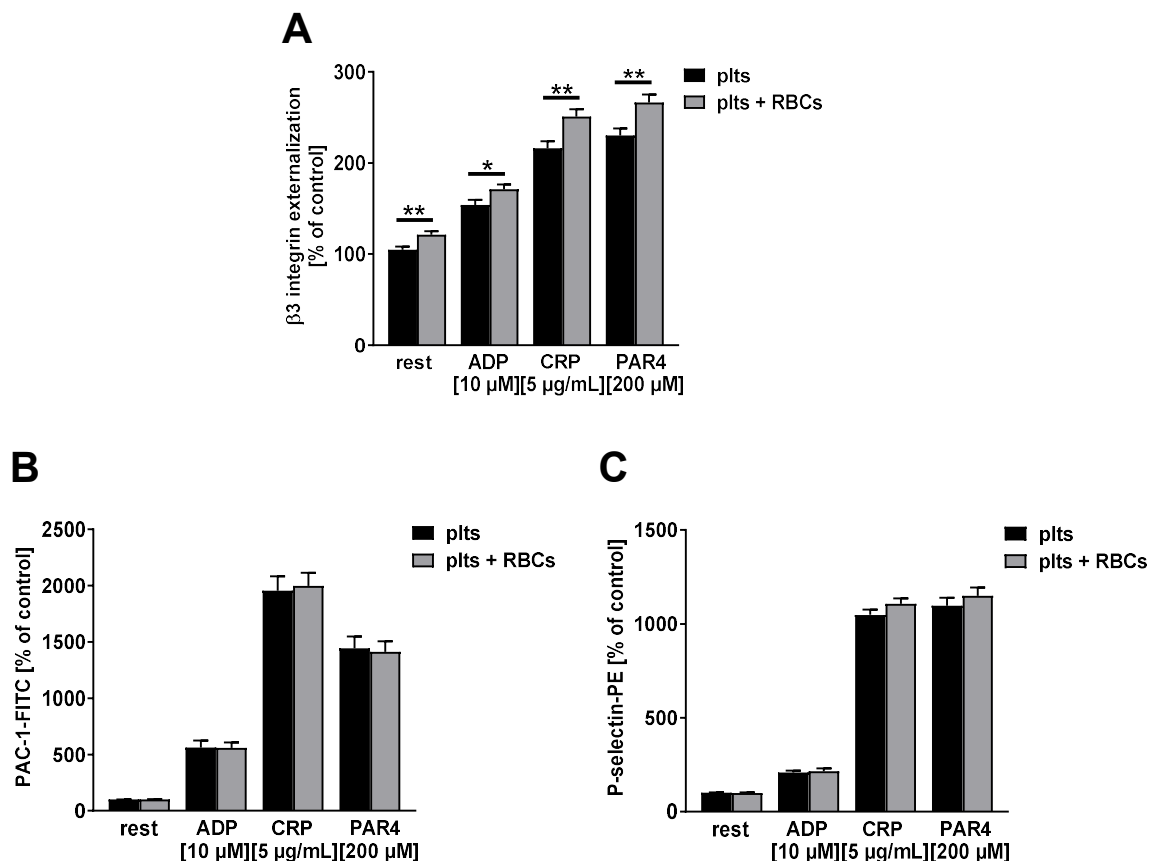
Figure 15: Increased β_3 integrin externalization on the platelet membrane in the presence of RBCs. (A – C) Human platelets were analyzed by flow cytometric analysis regarding their side scatter (SSC) and forward scatter (FSC) profile. (A) Externalization of the β_3 integrin subunit of integrin $\alpha_{IIb}\beta_3$ (CD61-PE) on the surface of human platelets in the absence or presence of RBCs was determined by flow cytometry after platelet activation with indicated agonists (n = 11). (B, C) Platelet activation was analyzed by determination of active integrin $\alpha_{IIb}\beta_3$ (PAC-1-FITC) (B) and P-selectin externalization (P-selectin-PE) (C) on the platelet surface in the absence or presence of RBCs (n= 12). Results represent mean values $\pm$ SEM. *p < 0.05; **p < 0.01 tested by unpaired student's t-test. Rest = resting, plts = platelets; RBCs = red blood cells; ADP = adenosine diphosphate; CRP = collagen related peptide; PAR4 = protease-activated receptor 4 activating peptide, MFI = mean fluorescence intensity.

4.2.2 FasR on the RBC surface is involved in β₃ integrin externalization on the platelet surface

Next, the question arises weather the FasL/FasR axis plays a role in RBC induced increase of β₃ integrin externalization on platelets. Thus, FasR and FasL antibody-mediated inhibition as well as *FasR*⁻/⁻ RBCs and FasL-deficient platelets were used to analyze the level of β₃ integrin on the platelet surface. Flow cytometric analysis of platelets in the presence of RBCs from healthy human volunteers showed elevated β₃ integrin externalization compared to platelets in the absence of RBCs under resting conditions (*p = 0.0347*) and after activation with CRP (*p = 0.0240*) (Fig. 16A).
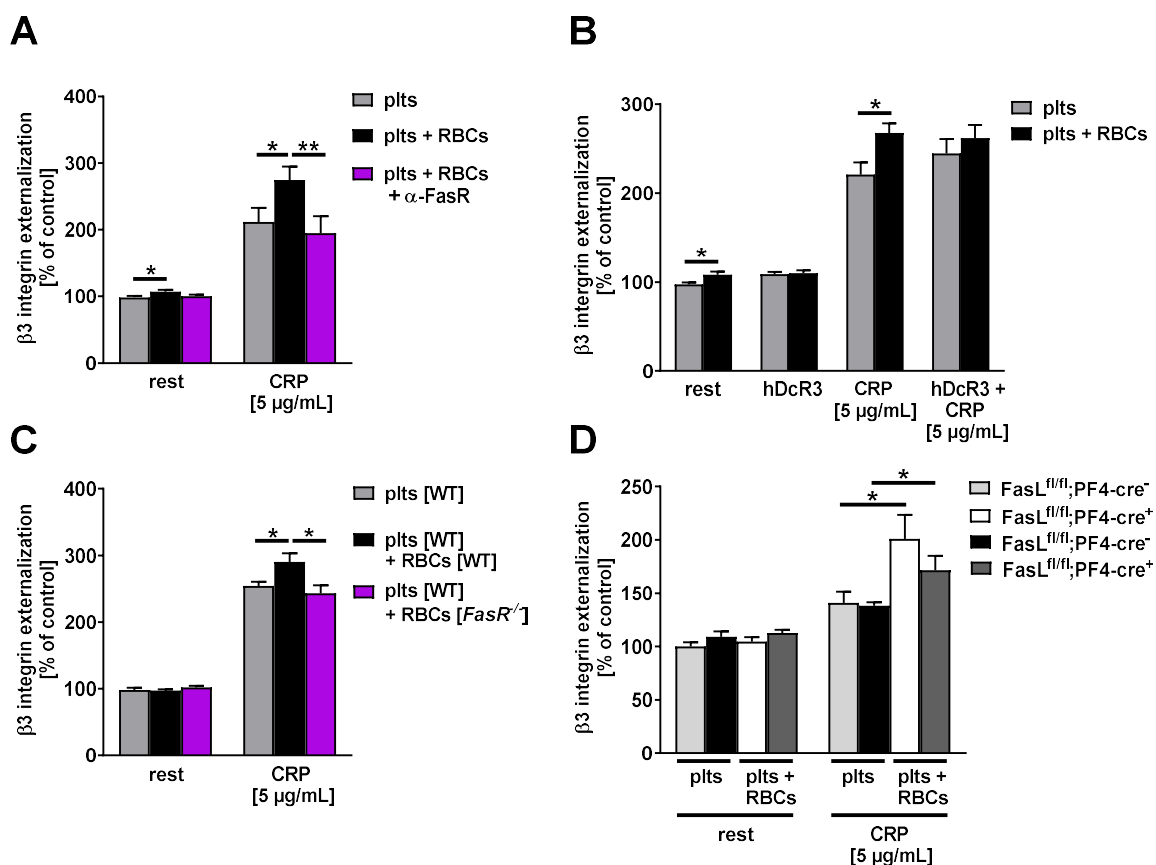
Figure 16: FasR inhibition or genetic deletion of FasR leads to impaired β₃ integrin externalization at the platelet surface. (A, B) Human and (C, D) murine platelets were analyzed by flow cytometry regarding their side scatter (SSC) and forward scatter (FSC) profile. (A – D) Externalization of the β₃ integrin subunit of integrin α$_{IIb}$β₃ on the surface of human (A, B; n = 8 - 9) and mouse (C, D; n = 5 - 7) platelets in the absence or presence of RBCs under resting or CRP-stimulated conditions was determined. (A, B) Human RBCs and platelets were isolated and treated with a FasR mAb (A) or hDcR3 as indicated (B). (C) WT platelets were incubated with either WT or *FasR*⁻/⁻ RBCs. (D) Either WT FasL$^{fl/fl}$;PF4-cre⁻ or FasL-deficient platelets (FasL$^{fl/fl}$;PF4-cre⁺) were incubated with WT RBCs. Results represent mean values ± SEM. *p < 0.05; **p < 0.01 tested by unpaired student's t-test (B) and by ordinary One-Way ANOVA with Sidak's multiple comparison post-hoc test (A, C, D). Rest = resting; plts = platelets; RBCs = red blood cells; α-FasR = FasR monoclonal antibody; hDcR3 = human decoy receptor 3; CRP = collagen related peptide; WT = wild type.

In addition, markedly reduced β_3 integrin externalization of platelets was observed when the FasR on RBCs was inhibited by antibody treatment compared to untreated RBCs ($p = 0.0124$) (Fig. 16A). The involvement of erythroid FasR on β_3 integrin externalization at the platelet membrane was confirmed with $FasR^{-/-}$ RBCs (Fig. 16C). Along the same lines of human platelets, β_3 integrin externalization on murine platelets was notably increased in the presence of RBCs compared to WT platelets alone following platelet stimulation with CRP ($p = 0.0325$). Moreover, CRP-stimulated murine platelets revealed significantly reduced β_3 integrin externalization in the presence of $FasR^{-/-}$ RBCs compared to CRP-stimulated platelets in the presence of WT RBCs ($p = 0.0093$) (Fig. 16C). In contrast, unaltered platelet β_3 integrin externalization in the presence of RBCs was observed when FasL was inhibited on the surface of human platelets (Fig. 16B) or FasL-deficient murine platelets were used (Fig. 16D).

4.2.3 Integrin $\alpha_{IIb}\beta_3$ serves as binding partner for FasR

To further investigate the potential of FasR ligands on platelet-RBC interactions, the adhesion of platelets to immobilized human FasR protein (CD95 protein [50 µg/mL]) was analyzed. To this end, either FasL (with hDcR3) or integrin $\alpha_{IIb}\beta_3$ or both were blocked to analyze if integrin $\alpha_{IIb}\beta_3$ plays a role in the activation of erythroid FasR and if this is an additive or a competitive effect to the already confirmed ligand FasL on the platelet surface. As indicated, tirofiban and abciximab were utilized to block integrin $\alpha_{IIb}\beta_3$. Both drugs are categorized as glycoprotein (GP)-IIb/IIIa-receptor-antagonists and are used to treat over 50,000 patients with acute coronary syndrome. Tirofiban is a "non-peptide-mimetica" (structural analog of RGD-sequence) and abciximab (c7E3 Fab) is a (GP)-IIb/IIIa-receptor-antibody [187].

The inhibition of integrin $\alpha_{IIb}\beta_3$ with tirofiban resulted in unaltered platelet adhesion to immobilized FasR under resting conditions but strongly reduced platelet adhesion under ADP-stimulated conditions ($p < 0.001$) (Fig. 17A). After inhibition of integrin $\alpha_{IIb}\beta_3$ with abciximab, the adhesion of resting ($p = 0.0184$) and ADP-stimulated platelets ($p < 0.001$) was severely decreased (Fig. 17B). Moreover, inhibition of platelet FasL with hDcR3 was accompanied by a significant reduction of platelet adhesion to immobilized FasR protein in the resting state ($p < 0.001$) and after ADP stimulation ($p < 0.001$). In addition, inhibition of both, FasL and integrin $\alpha_{IIb}\beta_3$ led to an additive effect of platelet adhesion to immobilized FasR compared to the inhibition of FasL alone when platelets were activated with ADP ($p = 0.0409$) (Fig. 17B). To confirm the data with human platelets, the adhesion of A5 CHO cells to immobilized fibrinogen [100 µg/mL] and FasR protein was investigated. As shown in

figure 17C, the adhesion of A5 CHO cells to both, immobilized fibrinogen ($p < 0.001$) and FasR ($p < 0.001$) was markedly increased compared to CHO cells that do not expose integrin $\alpha_{IIb}\beta_3$ at the cell surface (Fig. 17C). The adhesion of CHO cells to BSA (1%) served as controls. This data suggests that integrin $\alpha_{IIb}\beta_3$ binds to FasR and may serve as a potential ligand for FasR on the surface of RBCs.
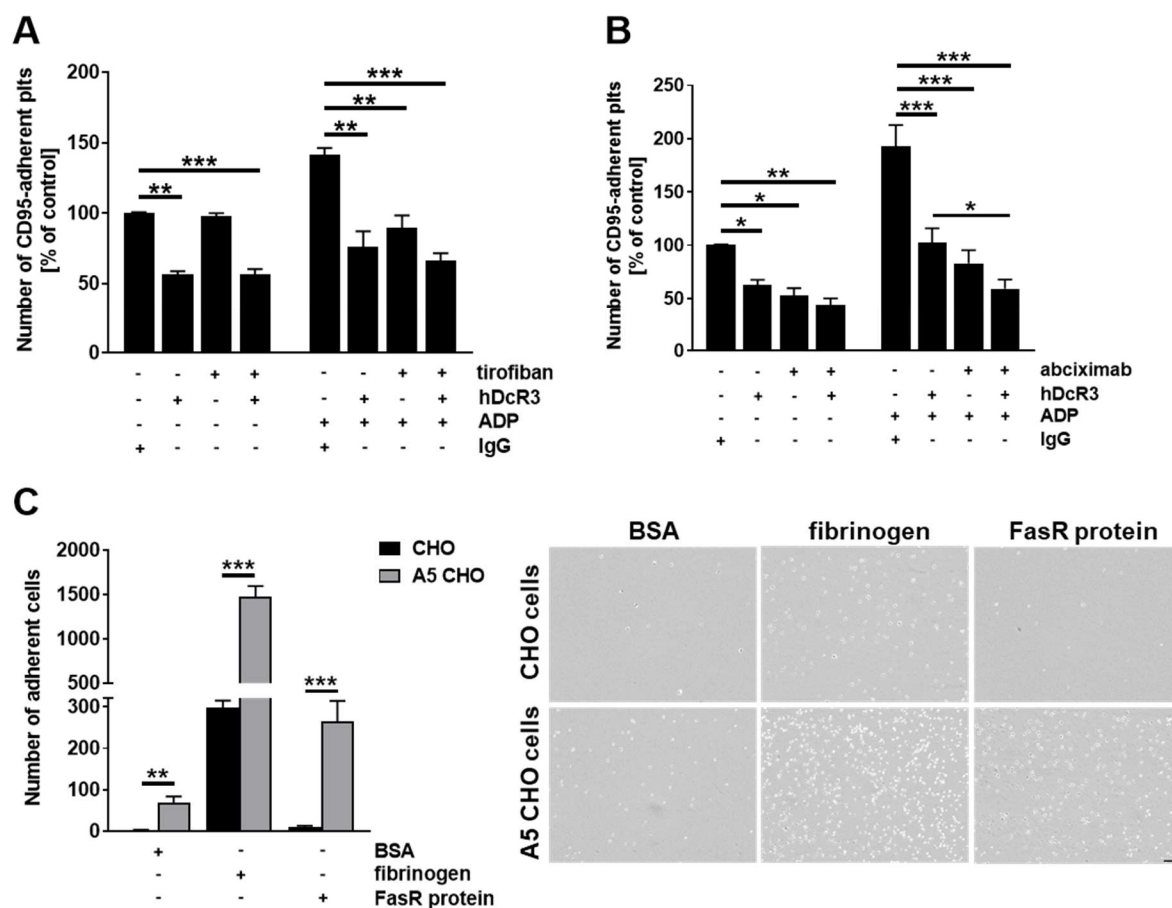
Figure 17: Impaired platelet adhesion on immobilized FasR protein after inhibition of FasL and integrin $\alpha_{IIb}\beta_3$. (A, B) Adhesion of platelets to immobilized recombinant FasR protein [50 µg/mL] in the presence of FasL (hDcR3 [10 µg/mL]) and integrin $\alpha_{IIb}\beta_3$ inhibitors (abciximab [10 µg/2mio. cells], n = 6); tirofiban [1 µg/mL] (n = 4)) in resting state and after ADP [10 µM] stimulation compared to IgG-FC control peptide [10 µg/ml]. (C) Adhesion of CHO cells and A5 CHO cells to immobilized recombinant FasR protein and fibrinogen [100 µg/mL] (n = 5). BSA (1%) served as control (n = 4). Representative DIC images with 100-fold magnification are shown. Scale bar: 100 µm. Results represent mean values $\pm$ SEM. *p < 0.05; **p < 0.01; ***p < 0.001 tested by ordinary One-Way ANOVA with Sidak's multiple comparison post-hoc test (A, B) and unpaired student's t-test (C). Plts = platelets; abciximab = integrin $\alpha_{IIb}\beta_3$ inhibitor, hDcR3 = human decoy receptor 3; ADP = adenosine diphosphate; BSA = bovine serum albumin; CHO cells = Chinese hamster ovary cells; A5 CHO cells = integrin $\alpha_{IIb}\beta_3$ transfected into Chinese hamster ovary cells.

4.2.4 Integrin α$_{IIb}$β$_3$ and FasL on platelets are important for PS exposure on RBCs in humans and mice

The adhesion experiments above indicate that integrin α$_{IIb}$β$_3$ plays a role in platelet-RBC interactions. To investigate if integrin α$_{IIb}$β$_3$-mediated interaction plays a role in the exposure of PS, Annexin V binding to platelets and RBCs after inhibition of FasL (with hDcR3) and integrin α$_{IIb}$β$_3$ (with abciximab) was determined by flow cytometry (Fig. 18). Accordingly, flow cytometric analysis of ADP [10 µM]-stimulated platelets coincubated with RBCs showed significantly reduced Annexin V binding when integrin α$_{IIb}$β$_3$ was blocked by abciximab ($p = 0.0182$), but unaltered PS exposure after FasL inhibition compared to IgG controls (Fig. 18A). The treatment with both inhibitors showed an equal decrease of exposed PS on the surface of platelets and RBCs compared to the single inhibition with hDcR3 and abciximab (Fig. 18A, B). In addition, Annexin V binding to RBCs was significantly decreased after the inhibition of ADP-stimulated platelets with abciximab ($p = 0.0170$), hDcR3 ($p = 0.0473$) and with both inhibitors ($p = 0.0171$) (Fig. 18B).

Similarly, platelets which where stimulated with CRP and coincubated with RBCs showed strongly reduced Annexin V binding to platelets in the presence of abciximab ($p < 0.001$) (Fig. 18A). In addition, PS exposure of CRP-stimulated platelets was markedly reduced when platelet FasL was inhibited ($p < 0.001$). However, no additive effect on the exposure of PS at the platelet surface was measured when integrin α$_{IIb}$β$_3$ and FasL at the platelet surface were blocked simultaneously (Fig. 18A). Similar results were observed for Annexin V binding to RBCs (Fig. 18B). Decreased PS exposure was detected on the RBC membrane after inhibition with abciximab ($p = 0.0101$) and with both inhibitors hDcR3 and abciximab after CRP stimulation ($p = 0.0171$). Additionally, hDcR3 treatment of CRP-stimulated platelets affected PS exposure of RBCs ($p = 0.0146$). Next, human data with FasL and integrin inhibitors were confirmed using platelets and RBCs from FasL-deficient mice and the integrin α$_{IIb}$β$_3$ inhibitor Leo.H4. Platelets (Fig. 18C) and RBCs (Fig. 18D) of FasL$^{fl/fl}$;PF4-cre$^-$ mice showed significantly increased Annexin V binding after CRP stimulation. The PS exposure of both cell types was only decreased after the treatment of FasL$^{fl/fl}$;PF4-cre$^-$ CRP-stimulated platelets with the antibody Leo.H4 [5 µg/mL] compared to IgG controls (Fig. 18C, D). Additionally, a significant reduction of Annexin V binding of FasL-deficient resting ($p = 0.0215$) and CRP-stimulated ($p < 0.001$) platelets was detected compared to FasL$^{fl/fl}$;PF4-cre$^-$ (Fig. 18C). Furthermore, RBCs from FasL$^{fl/fl}$;PF4-cre$^-$ mice showed a higher Annexin V binding in resting state ($p = 0.0131$) and after CRP stimulation ($p = 0.0411$) compared to RBCs from FasL-deficient mice. In contrast to the human results shown in figure 18A and B, FasL deficiency and integrin α$_{IIb}$β$_3$ inhibition showed an additive effect on the exposure of PS at the surface of both cell types (Fig. 18C). This could be observed for

the PS exposure of RBCs as well (Fig. 18D). Taken together, adhesion studies with CHO cells and human platelets to immobilized FasR protein (Fig. 17) and decreased PS exposure on the RBC membrane after coincubation with FasL-deficient platelets or antibody-mediated FasL inhibition indicated an interaction between FasR on RBCs and integrin $\alpha_{IIb}\beta_3$ at the platelet surface.
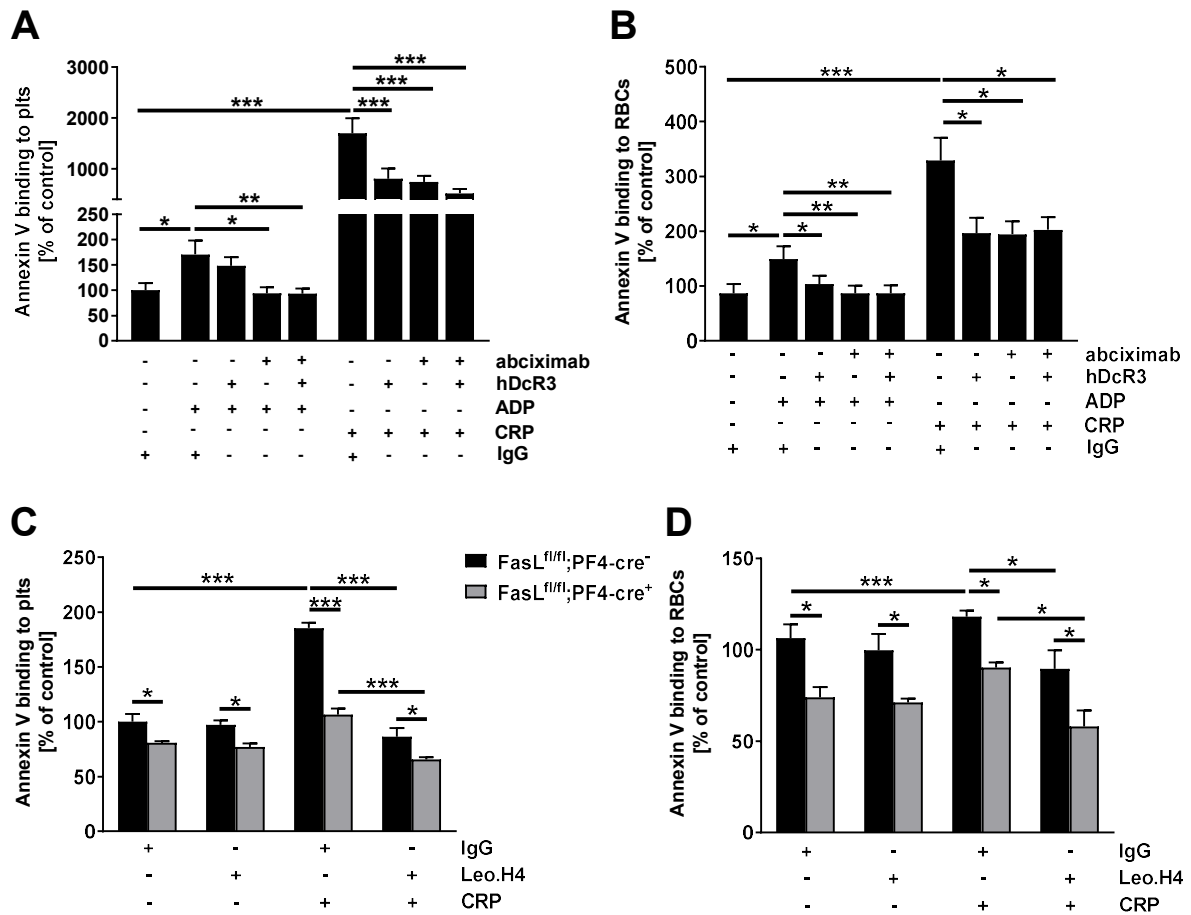
Figure 18: Impaired PS exposure of platelets and RBCs after inhibition of FasL and integrin $\alpha_{IIb}\beta_3$. (A, B) Human platelets and RBCs were determined by flow cytometric analysis regarding their cell specific markers CD235-FITC (RBCs) and CD42-PE (platelets). (C, D) Murine platelets and RBCs were determined by flow cytometric analysis regarding their side scatter (SSC) and forward scatter (FSC) profile. (A, B) Annexin V binding to human platelets (A) and RBCs (B) in the absence or presence of FasL (hDcR3 [10 µg/mL]) and integrin $\alpha_{IIb}\beta_3$ inhibitors (abciximab [10 µg/2mio. cells]) coincubated with RBCs in resting state and in response to indicated agonists compared to IgG-FC control peptide [10 µg/ml] (n = 7 - 9). (C, D) Annexin V binding to FasL-deficient and FasL^{fl/fl};PF4-cre^- platelets (C) and RBCs (D) in the absence or presence of integrin $\alpha_{IIb}\beta_3$ inhibitor (Leo.H4 [5 µg/mL]). Platelets were coincubated with RBCs in resting state and in response to indicated agonists (n = 6). Results represent mean values $\pm$ SEM. *p < 0.05; **p < 0.01; ***p < 0.001 tested by Two-Way ANOVA with Sidak's multiple comparison post-hoc test (A – D). Plts = platelets; RBCs = red blood cells; abciximab = integrin $\alpha_{IIb}\beta_3$ inhibitor; hDcR3 = human decoy receptor 3; ADP = adenosine diphosphate; CRP = collagen related peptide; Leo.H4 = integrin $\alpha_{IIb}\beta_3$ inhibitor.

4.3 The scavenger receptor CD36 on RBCs influences platelet signaling and thrombus formation

CD36 is known to be an adhesion molecule of monocytes, platelets and ECs but it is also expressed on normal human RBCs (healthy persons) [81]. This protein is expressed on the surface of platelets with a high copy number of 10,000 to 25,000. Additionally, a low number of CD36 copies are stored into platelet α-granules [70]. The copy number of RBCs is not defined yet. The crucial role of platelet-derived TSP-1 and CD36 for thrombus formation on a collagen and a collagen/TSP-1 matrix has been previously demonstrated [92, 114]. To identify a potential role of erythroid CD36 in platelet-driven thrombus formation, the expression of CD36 of human platelets and RBCs was studied by flow cytometry and Western blot analysis. Next, PS exposure and β_3 integrin externalization in the presence of a CD36 monoclonal antibody (mAb) was determined by flow cytometry. Furthermore, the impact of erythroid CD36 on three-dimensional thrombus formation on a collagen versus a collagen/TSP-1 matrix under flow conditions was investigated using an arterial shear rate of $1,700 \ s^{-1}$.

4.3.1 Erythroid CD36 modulates PS exposure and β_3 integrin signaling of platelets

To study the expression of CD36 on the RBC and platelet membrane, flow cytometric analysis under static conditions were performed (Fig. 19C). The results revealed a constitutive expression of CD36 on the surface of platelets and RBCs under resting conditions and after CRP stimulation of platelets without any significant alterations in the different samples. To investigate the protein expression level of CD36 in human platelets and RBCs, lysates and supernatants of platelets, RBCs and platelets coincubated with RBCs were analyzed for CD36 by Western blot. Western blot analysis of CD36 using platelet lysates revealed four different glycosylation and splicing forms (Fig. 19A). The highly glycosylated band appears at 88 kDa (black arrow) and is described as the major platelet band [188]. The 53 kDa band (black arrowhead) is at the predicted size of the unglycosylated full length form of the protein [188]. Quantification of the 88 kDa and 53 kDa band, revealed no significant differences between resting and activated platelets. Furthermore, no differences could be detected neither for the ~ 48 kDa nor for ~ 40 kDa bands (blue arrowheads).
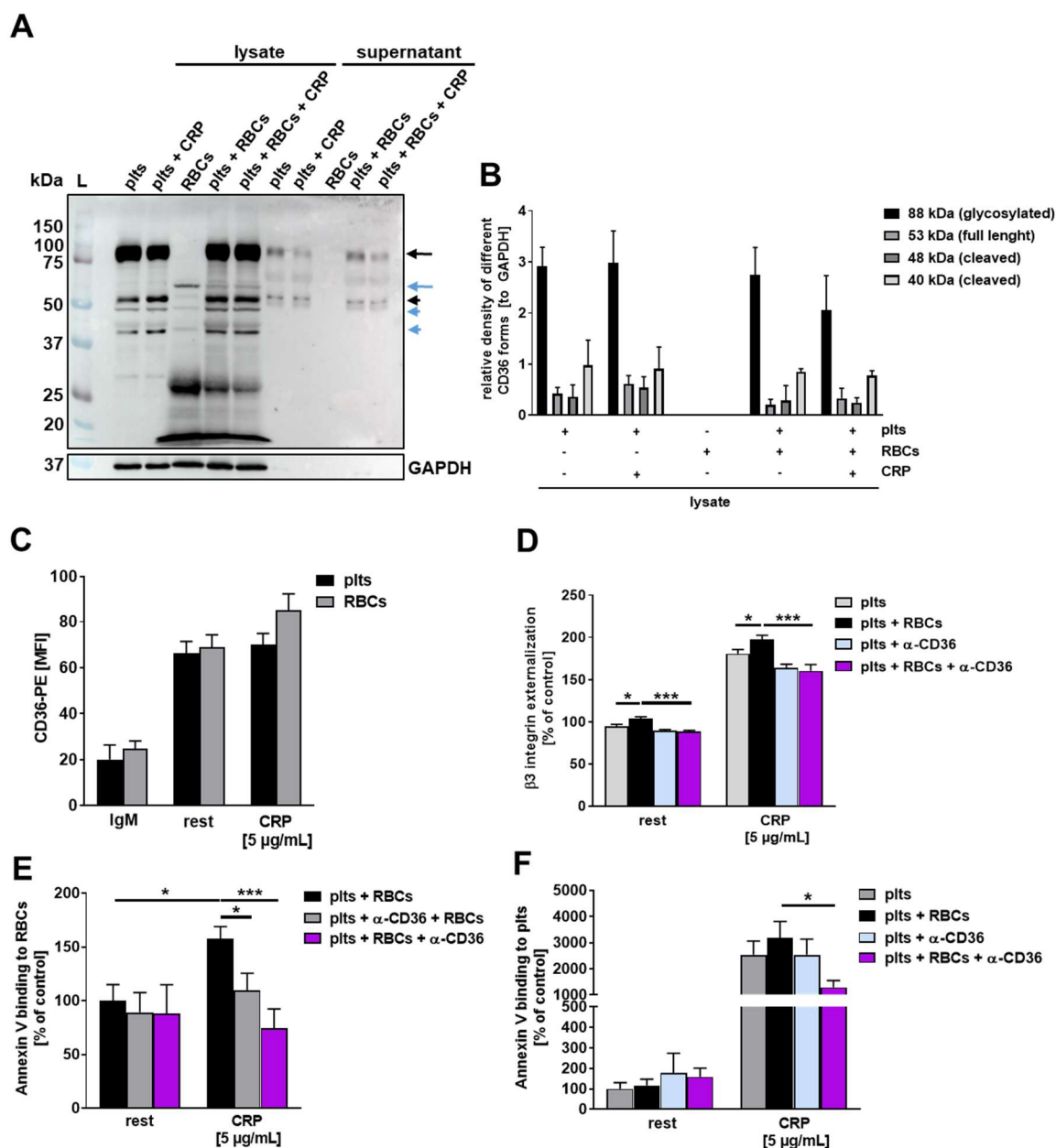
Figure 19: Impact of CD36 on β₃ integrin externalization of platelets and PS exposure of platelets and RBCs. (A) In the absence or presence of RBCs (2×10^5 RBCs/µL), isolated human platelets (4×10^5 platelets/µL) were activated with CRP [5 µg/mL] for 5 min at 37 °C or used under resting conditions. Subsequently lysates and supernatants were generated and Western blot analysis was performed (n = 3). GAPDH was used as housekeeping protein. (B) Statistical evaluation of CD36 expression normalized to GAPDH. (C) CD36 expression of human platelets and RBCs was determined by flow cytometric analysis regarding their specific SSC and FSC profile (n = 6). RBCs were detected with the cell specific marker CD235-FITC. (D) Externalization of the β₃ integrin subunit of integrin α$_{IIb}$β₃ (CD61-PE) on the surface of platelets in the absence and presence of RBCs was measured by flow cytometry (n = 11). RBCs and platelets were cell-specifically treated with a CD36 mAb [2 µg/mL] and RBCs were subsequently washed before they were coincubated with platelets. (E, F) Annexin V binding to human RBCs (E) and platelets (F) in the resting state and after CRP stimulation under static conditions was determined by flow cytometric analysis with the cell specific markers CD235-FITC (RBCs) and CD42-PE (platelets) (n = 4). Isolated cells were preincubated with a CD36 mAb [2 µg/mL] and RBCs were washed before coincubation with platelets. Results represent mean values $\pm$ SEM. *p < 0.05; ***p < 0.001 tested by Two-Way ANOVA with Sidak's multiple comparison post-hoc test. Rest = resting; plts = platelets; RBCs = red blood cells; α-CD36 = CD36 monoclonal antibody; CRP = collagen related peptide; L = ladder; MFI = mean fluorescence intensity.

The prominent band of 88 kDa was only detected in lysates containing platelets, while the unglycosylated full length form of 53 kDa was also detected in the supernatant of resting and activated platelets. Western blot analysis revealed a different glycosylation form of erythroid CD36 compared to platelet CD36. The apparent band of CD36 on the surface of RBCs was approximately ~ 65 kDa (blue arrow) in size and was only observed in the lysates of RBCs (Fig. 19A). While it is known that CD36 in erythroblasts appears at a size of ~ 78 kDa [189], the 65 kDa band has not been described yet. Also, no other band was detected in lysates using RBCs alone. No positive control was used for the detection of CD36 as no platelet-derived recombinant protein was available and cell type specific glycosylation patterns would not have been visible. Next, flow cytometric analysis was performed to investigate the externalization of platelet β_3 integrin and PS exposure of platelets and RBCs (Fig. 19D – F). After inhibition, RBCs were always washed with PBS to avoid CD36 inhibitory effects on platelets. The externalization of β_3 integrin on resting ($p = 0.0415$) and CRP-stimulated ($p = 0.0290$) platelet was significantly increased in the presence of RBCs compared to platelets alone (Fig. 19D). Inhibition of erythroid CD36 leads to significantly reduced β_3 integrin externalization of platelets compared to controls (resting: $p < 0.001$; CRP [5 µg/mL]: $p < 0.001$). To study the procoagulant surface of platelets and RBCs, Annexin V binding to platelets and RBCs was determined by flow cytometry (Fig. 19E, F). Annexin V binding to coincubated RBCs (Fig. 19E) and CRP-stimulated platelets (Fig. 19F) was significantly reduced after inhibition of erythroid CD36 (RBCs: $p < 0.001$; platelets: $p = 0.0190$). After stimulation of platelets with CRP, inhibition of CD36 on the platelet surface only affected PS exposure of RBCs ($p = 0.0488$) but not of platelets (Fig. 19E). Taken together, erythroid CD36 was detected in Western blot with an apparent molecular weight of ~ 68 kDa. Additionally, platelet β_3 integrin externalization as well as PS exposure of platelets and RBCs depends on erythroid CD36 rather than on platelets CD36.

4.3.2 Human erythroid CD36 supports thrombus formation under arterial shear rates

To investigate whether CD36 on the surface of RBCs supports platelet-driven thrombus formation on collagen [200 µg/mL] under flow conditions at a shear rate of 1,700 s^{-1}, the formation of three-dimensional thrombi and the procoagulant surface of platelets and RBCs were analyzed in the presence of an inhibiting CD36 mAb (Fig. 20 A – E). First, human whole blood was treated with an inhibiting CD36 mAb [2 µg/mL]. As shown in figure 20, antibody treatment resulted in a notable reduction of surface coverage compared to IgG controls ($p = 0.0081$).
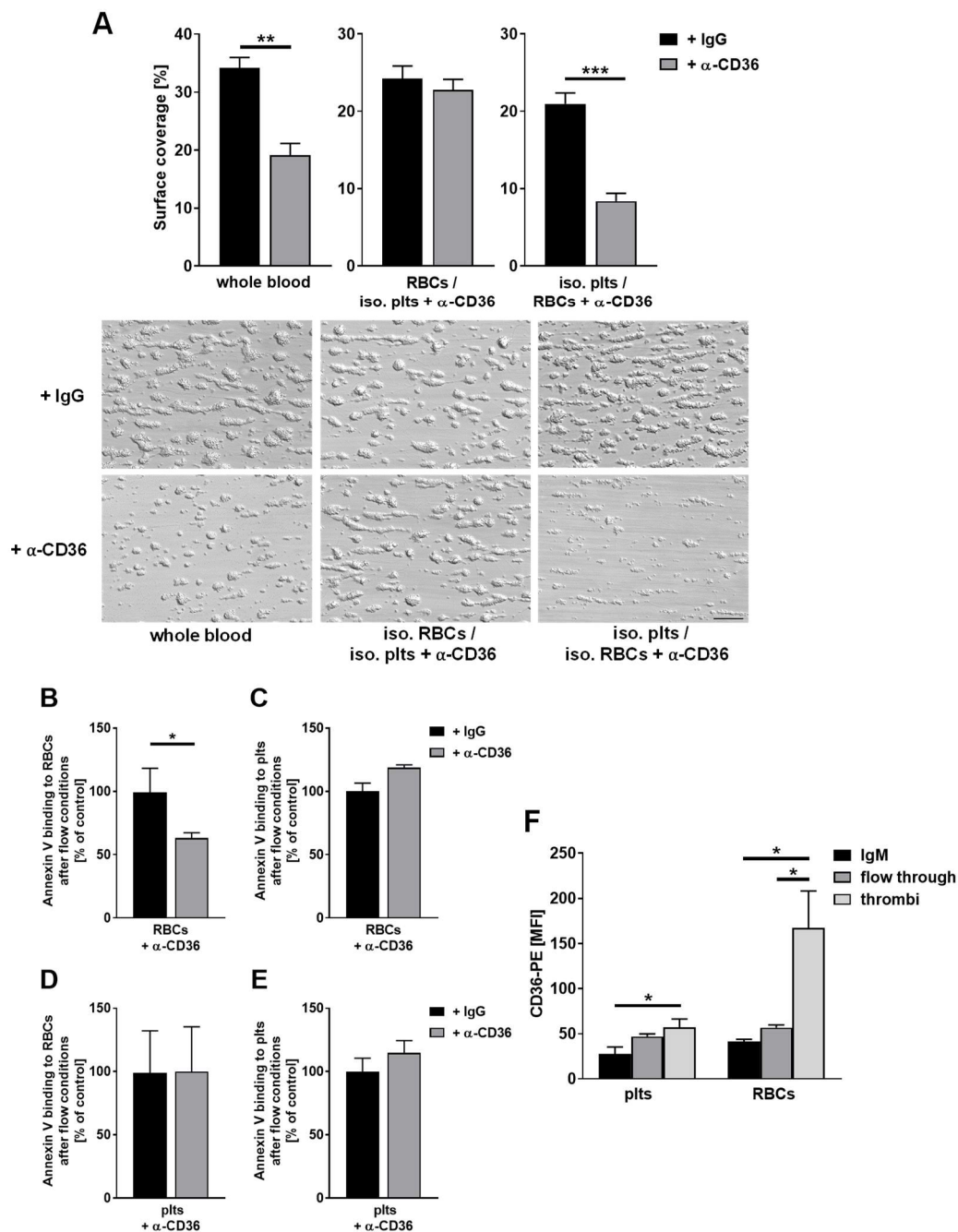
Figure 20: Role of CD36 for thrombus formation and PS exposure of platelets and RBCs under dynamic conditions. (A) Thrombus formation on a collagen matrix [200 µg/mL] was analyzed using a shear rate of 1,700 s^{-1}. Human whole blood was pretreated with an IgG antibody or a CD36 mAb [2 µg/mL]. Human platelets, RBCs and plasma were isolated and either RBCs or platelets were pretreated with an IgG antibody or a CD36 mAb (n = 5). Subsequently, RBCs were washed and supplemented with platelets and plasma using a concentration of 4 x 10^6 RBCs/µL and 2 x 10^5 platelets/µL. Representative DIC images are shown. Scale bar: 50 µm. (B – E) Annexin V binding to RBCs (B, D) and platelets (C, E) isolated from thrombi was measured by flow cytometry with the cell specific marker CD235-FITC (RBCs) and CD42-PE (platelets) (n = 4). (F) CD36 expression of platelets and RBCs isolated from thrombi (dissolved with Accutase®) was determined by flow cytometric analysis regarding their side scatter (SSC) and forward scatter (FSC) profile. Additionally, RBCs were detected with their cell specific marker CD235-FITC (n = 5). Results represent mean values ± SEM. *p < 0.05; **p < 0.01;***p < 0.001 tested by unpaired student's t-test (A – E) and by ordinary One-Way ANOVA with Sidak's multiple comparison post-hoc test (F). Plts = platelets; RBCs = red blood cells; iso. = isolated; α-CD36 = CD36 monoclonal antibody; MFI = mean fluorescence intensity.

To investigate cell specific inhibition of CD36, flow chamber experiments with isolated platelets and RBCs were performed using a concentration of 2 x 10^5 platelets/µL and 4 x 10^6 RBCs/µL at a shear rate of 1,700 s^{-1} (Fig. 20A). Platelets and RBCs were independently treated with a CD36 mAb and supplemented with plasma to allow thrombus formation under flow. RBCs were always washed after CD36 inhibition to avoid the binding of surplus CD36 antibody to platelets. The formation of three-dimensional thrombi was markedly reduced when CD36 was only inhibited at the RBC membrane (*p = 0.0017*) (Fig. 20A). Furthermore, CD36 inhibition on RBCs led to decreased Annexin V binding to RBCs that have been isolated from thrombi (*p = 0.0489*) (Fig. 20B). Moreover, erythroid CD36 was significantly upregulated in thrombi compared to RBCs from flow through (*p = 0.0201*) (Fig. 20F). Regarding platelets, no statistical differences were obtained in thrombi compared to flow through. Taken together, these results support the hypothesis for an important role of CD36 in thrombus formation on collagen, which depends on erythroid CD36 rather than on platelet CD36.

4.3.3 Inhibition of erythroid CD36 strongly reduces thrombus formation on a collagen/TSP-1 matrix under arterial shear rates

The ECM protein TSP-1 is released from platelets and binds to CD36 [114]. To clarify whether or not erythroid CD36 supports thrombus formation on a TSP-1/collagen matrix, the formation of three-dimensional thrombi under dynamic conditions were analyzed in the presence of an inhibiting CD36 mAb (Fig. 21A, B). RBCs were always washed after inhibition to avoid the binding of surplus CD36 antibody to platelets. Initial results revealed significantly enhanced thrombus formation on a TSP-1/collagen matrix compared to a collagen matrix using a shear rate of 1,700 s^{-1} (*p < 0.001*). Moreover, the formation of three-dimensional thrombi on a TSP-1/collagen matrix was dramatically reduced when CD36 was specifically inhibited on the RBC surface (*p < 0.001*) (Fig. 21A), but only moderately decreased after inhibition of CD36 on the platelet surface compared to IgG controls (*p = 0.0322*) (Fig. 21B). Only a few thrombi were observed using a TSP-1 matrix, which served as control (Fig. 21A). Taken together, these results indicate that TSP-1 binding to erythroid CD36 is important for thrombus formation under arterial shear rate.
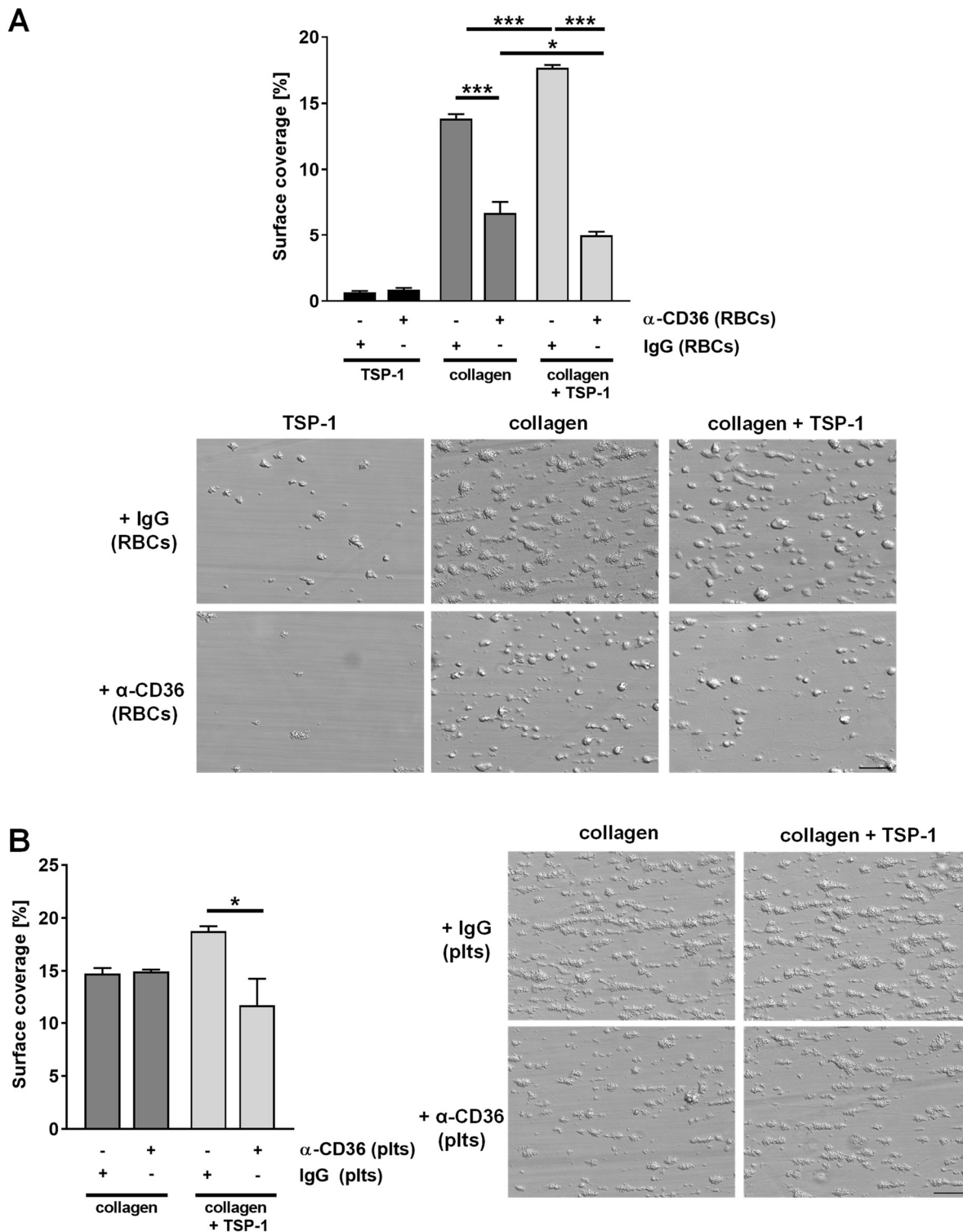
Figure 21: Defective thrombus formation on collagen-rich and collagen/TSP-1-rich matrices after CD36 inhibition under arterial shear rates. Thrombus formation on a TSP-1 [100 µg/mL], a collagen [200 µg/mL] or TSP-1/collagen matrix was analyzed using a shear rate of 1,700 s^{-1}. Human platelets, RBCs and plasma were isolated and either RBCs (A) or platelets (B) were incubated with or without a CD36 mAb [2 µg/mL]. Subsequently, RBCs were washed and supplemented with platelets and plasma using a concentration of 4 x 10^6 RBCs/µL and 2 x 10^5 platelets/µL (n = 3). Representative DIC images are shown. Scale bar: 50 µm. Results represent mean values ± SEM. *p < 0.05; ***p < 0.001 tested by Two-Way ANOVA with Sidak's multiple comparison post-hoc test. Plts = platelets; RBCs = red blood cells; iso. = isolated; α-CD36 = CD36 monoclonal antibody.

4.3.4 CD36-deficient RBCs are responsible for reduced thrombus formation, platelet aggregation, PS exposure and FasL externalization

To investigate whether the role of CD36 in thrombus formation, platelet aggregation, procoagulant surface and FasL externalization of platelets depends on erythroid CD36 rather than on CD36 at the platelet surface, experiments with platelets and RBCs from $Cd36^{-/-}$ mice were performed. WT or $Cd36^{-/-}$ platelets were incubated with WT or $Cd36^{-/-}$ RBCs as indicated (Fig. 22A – E).

In line with the results from CD36 blocking experiments using human platelets and RBCs (Fig. 20), strongly reduced thrombus formation was observed at a shear rate of 1,700 s^{-1} when WT platelets and $Cd36^{-/-}$ RBCs were used for flow chamber experiments (Fig. 22A). In detail, thrombus formation of WT platelets with $Cd36^{-/-}$ RBCs was significantly decreased compared to WT platelets coincubated with WT RBCs ($p < 0.001$) and WT RBCs in the presence of $Cd36^{-/-}$ platelets ($p < 0.001$) assed by surface coverage. In addition, thrombus formation in flow chamber experiments using WT platelets with $Cd36^{-/-}$ RBCs was altered compared to whole blood of C57BL/6J mice ($p < 0.001$). Moreover, flow cytometric analysis of PS exposure of WT RBCs in the presence of CRP-stimulated $Cd36^{-/-}$ platelets ($p < 0.001$) and of $Cd36^{-/-}$ RBCs in the presence of activated WT platelets ($p < 0.001$) was significantly decreased compared to RBCs and platelets both from WT mice (Fig. 22B). PS exposure of platelets and RBCs under resting conditions was unaltered. In addition, CD36 deficiency of RBCs and platelets showed no alterations in PS exposure of platelets (Fig. 22C).

Furthermore, FasL externalization on resting WT platelets was markedly decreased in the presence of RBCs from $Cd36^{-/-}$ mice compared to either WT platelets ($p = 0.0368$) or $Cd36^{-/-}$ platelets ($p = 0.0437$) in the presence of WT RBCs (Fig. 22D).

In addition, platelet aggregation was analyzed by impedance measurements using indicated compositions of RBCs and platelets from WT or $Cd36^{-/-}$ mice. These results revealed strongly reduced aggregation of $Cd36^{-/-}$ platelets in the presence of WT RBCs ($p = 0.0385$) and almost no aggregation of WT platelets in the presence of $Cd36^{-/-}$ RBCs ($p < 0.001$) compared to platelets and RBCs from WT mice (Fig. 22E). These results clearly identify a role of erythroid CD36 in thrombus formation, aggregation and PS exposure that only partially depends on platelet CD36.
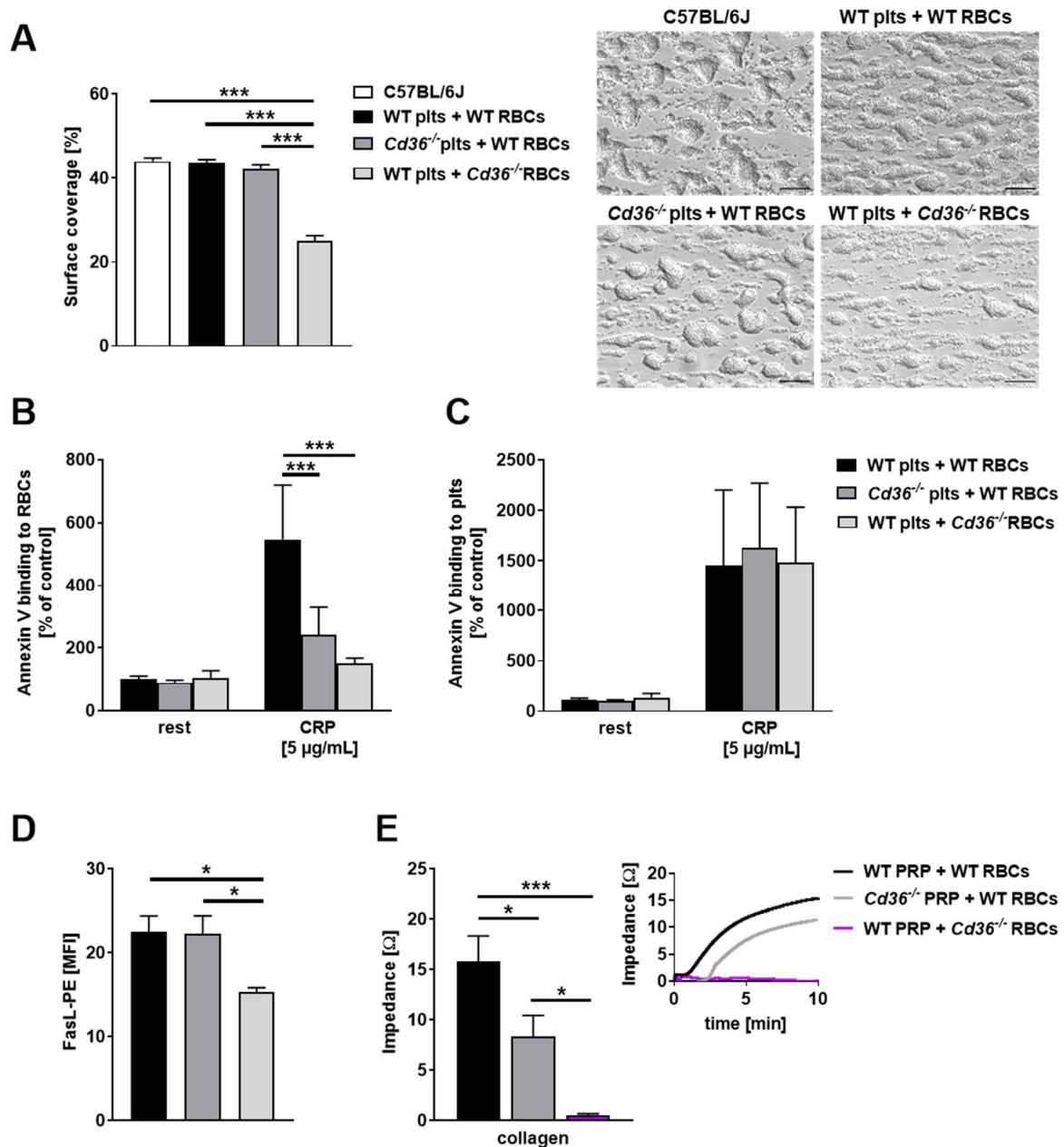
Figure 22: Deficiency of erythroid CD36 modulates platelet aggregation, PS exposure, FasL externalization and thrombus formation under arterial shear rates. (A – E) Murine WT or *Cd36*^{-/-} platelets and RBCs were isolated and the three indicated cell compositions were coincubated. (A) Thrombus formation on collagen [200 µg/mL] at a shear rate of 1,700 s^{-1} was assessed by surface coverage. The three indicated cell compositions were adjusted with plasma to 4×10^6 RBCs/µL and 3×10^5 platelets/µL or whole blood of C57BL/6J mice were used (n = 4). Representative DIC images are shown. Scale bars: 50µm. (B, C) Annexin V binding to RBCs (B) and platelets (C) of the three indicated cell compositions (adjusted to 5×10^4 platelets/µl and 5×10^4 RBCs/µl) was determined by flow cytometric analysis regarding the platelet and RBC specific side scatter (SSC) and forward scatter (FSC) profile (n = 9 - 12). (D) FasL externalization on platelets (FasL-PE) was measured via flow cytometry. Platelets were determined with the cell specific marker CD42-FITC (n = 11). (E) Impedance measurement were performed to analyze platelet aggregation using the three indicated cell compositions that were stimulated with collagen [20 µg/mL] (n = 6). Representative aggregation curves are shown. Results represent mean values ± SEM. *p < 0.05; ***p < 0.001 tested by ordinary One-Way ANOVA (A, D, E) and Two-Way ANOVA with Sidak's multiple comparison post-hoc test (B, C). Rest = resting; plts = platelets; PRP = platelet rich plasma; RBCs = red blood cells; WT = wild type; MFI = mean fluorescence intensity.

4.4 Platelet-released TSP-1 binds to CD36 of human and murine platelets and RBCs

As described above platelet-derived TSP-1 and erythroid CD36 are essential for thrombus formation on a collagen and a collagen/TSP-1 matrix, for PS exposure and platelet aggregation. However, no direct binding of TSP-1 to erythroid CD36 or platelet CD36 was investigated so far. Therefore, the role of TSP-1 binding to RBC was evaluated by flow cytometric analysis under static conditions and under dynamic conditions using whole blood of humans and $Cd36^{-/-}$ mice.

4.4.1 Altered thrombus formation after TSP-1 inhibition in human whole blood

First, Western blot analysis of lysates and supernatants from isolated platelets, RBCs and platelets in the presence of RBCs under resting and CRP-stimulated conditions were performed to verify TSP-1 existence. Two different forms of TSP-1 were detected with apparent bands of 185 kDa (black arrow) and approximately ~ 110 kDa (Fig. 23A, black arrowhead). The upper band could represent the monomeric full length form (185 kDa) [99] and was notably decreased after the activation of platelets compared to resting controls ($p < 0.001$), indicating the secretion of the 185 kDa form after platelet activation (Fig. 23A, B). Under resting conditions, the apparent band of 185 kDa was abolished in the presence of RBCs independently of platelet activation, whereas the band representing the cleaved TSP-1 fragment around ~ 110 kDa increases (Fig. 23A). This suggested a role of RBCs in the protolytical cleavage of TSP-1. As for the full length monomeric form of TSP-1, the amount of the cleaved TSP-1 form (110 kDa) decreased upon platelet activation ($p = 0.0124$). Furthermore, the lysates of RBCs without platelets show that RBCs do not possess TSP-1 on their own. The release of the full length monomeric form and the cleaved TSP-1 fragment was shown by the analysis of the supernatant (Fig. 23A). In detail, the TSP-1 band of 185 kDa was increased upon platelet activation with CRP in the absence ($p < 0.001$) or presence ($p < 0.001$) of RBCs in the supernatant compared to the corresponding lysates. Besides that, a significant decrease in the 185 kDa band was observed between the supernatant of resting platelets compared to the corresponding lysates ($p < 0.001$). The cleaved fragment (110 kDa) was significantly increased in the supernatant after CRP stimulation in the absence ($p = 0.0086$) and presence of RBCs ($p = 0.0042$) compared to the corresponding lysates. Next, flow chamber experiments with human whole blood in the absence and presence of a TSP-1 mAb were performed. As shown in figure 23C, markedly reduced surface coverage was detected when TSP-1 was inhibited. Platelets and RBCs

were isolated from the thrombi and Annexin V binding to both cell types revealed no differences when TSP-1 was inhibited by antibody treatment compared to controls (Fig. 23D, E).
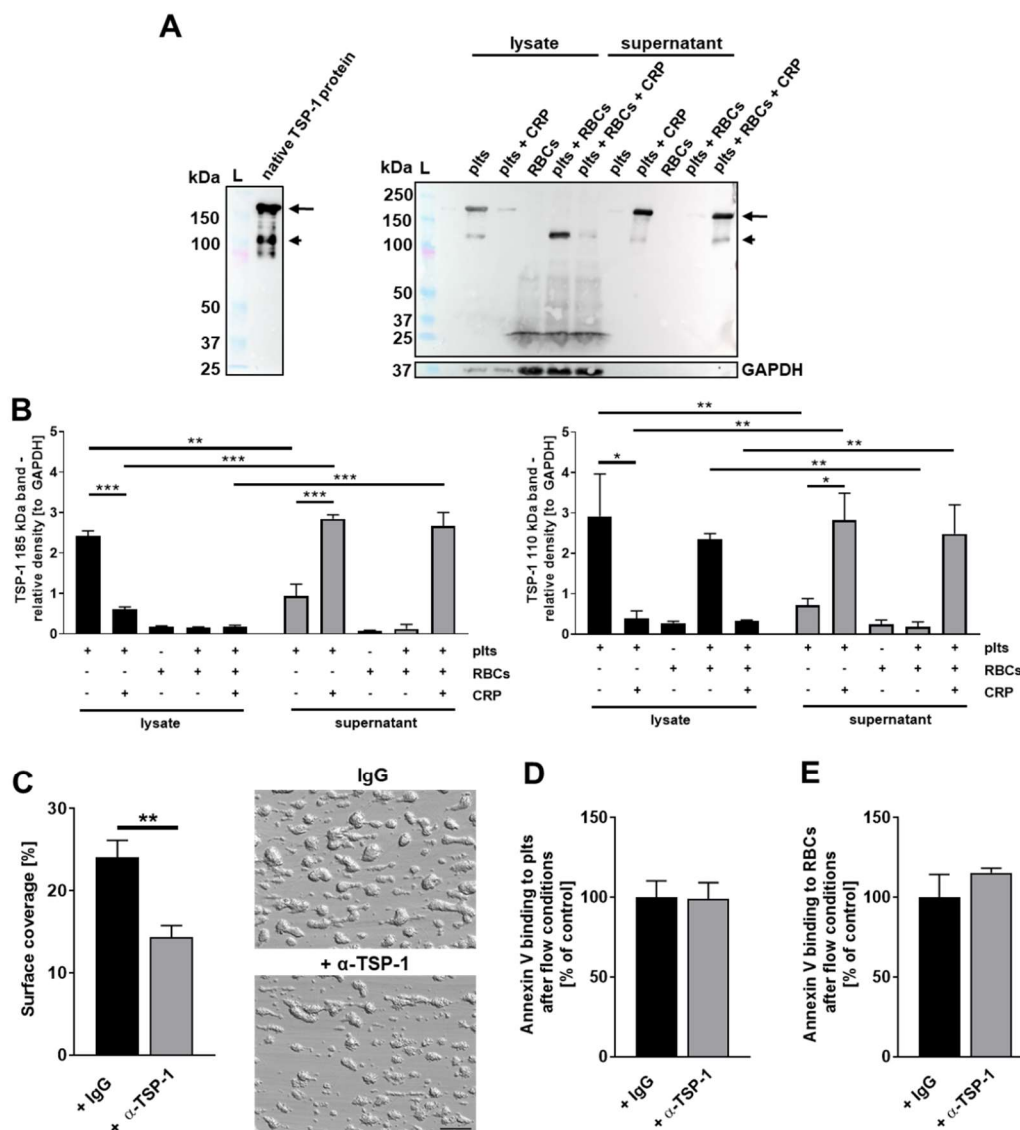
Figure 23: TSP-1 is important for thrombus formation under dynamic conditions. (A) Western blot of native TSP-1 [10 µg/mL] purified from human platelets. In the absence or presence of RBCs (2 x 10^6 RBCs/µL), isolated human platelets (4 x 10^5 platelets/µl) were activated with CRP [5 µg/mL] for 5 min at 37 °C or used under resting conditions. Subsequently lysates and supernatants were generated and Western blot analysis was performed (n = 3). GAPDH was used as housekeeping protein. (B) Statistical evaluation of TSP-1 protein expression normalized to GAPDH. (C) Human whole blood was used to analyze thrombus formation on collagen [200 µg/mL] at a shear rate of 1,700 s^{-1} in the absence or presence of a TSP-1 mAb [2 µg/mL] (n = 5). Platelets were fluorescently labeled. Representative DIC images are shown. Scale bar: 50 µm. (D, E) Annexin V binding to RBCs (D) and platelets (E) isolated from thrombi was measured by flow cytometry with the cell specific marker CD235-FITC (RBCs) and CD42-PE (platelets) (n = 4). Results represent mean values $\pm$ SEM. *$p < 0.05$; **$p < 0.01$; ***$p < 0.001$ tested by Two-Way ANOVA with Sidak's multiple comparison post-hoc test (B) and by student's t-test (C – E). Plts = platelets; RBCs = red blood cells; α-TSP-1 = TSP-1 monoclonal antibody; CRP = collagen related peptide.

4.4.2 Increased TSP-1 binding to RBCs under dynamic conditions

To investigate the binding of platelet-released TSP-1 to platelets and RBCs, flow cytometric analysis was performed using human whole blood that was stimulated with indicated agonists under static and dynamic conditions. Under static conditions, significant differences of TSP-1 binding to platelets compared to resting platelets were observed with intermediate and high concentration of CRP and PAR4 peptide (Fig. 24A). However, TSP-1 binding to RBCs could be detected but no differences were observed in the presence of resting platelets compared to activated platelets (Fig. 24B).
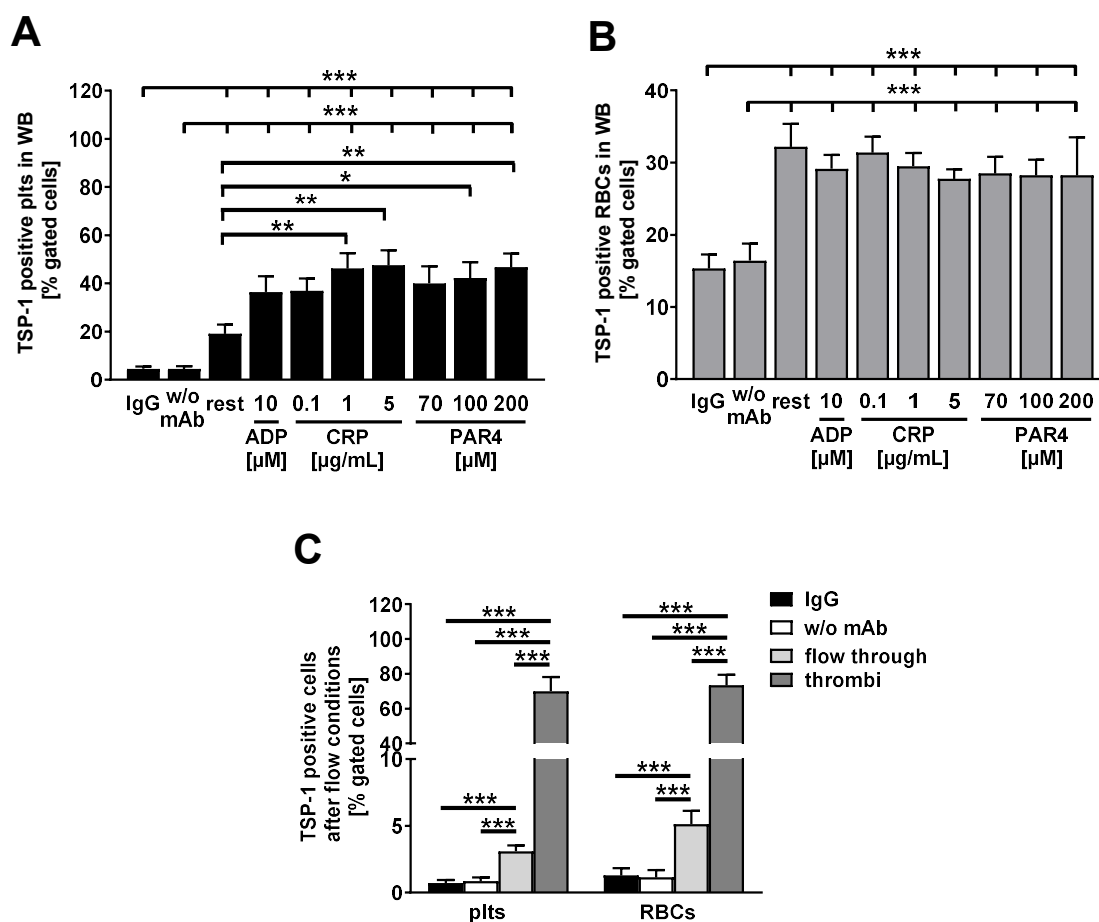
Figure 24: Platelets and RBCs show increased TSP-1 binding when incorporated into the growing thrombus under flow conditions. (A – C) TSP-1 binding to human platelets and RBCs was determined by flow cytometric analysis regarding their specific side scatter (SSC) and forward scatter (FSC) profile. (A, B) TSP-1 binding to platelets (A) and RBCs (B) of human whole blood under static conditions (n = 5). (C) TSP-1 binding to platelets and RBCs isolated from thrombi (dissolved with Accutase®) or from flow through after flow chamber experiments at a shear rate of 1,700 s^{-1} (n = 5). Results represent mean values ± SEM. *p < 0.05; **p < 0.01; ***p < 0.001 tested by ordinary One-Way ANOVA with Sidak's multiple comparison post-hoc test. Rest = resting; plts = platelets; RBCs = red blood cells; WB = whole blood; ADP = adenosine diphosphate; CRP = collagen related peptide; PAR4 = protease-activated receptor 4 activating peptide; w/o mAb = without primary TSP-1 monoclonal antibody.

Under dynamic conditions, TSP-1 binding to platelets that have been isolated from the thrombi as well as from the flow through were notably elevated compared to IgG controls. Interestingly, TSP-1 binding to platelets in the thrombus was strongly upregulated compared to platelets from the flow through ($p < 0.001$) (Fig. 24C). Furthermore, TSP-1 binding to RBCs isolated from thrombi and from the flow through was strongly increased compared to IgG controls. Again, significantly enhanced TSP-1 binding to RBCs isolated from the thrombus was observed compared to TSP-1 binding to RBCs from the flow through ($p < 0.001$) (Fig. 24C). These results suggest that not the shear stress leads to enhanced TSP-1 binding to platelets and RBCs but the incorporation of cells into the thrombus.

4.4.3 Unaltered TSP-1 binding to platelets and RBCs under static and dynamic conditions after inhibition of PS or CD36

Next, it was of utmost interest if PS serves as a potential binding partner for TSP-1 as described for RBCs [190], or if CD36 might be a receptor for TSP-1 binding to platelets and RBCs under static and dynamic conditions. Flow cytometric analysis of TSP-1 binding to the platelet and RBC surface was measured in human whole blood.
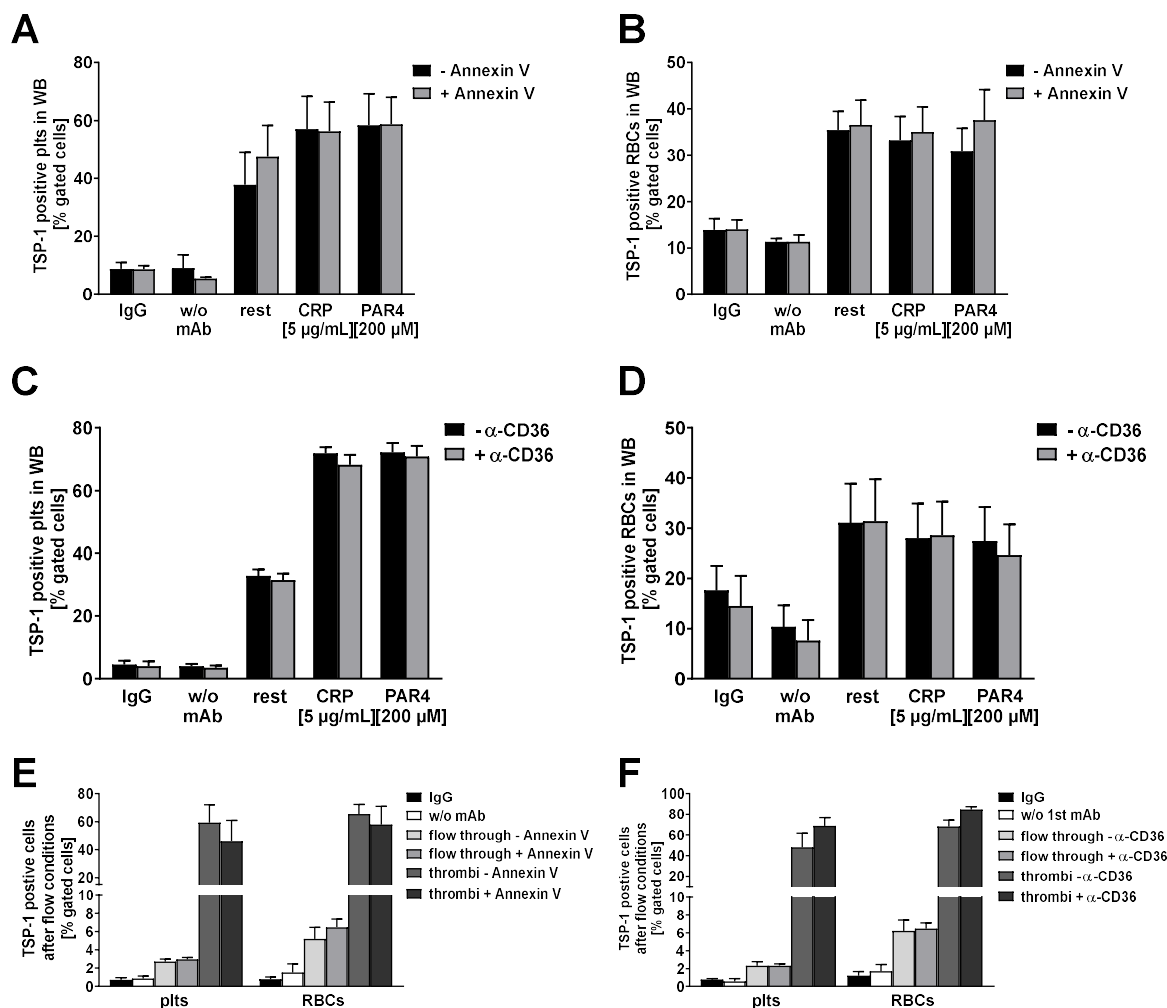
Figure 25: Unaltered TSP-1 binding to platelets and RBCs under static and dynamic conditions after CD36 or PS inhibition. (A – F) Human platelets and RBCs were analyzed by flow cytometric analysis regarding their specific side scatter (SSC) and forward scatter (FSC) profile. (A, B) TSP-1 positive platelets (A) and RBCs (B) in the absence and presence of recombinant Annexin V inhibiting protein [5 µg/mL] were analyzed using human whole blood (n = 4). (C, D) TSP-1 positive platelets (C) and RBCs (D) in the absence and presence of a CD36 mAb [2 µg/mL] were analyzed in human whole blood (n = 4). (E, F) TSP-1 binding to platelets (E) and RBCs (F) under dynamic conditions after flow chamber experiments at a shear rate of 1,700 s^{-1}. Indicated cells were isolated from thrombi (dissolved with Accutase®) (n = 5). Results represent mean values ± SEM. Rest = resting; plts = platelets; RBCs = red blood cells; WB = whole blood; CRP = collagen related peptide; PAR4 = protease-activated receptor 4 activating peptide; w/o mAb = without primary TSP-1 monoclonal antibody.

As shown in figure 25, inhibition of PS with recombinant Annexin V inhibiting protein [5 µg/mL] (Fig. 25A, B) or CD36 with a CD36 mAb [2 µg/mL] (Fig. 25C, D) resulted in unaltered TSP-1 binding to both, platelets and RBCs under static conditions. Additionally, no alterations in TSP-1 binding to platelets and RBCs after the inhibition with both inhibitors under dynamic conditions were observed (Fig. 25E, F).

4.4.4 Altered TSP-1 binding to murine CD36-deficient RBCs under static and dynamic conditions

To clarify the role of PS and/or CD36 for TSP-1 binding on the platelet and RBC surface, flow cytometric analysis was performed. TSP-1 binding to both $Cd36^{-/-}$ or WT platelets and RBCs in whole blood under static conditions as well as in thrombi and flow through after flow chamber experiments at a shear rate of 1,700 s^{-1} was analyzed. Under static conditions, no alterations in TSP-1 binding to $Cd36^{-/-}$ resting or CRP-stimulated platelets were detected (Fig. 26A). However, TSP-1 binding to $Cd36^{-/-}$ RBCs after platelet activation with CRP was significantly decreased compared to WT RBCs ($p = 0.0174$) (Fig. 26B). In addition, TSP-1 binding to isolated RBCs from thrombi after flow chamber experiments revealed a significant reduction of TSP-1 binding to $Cd36^{-/-}$ RBCs compared to WT RBCs ($p = 0.0180$) (Fig. 26C). TSP-1 binding to platelets was unaltered as already observed under static conditions. No statistical differences in TSP-1 binding to platelets and RBCs were obtained after PS inhibition. These results demonstrate that erythroid CD36 plays a major role for TSP-1 binding of RBCs under static and dynamic conditions while CD36 plays no major role for TSP-1 binding to platelets, neither under static nor under dynamic conditions.
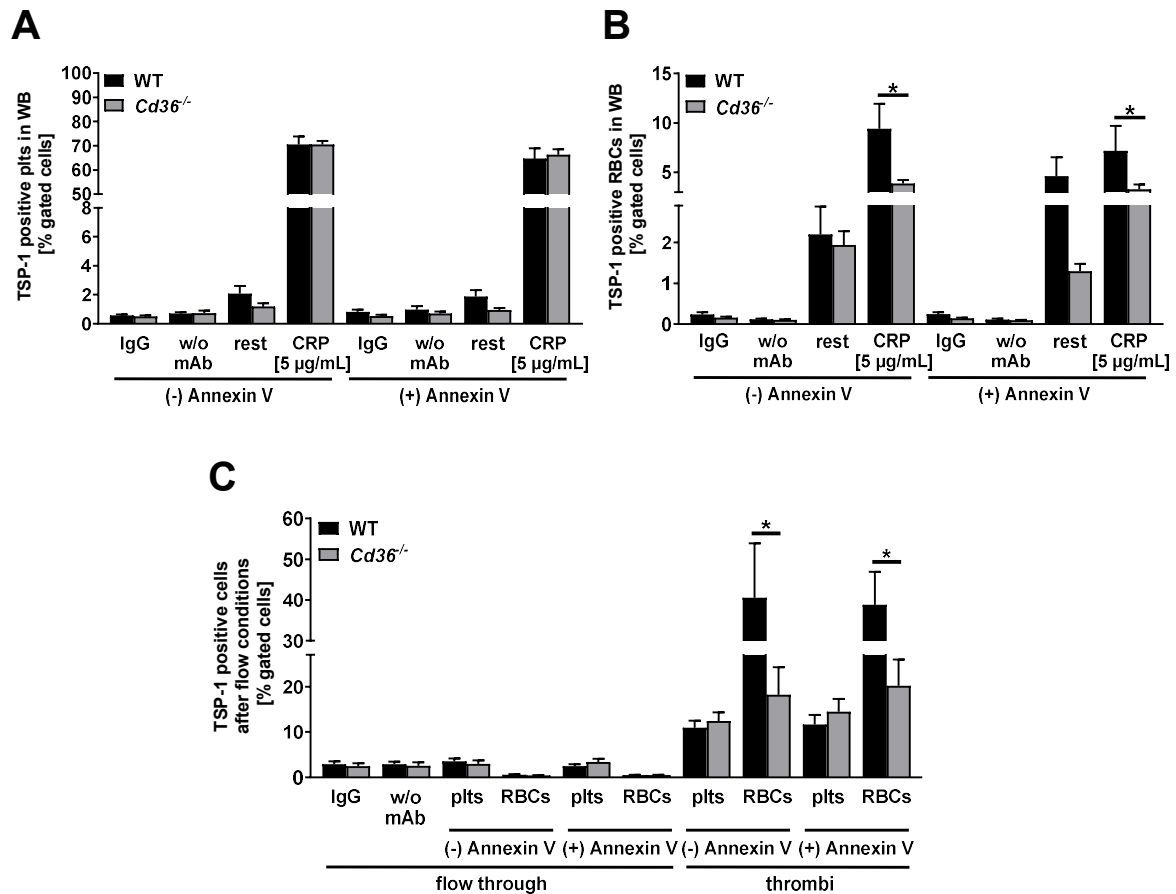
Figure 26: Genetic deletion of erythroid CD36 leads to decreased TSP-1 binding under static and dynamic conditions. (A – C) Murine *Cd36^-/-* or WT platelets and RBCs isolated from whole blood were analyzed by flow cytometric analysis regarding their specific side scatter (SSC) and forward scatter (FSC) profile. (A, B) TSP-1 positive platelets (A) and RBCs (B) were analyzed in the absence and presence of recombinant Annexin V inhibiting protein [5 µg/mL] (n = 10). (C) TSP-1 binding to platelets and RBCs isolated from thrombi (dissolved with Accutase®) after flow chamber experiments measured by flow cytometric analysis (n = 9). Flow cytometric analysis of TSP-1 binding (static conditions) was performed together with Alicia B. (M. Sc.). Results represent mean values ± SEM. *p < 0.05 tested by Two-Way ANOVA with Sidak's multiple comparison post-hoc test. Rest = resting; plts = platelets; RBCs = red blood cells; WB = whole blood; CRP = collagen related peptide; w/o mAb = without primary TSP-1 monoclonal antibody; WT = wild type.

4.5 Active recruitment of RBCs to collagen-adherent platelets

Decades ago, the general knowledge about RBCs was that they are essential for oxygen transport and supply to cells and tissues, the delivery of carbon dioxide to the lungs and influence rheology in a passive manner. However, no active role for RBCs in hemostasis and procoagulant activity for thrombus formation was assumed.

Recently it was shown that platelet-RBC interactions are important for the externalization of PS at the RBC membrane that attributes a direct role for RBCs in thrombin generation, thrombus formation and –stabilization in hemostasis and thrombosis [63]. However, little is

known about the interaction of RBCs to other cells. It was demonstrated that the interaction of RBCs to ECs is limited under physiological conditions. Under pathophysiological conditions it was shown that the adhesion of RBCs to ECs is mediated by adhesion molecules, e. g. ICAM-4 and VCAM-1 [66]. In addition, RBCs can bind to the subendothelial matrix when the endothelium is damaged [66].

Due to the fact that RBCs can directly bind to platelets under venous shear rates [67], the active recruitment of RBCs to collagen-adherent platelets at arterial shear rate was investigated. Furthermore, these experiments were performed with inhibition of several surface molecules of platelets and RBCs and TSP-1 which is released after the activation of platelets to analyze which interaction partners were responsible for the recruitment of RBCs to the growing thrombus.

4.5.1 Several surface molecules are involved in the active recruitment of RBCs to collagen-adherent platelets

Flow chamber experiments were performed to investigate the active recruitment of RBCs to collagen-adherent platelets. Briefly, isolated human platelets were stimulated with ADP [10 µM] and allowed to adhere to collagen [200 µg/mL] coated coverslips to establish a uniform collagen-adherent platelet matrix (Fig. 27A). Four million isolated human RBCs per µL were utilized for flow chamber experiments that were performed using a shear rate of 1,700 s^{-1}. Tethering RBCs were detected during a 3 min video (representative single image; Fig. 27B). In sharp contrast to venous conditions [67], no stable adherent RBCs were observed under arterial shear rates. After inhibition of PS on both cell types, a significant decrease of tethered RBCs on collagen-adherent platelets under flow was detected ($p = 0.0022$) (Fig. 27C). To distinguish between the influence of PS exposure on platelets and RBCs, either collagen-adherent platelets or isolated RBCs were preincubated with recombinant Annexin V inhibiting protein. The treatment of collagen-adherent platelets ($p = 0.0334$) and isolated RBCs ($p = 0.0356$) with recombinant Annexin V inhibiting protein led to notably decreased tethering of RBCs compared to control experiments without recombinant Annexin V inhibiting protein (Fig. 27D). To investigate if the interaction of platelets and RBCs via FasL and FasR is also responsible for the recruitment of RBCs to the growing thrombus, RBCs were coincubated with a FasR blocking antibody and platelets with hDcR3. Thereby the tethering of RBCs to collagen-adherent platelets was significantly decreased after the blocking of FasL ($p = 0.0353$) and FasR ($p = 0.0094$) (Fig. 27E, F). Also the blocking of CD36 at the surface of platelets ($p = 0.0379$) and RBCs ($p = 0.0457$) led to strongly decreased tethering of RBCs on collagen-adherent platelet compared to IgG

controls (Fig. 27G, H). In addition, blocking of TSP-1 on the surface of collagen-adherent platelets using a mAb revealed a reduction in tethering of RBCs compared to controls ($p = 0.032$) (Fig. 27I). Only the inhibition of integrin $\alpha_{IIb}\beta_3$ on platelets with abciximab showed unaltered numbers of tethered RBCs (Fig. 27J).

Taken together, the recruitment of RBCs to collagen-adherent platelets is an active process controlled by several surface molecules on the platelet and the RBC membrane including CD36, PS and FasR on RBCs and the release of TSP-1 from platelets together with PS, CD36 and FasL on the platelet membrane.
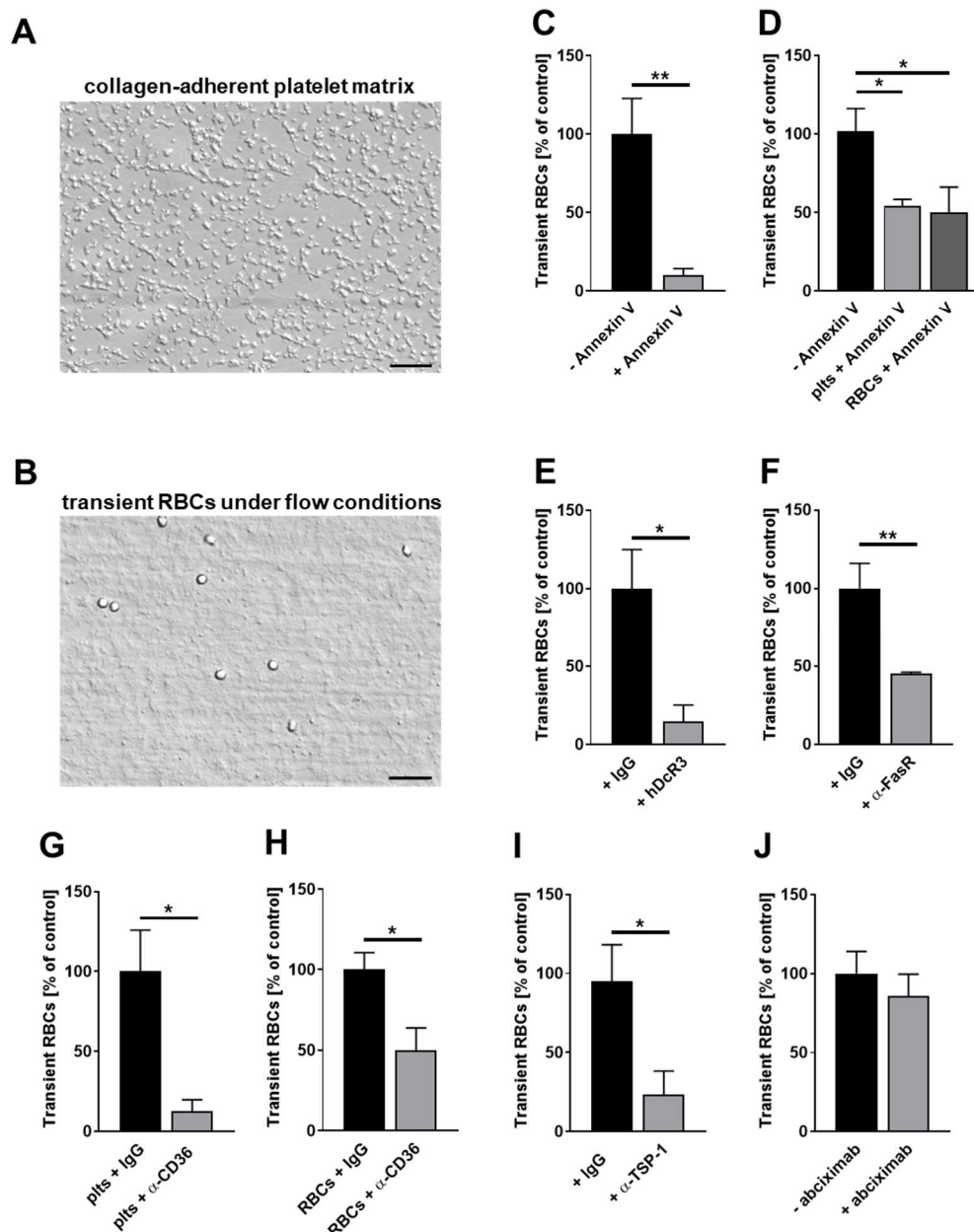
Figure 27: Inhibition of various surface molecules on RBCs and platelets as well as TSP-1 blockage leads to impaired recruitment of RBCs to collagen-adherent platelets under arterial shear rates. (A) Representative image of the collagen-adherent platelet matrix. Isolated human platelets were stimulated with ADP [10 µM] and subsequently allowed to adhere on collagen [200 µg/mL] coated coverslips for 10 min. Scale bar: 50 µm. (B) Representative image of tethered RBCs during a 3 min time period using a shear rate of 1,700 s^{-1}. Scale bar: 50 µm. (C) Simultaneously, both cell types were incubated with recombinant Annexin V inhibiting protein [5 µg/mL] before flow chamber experiments compared to untreated cells (n = 4). (D) Experiments with isolated platelets and RBCs independently treated with or without recombinant Annexin V inhibiting protein (n = 4). (E – J) Experiments with isolated platelets and RBCs treated with: hDcR3 (platelets [10 µg/mL]) (E); a FasR mAb (RBCs [10 µg/mL]) (F); a CD36 mAb (G, platelets and H, RBCs [2 µg/mL]); a TSP-1 mAb (platelets [2 µg/mL] compared to IgG controls (I) (n = 3 – 5). (J) Abciximab treated platelets [10 µg/2 million cells] compared to platelets without treatment (n = 4). Results represent mean values $\pm$ SEM. *p < 0.05; **p < 0.01 tested by One-Way ANOVA with Sidak's multiple comparison post-hoc test (D) and by student's t-test (C, E – J). Plts = platelets; RBCs = red blood cells; Annexin V = recombinant Annexin V; hDcR3 = human decoy receptor 3; α-TSP-1 = TSP-1 monoclonal antibody; α-CD36 = CD36 monoclonal antibody; α-FasR = FasR monoclonal antibody; abciximab = integrin α$_{IIb}$β$_3$ inhibitor.

4.6 Translational approach in abdominal aortic aneurysm

Platelet-RBC interactions could be of utmost interest in cardiovascular diseases under pathophysiological conditions such as AAA. AAA is often combined with the formation of an intraluminal thrombus (ILT), a multi-layered, biological active neo-tissue with its own microenvironment, which occurs in 70 – 80% of the cases [168]. AAA is associated with increased thrombin generation but unaltered fibrinolysis [191, 192]. The analysis of makers for coagulation such as D-dimer or thrombin-antithrombin III-complex (TAT) in AAA patients showed increased plasma levels [193]. According to the recent literature, platelets play a role in AAA progression [8], but the complexity and the underlying mechanisms have not been identified yet. In addition, RBCs were found in the ILT, but it is believed so far that this is because of a passive entrapping of RBCs. However, RBCs are incorporated into the mural thrombus and due to hemagglutination at the ILT ROS is generated through increased oxidative stress and the participation of released hemoglobin in chemical reactions [122]. Nevertheless, the role of RBCs in AAA development and possible interactions with platelets need to be investigated in further detail to answer the question, if the above mentioned molecular mechanisms between platelets and RBCs such as FasL/FasR and TSP-1/CD36 do play a role in the progression of AAA.

First, platelet activation and PS exposure of platelets and RBCs isolated from whole blood of AAA patients and AMCs were analyzed using flow cytometry. Next, FasL on the platelet surface and FasR on the RBC surface as well as TSP-1 binding to RBCs and platelets and CD36 expression of both cell types were determined by flow cytometric analysis. Moreover, Western blot analysis was performed to investigate protein expression of TSP-1 and CD36 of platelets and RBCs. Finally, histological analysis using immunofluorescence staining of platelets and RBCs as well as the presence and distribution of TSP-1 in the ILTs and the aortic wall of AAA patients was performed.

4.6.1 Preactivated platelets in patients with AAA

To study platelet activation, β_3 integrin externalization, P-selectin externalization and activation of integrin $\alpha_{IIb}\beta_3$ was determined by flow cytometry using whole blood from AAA patients and AMCs. As shown in figure 28A, the exposure of β_3 integrin at the platelet surface was unaltered following platelet activation with indicated agonists. The activation of integrin $\alpha_{IIb}\beta_3$ was significantly increased in resting platelets ($p = 0.015$), after stimulation with ADP ($p = 0.0362$), low concentrations of CRP ($p = 0.0411$) and PAR4 peptide stimulation ($p = 0.0461$) compared to AMCs (Fig. 28B). In addition, significantly enhanced P-selectin

externalization was observed in resting platelets (*p = 0.0402*) and after platelet activation with low concentrations of CRP (*p = 0.0226*).
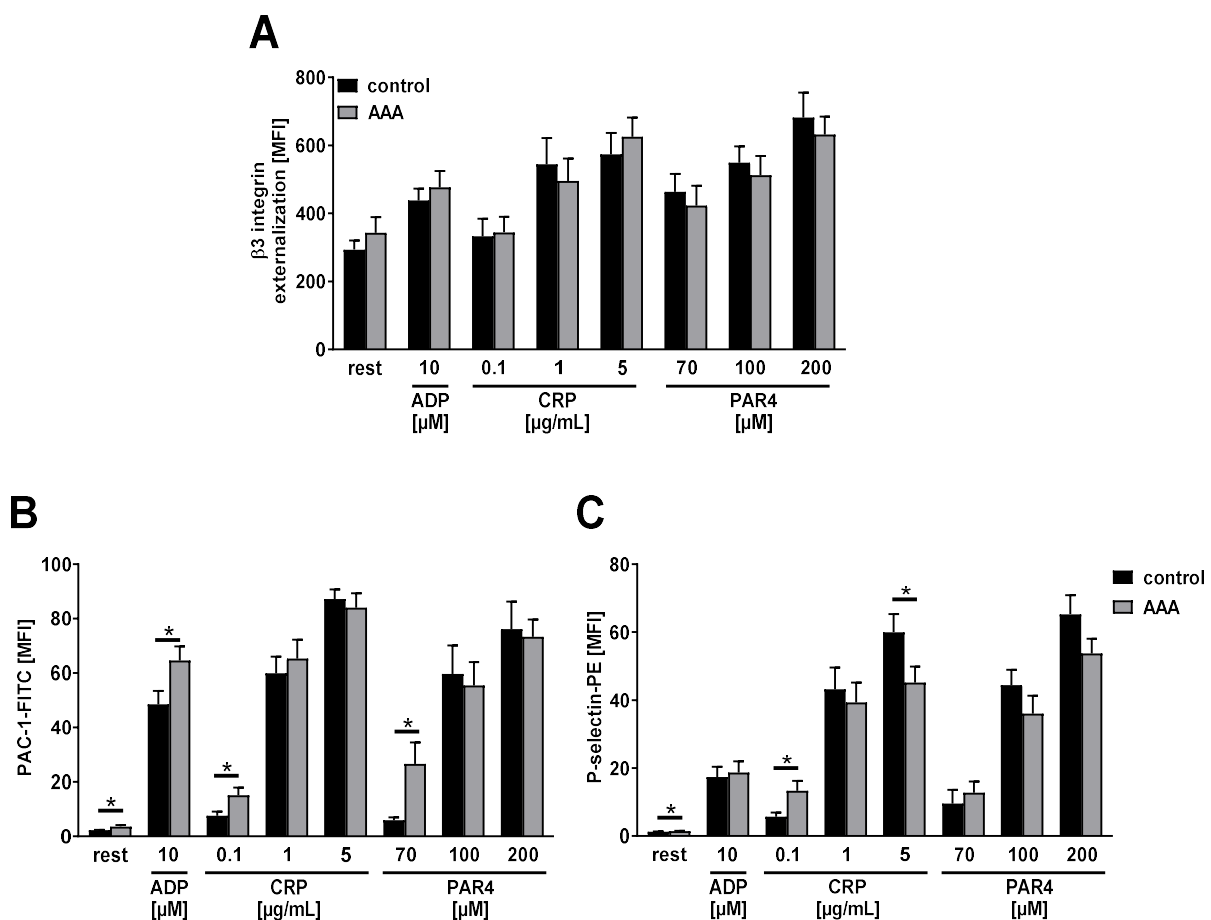
Figure 28: Altered platelet activation in patients with AAA. (A – C) Human platelets isolated from whole blood of AAA patients were activated with indicated agonists and analyzed by flow cytometric analysis regarding their specific side scatter (SSC) and forward scatter (FSC) profile. (A) Externalization of the β_3 integrin subunit of integrin $\alpha_{IIb}\beta_3$ (CD61-PE) on the surface of platelets was measured by flow cytometry (n = 8). (B, C) Platelet activation was analyzed by determination of active integrin $\alpha_{IIb}\beta_3$ (PAC-1-FITC, n = 12) and P-selectin externalization on the platelet surface (P-selectin-PE, n = 10). AMCs served as controls (n = 6 - 12). Results represent mean values $\pm$ SEM. *p < 0.05 tested by unpaired student's t-test. AAA = abdominal aortic aneurysm; control = age-matched controls; rest = resting; ADP = adenosine diphosphate; CRP = collagen related peptide; PAR4 = protease-activated receptor 4 activating peptide; MFI = mean fluorescence intensity.

In contrast, strong platelet activation with high concentrations of CRP showed decreased P-selectin exposure of platelets from AAA patients compared to AMCs (*p = 0.0491*) (Fig. 28C). These results provide strong evidence that platelets are in a preactivated state in the peripheral circulation of AAA patients. Moreover, the threshold of platelet activation with low agonist concentrations is decreased in AAA patients. Taken together these data suggests elevated platelet activation in AAA patients.

4.6.2 FasL externalization and PS exposure is enhanced under pathological conditions in AAA

Next, we followed up the question if PS exposure at the surface of platelets and RBCs was altered in whole blood of AAA patients compared to AMCs.
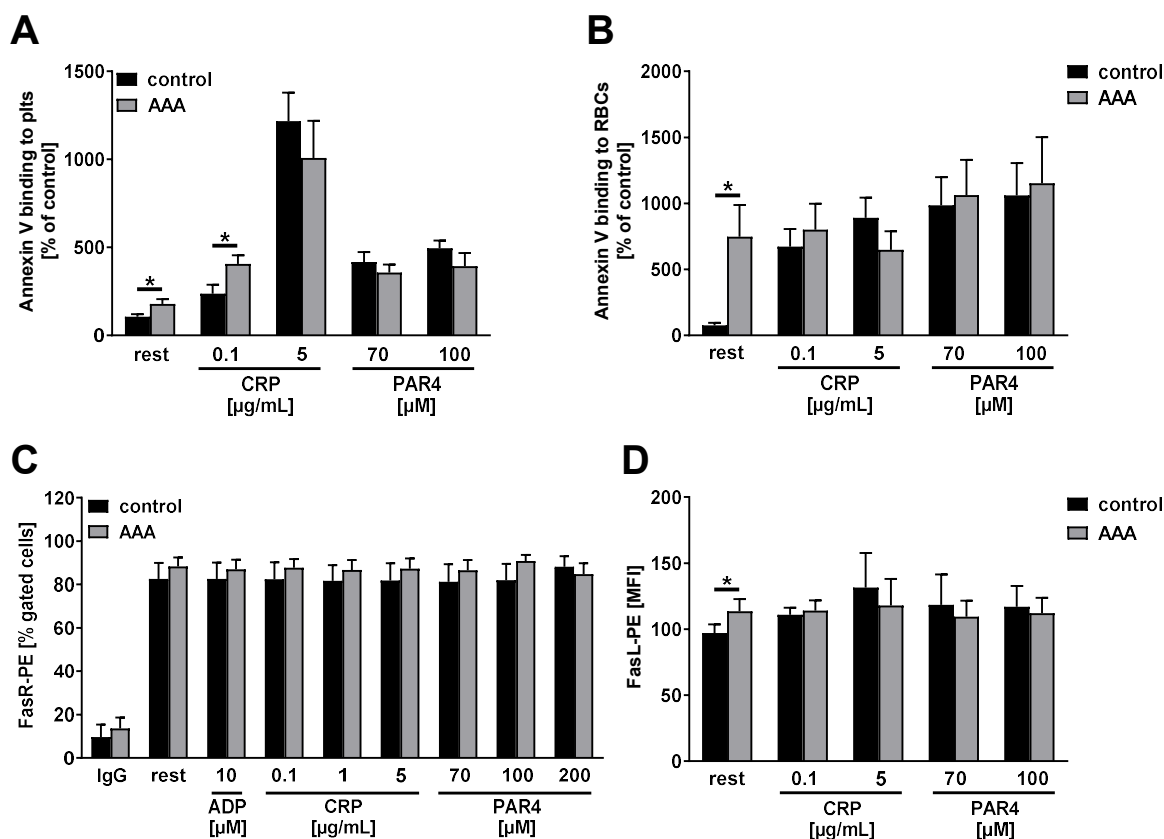
Figure 29: Enhanced FasL externalization and PS exposure of platelets and RBCs from AAA patients. (A – D) Human platelets isolated from whole blood of AAA patients were activated with indicated agonists and analyzed by flow cytometric analysis regarding their specific CD235-FITC (RBCs) and specific CD42-PE/FITC (platelets) profile. (A, B) Annexin V binding to platelets (A) and RBCs (B) was measured by flow cytometry with the cell specific markers CD235-FITC (RBCs) and CD42-PE (platelets) (n = 7). (C) FasR externalization at the surface of RBCs (FasR-PE) was measured via flow cytometry. RBCs were detected with the cell specific marker CD235-FITC (n = 8). (D) FasL externalization at the platelet surface (FasL-PE) was determined via flow cytometry. Platelets were detected with the cell specific marker CD42-FITC (n = 7). AMCs served as controls (n = 5 – 7). Results represent mean values $\pm$ SEM. *p < 0.05 tested by unpaired student's t-test. AAA = abdominal aortic aneurysm; control = age-matched controls; rest = resting; ADP = adenosine diphosphate; CRP = collagen related peptide; PAR4 = protease-activated receptor 4 activating peptide; MFI = mean fluorescence intensity.

Platelets and RBCs isolated from AAA patients showed increased Annexin V binding to resting platelets ($p = 0.0415$) and RBCs ($p = 0.0417$) (Fig. 29A, B). In addition, Annexin V binding to platelets was increased following the activation of platelets with low concentrations of CRP [0.1 µg/mL] ($p = 0.0377$) (Fig. 29A). Furthermore, FasL externalization on the surface

of platelet from AAA patients was enhanced under resting conditions (*p = 0.0148*) (Fig. 29D) compared to AMCs, while no change was detected for FasR externalization at the surface of RBC surface (Fig. 29C). These results are in line with the above described preactivated state of platelets isolated from AAA patients compared to AMCs (Fig. 28B, C).

4.6.3 Impaired TSP-1 and CD36 protein expression in patients with AAA

To investigate if the interaction of platelets and RBCs via TSP-1 and CD36 plays a role in the pathology of AAA, Western blot analysis of lysates and supernatants from isolated platelets, RBCs and platelets in the presence of RBCs from AAA patients and AMCs were performed. For TSP-1 as shown in figure 30A, one band in platelet lysates was detected at the predicted size of 185 kDa (black arrow) [99] without any differences between AAA patients compared to AMCs. However, platelet activation led to a decrease in the signal of the 185 kDa band in platelet lysates of AAA patients. The platelet lysates of the AMCs showed the same trend (Fig. 30A). In contrast to the 185 kDa full length TSP-1 form, the cleaved 110 kDa (black arrowhead) fragment was increased in lysates of resting platelet (*p = 0.014*) and CRP-stimulated platelets (*p = 0.011*) of AAA patients compared to AMCs (Fig. 30A). The most apparent effect visible in the lysates is that the 185 kDa and 110 kDa bands are reduced in activated platelets and almost disappeared in the presence of RBCs. Furthermore, the lysates using RBCs alone showed that RBCs do not express TSP-1. The most prominent band in the supernatants of platelet samples was the monomeric full length form of TSP-1 (185 kDa), which was increased upon platelet activation with CRP in the absence or presence of RBCs. Again, no difference could be observed between the supernatant of AAA patients or AMCs. Besides that, a decrease in the 185 kDa band was detected in the supernatant of resting platelets from AAA patients and AMCs compared to their corresponding lysates (Fig. 30A, B). Furthermore, the 185 kDa form of TSP-1 was increased in the supernatant of CRP-stimulated platelets coincubated with RBCs from AAA patients or AMCs compared to the corresponding lysate. This was also observed for the cleaved form of TSP-1 using platelets and RBCs form AAA patients and AMCs. Besides the expression pattern of TSP-1 in AAA patients and AMCs, CD36 protein expression was determined as well. CD36 expression of the highly glycosylated form at 88 kDa (black arrow) and the native form at 53 kDa (black arrowhead) was unaltered in AAA patients compared to AMCs (Fig. 30C). Additionally, the two other bands with molecular weights of ~ 48 kDa and ~ 40 kDa (blue arrowheads) were detectable in platelet lysates. Despite this, no differences could be detected neither for the ~ 48 kDa nor for the ~ 40 kDa. In the lysates where RBCs were added another band appeared at a size of ~ 65 kDa (blue arrow) which was already shown above in RBC lysates of healthy human volunteers (Fig. 19A). This band has not

been described yet. Also, no other band was detectable in the lysates where only RBCs were present.
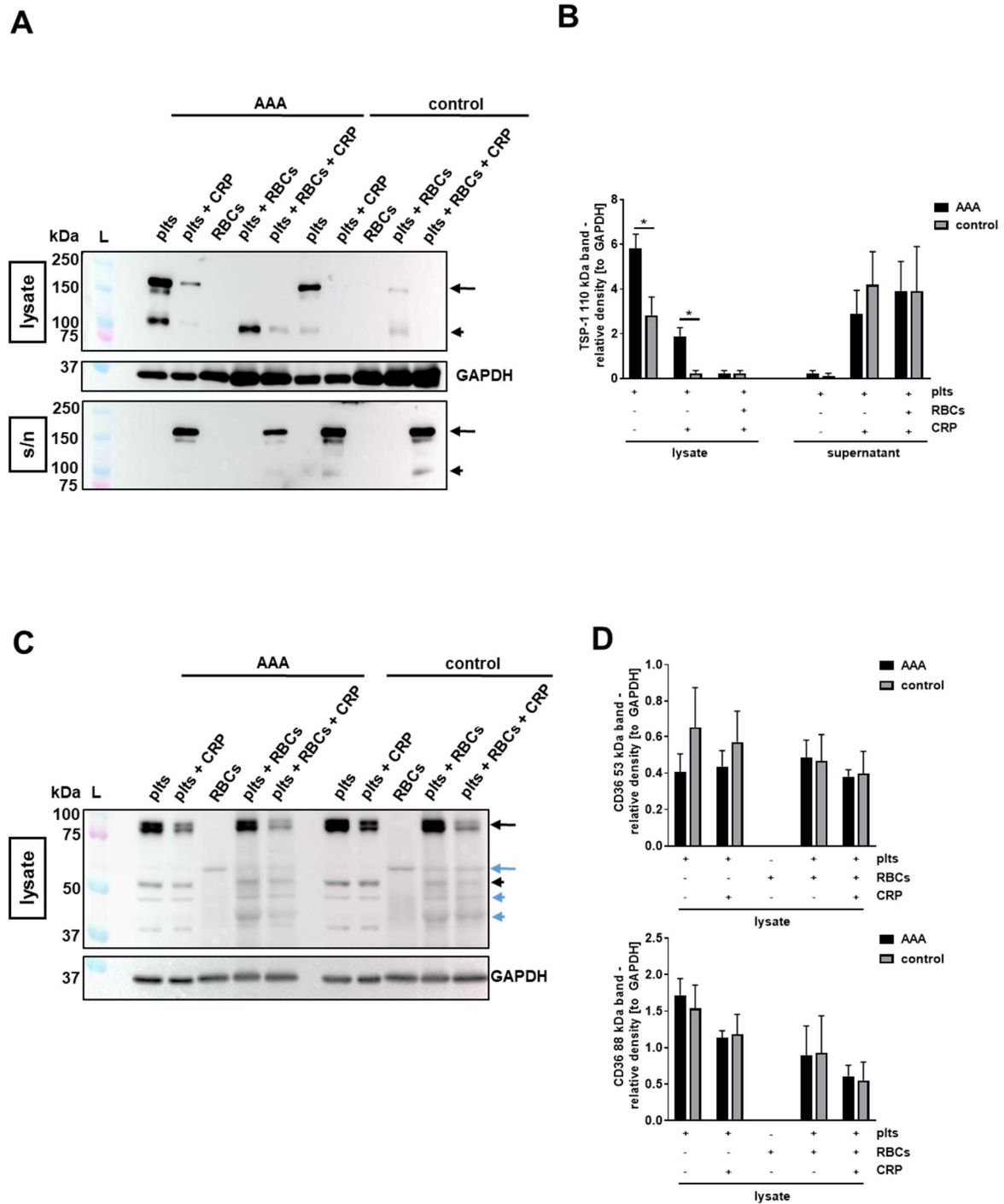
Figure 30: Altered TSP-1 and unaltered CD36 expression pattern in AAA patients compared to AMCs. (A, C) In the absence or presence of RBCs, isolated human platelets were activated with CRP [5 µg/mL] for 5 min at 37 °C or used under resting conditions. Subsequently lysates and supernatants were generated and Western blot analysis was performed (n = 3). GAPDH was used as housekeeping protein. (B, D) Statistical evaluation of TSP-1 and CD36 protein expression normalized to GAPDH. Plts = platelets; RBCs = red blood cells; AAA = abdominal aortic aneurysm; controls = age-matched controls; ADP = adenosine diphosphate; CRP = collagen related peptide; L = ladder. Results represent mean values $\pm$ SEM. *$p < 0.05$ tested by Two-Way ANOVA with Sidak's multiple comparison post-hoc test.

4.6.4 Role of TSP-1 under pathophysiological conditions in AAA

To study protein expression of CD36 at the surface of platelets and RBCs and TSP-1 binding to these cells, flow cytometric analysis was performed using whole blood from AAA patients and AMCs. CD36 protein expression on the platelet and RBC surface of AAA patients was unaltered compared to AMCs (Fig. 31A, B). In contrast, TSP-1 binding to platelets of AAA patients was significantly increased following platelet activation with low concentrations of CRP ($p = 0.0236$) and PAR4 peptide ($p = 0.0203$) compared to AMCs (Fig. 31C), whereas no alterations of TSP-1 binding to RBCs could be observed (Fig. 31D).
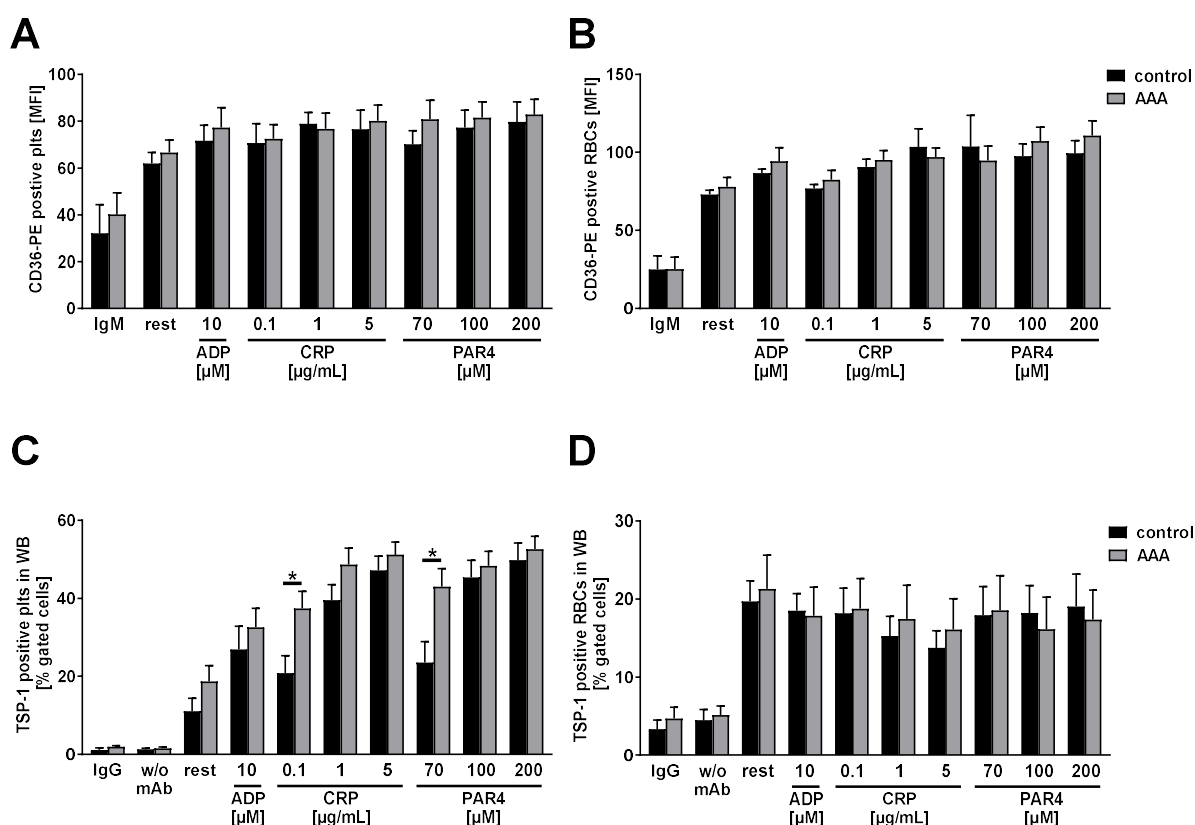
Figure 31: Enhanced TSP-1 binding to activated platelets of AAA patients. (A, B) CD36 expression of human platelets (A) and RBCs (B) from AAA patients was determined by flow cytometric analysis regarding their specific side scatter (SSC) and forward scatter (FSC) profile with indicated agonists (n = 8). RBCs were detected with the cell specific marker CD235-FITC. (C, D) TSP-1 positive platelets (C) and RBCs (D) were determined regarding their specific side scatter (SSC) and forward scatter (FSC) profile following platelet activation with indicated agonists (n = 10). AMCs served as controls (n = 5 – 6). Results represent mean values $\pm$ SEM. *$p < 0.05$ tested by unpaired student's t-test. Rest = resting; plts = platelets; RBCs = red blood cells; WB = whole blood; AAA = abdominal aortic aneurysm; control = age-matched controls; ADP = adenosine diphosphate; CRP = collagen related peptide; PAR4 = protease-activated receptor 4 activating peptide; w/o mAb = without primary TSP-1 monoclonal antibody; MFI = mean fluorescence intensity.

4.6.5 Deposition of platelets, RBCs and TSP-1 in the ILT of AAA patients

TSP-1 is important for vascular remodeling by regulating the vascular response to injury [162]. Besides the role of TSP-1 in angiogenesis, platelet-released TSP-1 is known to be important for thrombus formation and –stabilization [92, 114]. Of note, TSP-1 levels can increase rapidly after tissue injury as observed in cardiovascular diseases [101]. Therefore, the impact of TSP-1 for the progression of AAA was analyzed by histological staining of the ILT and the aortic wall of AAA patients. The same histological staining was performed with thrombi from peripheral vessels of patients who underwent thrombectomy. The thrombi of these two patient groups were analyzed to gain new insights in the structure of thrombi which are generated through a peripheral vessel occlusion in comparison to thrombi which are generated through a chronic event as it occurs in AAA (Fig. 32). CD235-positive RBCs and GPIX-positive platelets in the ILT of AAA patients were observed as well as in thrombi from patients who underwent thrombectomy (Fig. 32).
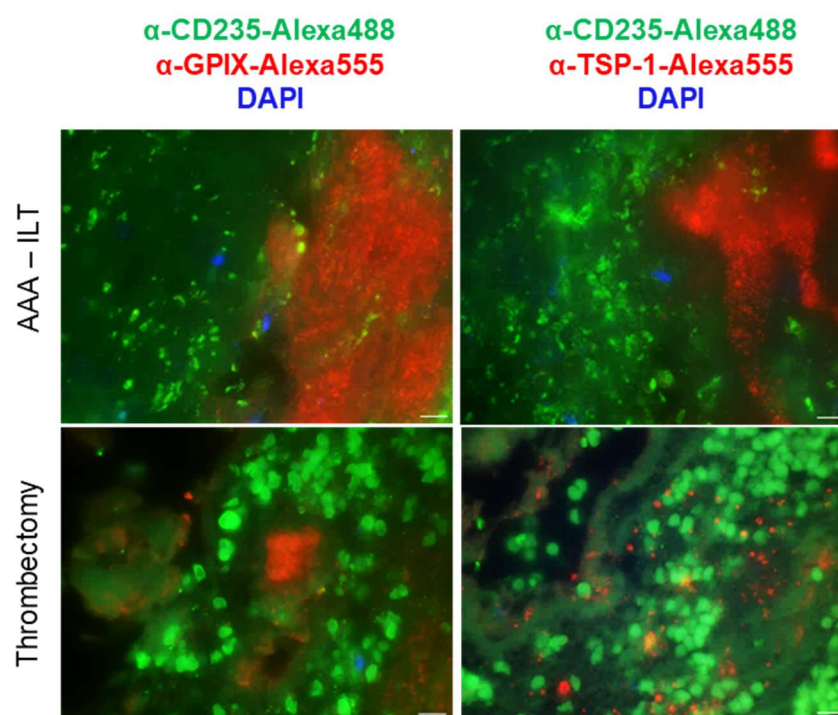
Figure 32: Deposition of platelets, RBCs and TSP-1 in the ILT of AAA patients and in thrombi isolated from patients who underwent thrombectomy. Paraffin-embedded sections (5 micron) of ILT from AAA patients and of thrombi from patients who underwent thrombectomy (thrombi from peripheral vessels) were stained with a GPIX antibody [20 µg/mL] to detect platelets, with a CD235 antibody [0.5 µg/ml] to detect RBCs and with a TSP-1 mAb [20 µg/mL] (n = 4). (IgG served as control, same concentration as respective primary antibody were used, shown in figure 35, appendix). 4',6-diamidino-2-phenylindole (DAPI) was used for nucleus staining. Representative fluorescent images with 1000-fold magnification are shown. Scale bar: 10 µm. AAA = abdominal aortic aneurysm; ILT = intraluminal thrombus.

GPIX-positive platelets are bundled in indefinite areas in thrombi of AAA patients and patients who underwent thrombectomy. Furthermore, immunofluorescence staining of TSP-1 in thrombi from peripheral vessels showed a distribution of TSP-1 all over the analyzed samples, while the ILT of AAA patients showed only areas of TSP-1 accumulation. In both thrombi RBCs were located near to platelets and TSP-1-rich areas. Nucleated cells were of high diversity in all individual samples. For the ILT samples this is in line with the current literature [194]. It is of utmost interest to analyses different parts of the ILT to determine the detailed distribution of platelets, RBCs and TSP-1 and to clarify the role of these cells and TSP-1 in the progression of an ILT in near future.

4.6.6 Platelets and RBCs in the aortic wall of AAA patients

To investigate the distribution of platelets and RBCs and TSP-1 in the aortic wall of AAA patients, immunofluorescence staining was performed. GPIX-positive platelet aggregates in the aortic wall of AAA patients was observed, accompanied by platelets located near to nuclear cells and CD235-positive RBCs, providing a first hint for a direct cell-cell contact of platelets with immune cells, smooth muscle cells, ECs or RBCs (Fig. 33). In addition, TSP-1 becomes visible in the extended media near to the former intima and in the upper part of the adventitia (Fig. 33).

These results suggest that platelets and RBCs as well as TSP-1 accumulate in the aortic wall of AAA patients. However, if this represents a pathological mechanism and/or if the accumulation of platelets, RBCs and TSP-1 is relevant for the progression of the AAA remains elusive and has to be investigated in near future to increase our understanding of the AAA pathology.
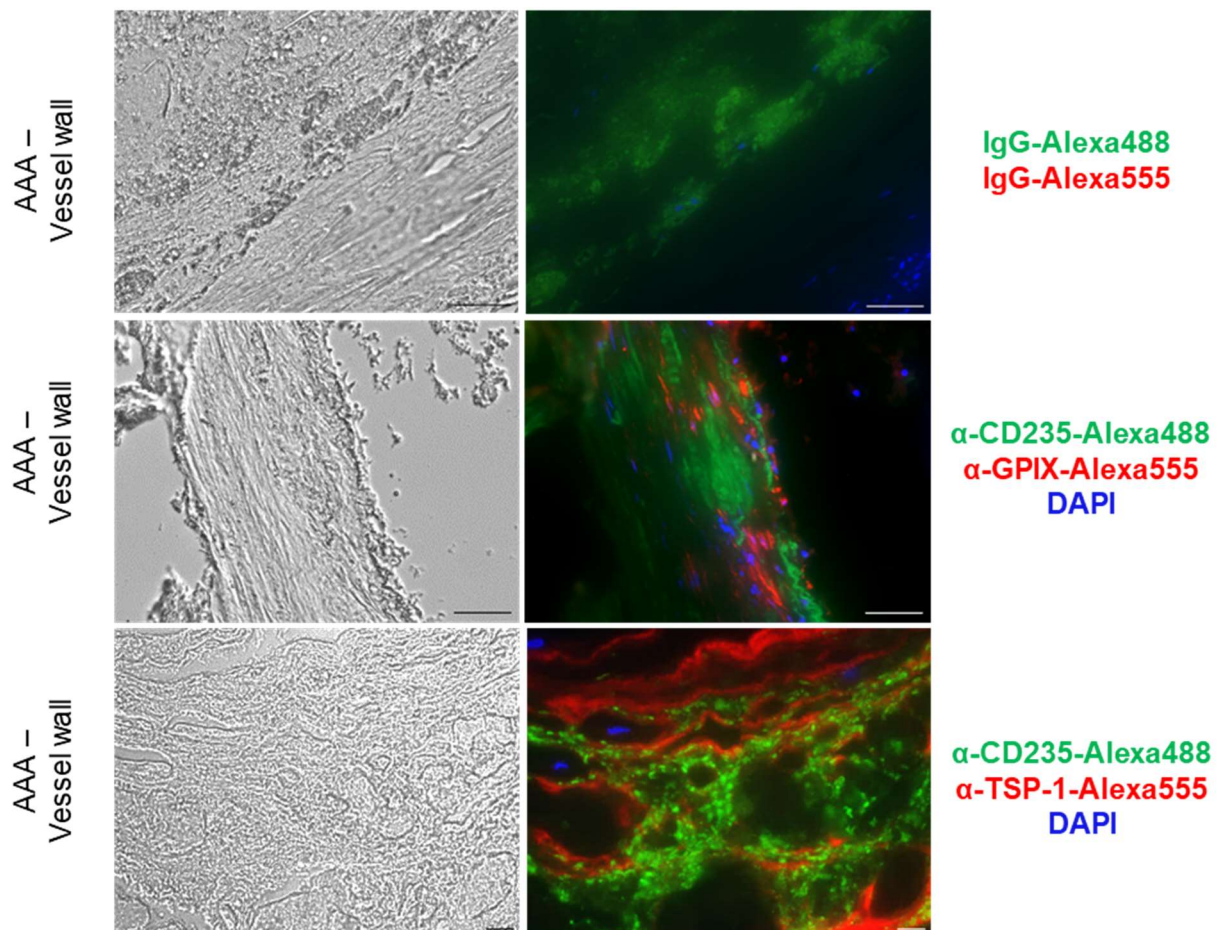
Figure 33: Deposition of platelets, RBCs and TSP-1 in the aortic wall of AAA patients. Paraffin-embedded sections (5 micron) of the aortic wall of AAA patients were stained with a GPIX antibody [20 µg/mL] to detect platelet, with a CD235 antibody [0.5 µg/ml] to detect RBCs and with a TSP-1 mAb [20 µg/mL] (n = 4). IgG served as control (same concentration as respective primary antibody) (n = 4). Additionally, fluorescence emission at 488 nm showed autofluorescence of red blood cells in IgG control and autofluorescence of elastic lamina in vessel wall samples. 4',6-diamidino-2-phenylindole (DAPI) was used for nucleus staining. Representative DIC and fluorescent images with 400-fold (upper and middle panels; Scale bar: 50 µm) and 1000-fold magnification (bottom panel; Scale bar: 10 µm) are shown. All channels are shown in the fluorescent images in figure 36, appendix. AAA = abdominal aortic aneurysm; DIC = Differential interference contrast.

5. Discussion

Platelets are relevant in many physiological and pathophysiological processes, but their main function is the regulation of hemostasis and thrombosis. It is important to note the role of platelets and platelet activation in cardio- and cerebrovascular diseases. It was shown that uncontrolled platelet activation, accompanied by three-dimensional thrombus formation, leads to vessel occlusion, loss of oxygen supply and tissue injury resulting in stroke or myocardial infarction [3, 4, 6]. Furthermore, platelets are relevant in the pathology of arteriosclerosis because of their proinflammatory properties. They release proinflammatory mediators, which affect the inflammatory processes of other cells such as ECs, SMCs, and leukocytes [3]. Their ability to interact with various cell types like ECs, monocytes, macrophages and RBCs is essential for the modulation of these pathological events. For a long time RBCs were considered as passive bystanders to support thrombus formation and hemostasis; however, recent studies revealed that RBCs are crucial for thrombus formation and actively support hemostasis [55]. After vessel wall injury, RBCs, the forgotten players in hemostasis and thrombosis, interact with several peripheral blood components such as ECs, monocytes, lymphocytes, other RBCs, platelets, bacteria, plasma proteins and the ECM [56]. An increased or abnormally high hematocrit leads to enhanced blood viscosity and thrombotic events, e.g. in polycythemia vera [59], whereby anemic mice showed attenuated hemostasis and prolonged occlusion times [63]. RBCs can not only modulate hemostatic events by influencing rheology, but also by direct cell-cell interactions with ECs and platelets as well as by providing a procoagulant surface upon activation [63, 195-197]. However, the impact of platelet-RBC interaction in thrombus formation and hemostasis and the underlying mechanism are poorly understood.

5.1 Platelet-RBC interaction mediated by FasL/FasR is essential for platelet adhesion, aggregation, and three-dimensional thrombus formation *in vitro*

Recently, Klatt *et al.* (2018) were able to demonstrate that a direct cell-cell contact of platelets and RBCs via FasL/FasR interaction plays a pivotal role for the externalization of PS on the RBC membrane that attributes a direct role for RBCs to thrombin generation, thrombus formation and –stabilization in hemostasis and thrombosis [63].

Results of this thesis were published in Klatt *et al.* (2018) and showed that FasL/FasR-mediated signaling of platelets and RBCs is essential for effective thrombus formation, aggregation and clotting *ex vivo*. Flow chamber experiments with either cell type specific

deletion of FasR on RBCs or FasL on platelets revealed a reduced thrombus formation compared to WT controls (Fig. 9). Furthermore, a reduced number of incorporated RBCs were detected in these thrombi (Fig. 10). These results provide strong evidence for an interaction of FasL on the platelet and FasR on the RBC surface that accounts for reduced thrombus formation. In the same study of Klatt *et al.* (2018), the loss of platelet-RBC interactions in *FasR*^{-/-} and *FasL*^{-/-} mice led to significantly decreased PS exposure on the surface of platelets and RBCs under static and dynamic conditions (Fig. 11). Furthermore, a direct mechanism, and a human relevance, for the induction of PS exposure on RBCs via FasL/FasR interaction were confirmed by antibody-mediated blocking studies with FasL and FasR [63]. Thus, a direct mechanism for the induction of PS exposure on RBCs in a growing thrombus was shown. To date, this is one of the first studies which demonstrates a direct mechanism of platelet-RBC interaction and the influence of RBCs by providing a procoagulant surface in thrombus formation.

Furthermore, RBCs are necessary for platelet aggregation which was shown in aggregometry experiments (Fig. 12). While PRP in the presence of RBCs showed aggregation comparable to whole blood in humans and mice, samples of PRP without RBCs revealed decreased aggregation (Fig. 12A, B). In contrast, dextran induced RBC aggregation and the reduction of RBCs electrostatic repulsion by neuraminidase showed no influence on platelet aggregation [198]. In this study of Reinhart and colleagues they came to the conclusion that platelet aggregation without flow was not affected by RBC aggregation, but they did not compared PRP in the absence or presence of RBCs and the influence of the release of chemical components by RBCs. These results might lead to the assumption that the effect of RBCs on platelet aggregation in our experiments (Fig. 12A, B) is independent of RBC aggregation, but may depend on the influence of released chemical components of RBCs. The release of ADP and ATP induce platelet activation [180, 181] thus might influence platelet aggregation. Therefore, experiments with "ghosts" (cell component free RBCs) have to be performed in near future.

Using whole blood of *FasR*^{-/-} mice and platelet-specific FasL KO mice revealed a defective platelet aggregation after collagen stimulation (Fig. 12C, E), which supports the hypothesis that FasL/FasR interaction of platelets and RBCs is important for aggregate formation and stable clotting. Surprisingly, whole blood samples from *FasR*^{-/-} mice showed unaltered platelet aggregation after PAR4 peptide stimulation (Fig. 12D), whereas whole blood from platelet-specific FasL KO mice showed decreased aggregation after this stimulation (Fig. 12F). On the one hand, these results might account for a platelet aggregation defect that is independent of FasL/FasR-mediated signaling, or on the other hand, one explanation could be the different agonist-dependent platelet activation using collagen or thrombin.

Thrombin caused a notable increase of PS externalization on the surface of platelets in *FasR*^{-/-} mice compared to the collagen-dependent stimulation. In line with these results, stimulation with thrombin leads to a higher calcium mobilization in platelets compared to collagen-dependent stimulation [199], which is necessary for PS exposure [200]. Noteworthy, platelet-specific FasL KO mice showed decreased PS exposure of FasL-deficient platelets in resting state and after agonist stimulation compared to WT mice (Fig. 18C, D), which might explain the platelet aggregation defect of these mice. These results could account for an integrin $\alpha_{IIb}\beta_3$ defect resulting in defective outside-in signaling. Furthermore, decreased PS in these mice suggests a dysfunctional inside-out signaling of FasL-deficient platelets after stimulation. Both aspects have to be investigated in near future.

Alongside platelet aggregation, clot retraction experiments with PRP in the absence or presence of RBCs were performed. Samples with PRP alone showed a significantly higher volume of the remaining fluid after clot retraction compared to samples with PRP in the presence of RBCs, indicating a higher contractility of platelets without RBCs in their proximity (Fig. 13). As it is known that RBCs decrease clot contractility in clot retraction experiments in a non-biochemical manner [201], this explains these differences in the volume of the remaining fluid from PRP in the absence or presence of RBCs (Fig. 13D). Interestingly, clot retraction experiments with FasL-deficient platelets in the presence of WT RBCs revealed decreased contractility compared to either WT RBCs and platelets or *FasR*^{-/-} RBCs in the presence of WT platelets (Fig. 13D). This suggests that the defective contractility of FasL-deficient platelet is independent of FasL/FasR-mediated signaling. Furthermore, platelet-specific FasL KO mice showed decreased PS exposure that is important for local thrombin generation and thus fibrin formation. It is tempting to speculate that these results of FasL-deficient platelets in clot retraction experiments might be explained by a defective outside-in signaling due to disturbed integrin $\alpha_{IIb}\beta_3$ ligand binding or signaling. This disturbed $\alpha_{IIb}\beta_3$ could lead to defective PS exposure of FasL-deficient platelets, resulting in altered clot retraction. Furthermore, it is of utmost interest to investigate intracellular signaling of FasL-deficient platelets to exclude possible defects in PLCγ2 and Src signaling important for clot retraction. Nevertheless, in both aggregation and clot retraction experiments, integrin inside-out and integrin outside-in signaling plays a dominant role and FasL/FasR interaction influenced aggregation. This suggests that FasL/FasR-mediated interaction of platelets and RBCs affect integrin signaling and is important for secondary hemostasis.

FasL/FasR interaction is a key regulator of apoptosis under physiological [202] and pathophysiological conditions [203]. In general, FasL/FasR interactions lead to intracellular caspase-8 signaling, followed by direct or indirect (via mitochondria) caspase-3 activation, which results in PS exposure and cell apoptosis [204]. This signaling pathway plays an

important role in the regulation of the immune system and the progression of cancer [183, 205, 206]. The apoptosis of FasR positive tumor cells is induced by FasL exposure on activated platelets [207] and was relevant in a mouse model of stroke *in vivo* [208]. Unexpectedly, thrombus formation in human whole blood and PS exposure of isolated platelets and RBCs was shown to be not dependent on caspases (Fig. 14), although caspase signaling following FasL binding to FasR has been shown to reflect a general mechanism to induce apoptosis in target cells [183, 184]. However, in RBCs there might be another signaling pathway that leads to PS exposure after the activation of FasR. Bratosin and Berg demonstrated that the ionophore ionomycin (induces intracellular calcium changes) rapidly induced RBC shape changes and PS exposure [209, 210]. Moreover, calcium mobilization in murine platelets leads to flippase activity, followed by PS exposure to the outer membrane of the cell [211]. Thus, calcium mobilization and intracellular calcium changes in RBCs might also account for PS exposure on RBCs after FasR activation, this has to be investigated in near future. It is tempting to speculate that the formation of a procoagulant surface of RBCs is driven by intracellular calcium mobilization, whereas caspase signaling seems to play no role. An acid sphingomyelinase is also activated in response to FasR activation, leading to ceramide production and cell stress that also might account for PS exposure at the surface of RBCs [212].

Taken together, platelet FasL is a ligand for FasR on the RBC membrane that is important for direct cell-cell contacts of platelets and RBCs upon thrombus formation. The findings in this study demonstrated a new mechanism of FasL/FasR interaction on the surface of platelets and RBCs that mediates the exposure of PS on the surface of RBCs important for thrombus formation and platelet aggregation of platelets. Apart from this, FasR-mediated effects on thrombus formation seem to exceed the effects of FasL [63]. This suggests that other interaction partners on platelets are present, which induces FasR activation on RBCs besides FasL.

5.2 The integrin $\alpha_{IIb}\beta_3$ serves as a potential binding partner for FasR

It is known that platelets have different integrin receptors on their surface such as integrin $\alpha_{IIb}\beta_3$ (fibrinogen receptor), integrin $\alpha_5\beta_1$ (fibronectin receptor) or $\alpha_6\beta_1$ (laminin receptor). Each integrin binds to different ligands of the ECM to induce intracellular signaling cascades in platelets. The constitutive and the activation-dependent expression of different integrins mediate platelet adhesion, aggregation, and thrombus formation after vascular injury [40]. Furthermore, integrins mediate cell-cell attachment and they are important for cell migration [213]. However, the platelet-RBC interaction mediated by integrins on the surface of platelets

is currently poorly understood. Erythroid ICAM-4 was suggested to be a novel ligand for integrin $\alpha_{IIb}\beta_3$ on the platelets surface [214, 215]. Furthermore, inhibition of ICAM-4/$\alpha_{IIb}\beta_3$ interactions revealed decreased incorporation of RBCs into thrombi providing strong evidence for integrin $\alpha_{IIb}\beta_3$ to play a role in platelet-RBC interaction [216]. Here, β_3 integrin externalization, platelet degranulation and integrin activation was determined to study the influence of RBCs on platelet activation (Fig. 15). This study showed an increased externalization of β_3 integrin on the surface of platelets in the presence of RBCs compared to platelets alone (Fig. 15A), whereas no alteration in integrin activation or platelet degranulation was detected (Fig. 15B, C). This was in contrast to other studies, which showed that platelet-RBC interaction is necessary for platelet activation. They showed enhanced integrin activation, P-selectin externalization, thromboxane production, and ADP release in platelet suspension in the presences of RBCs [217-219]; however, they did not determine β_3 integrin on the surface of platelets. As mentioned above, RBCs are able to release ADP and ATP, resulting in platelet activation [180, 181] and thus might influence the upregulation of β_3 integrin. To prove if β_3 integrin externalization on platelets is upregulated following direct cell-cell contact of RBCs and platelets or the release of chemicals from RBCs, experiments with "ghosts" could be performed as well. An impact of RBCs in the upregulation of β_3 integrin was supported by the fact that inhibition of FasR at the RBC surface led to decreased β_3 integrin externalization on platelets (Fig. 16A). This result was also confirmed with *FasR*$^{-/-}$ RBCs (Fig. 16C). In contrast, genetic deletion or antibody-mediated inhibition of FasL on platelets revealed no changes in β_3 integrin externalization (Fig. 16B, D). This gave a first hint that platelet-RBC interaction affects the regulation of β_3 integrin on the surface of platelets. Furthermore, it suggests that integrin $\alpha_{IIb}\beta_3$ could be involved in platelet-RBC interaction upon thrombus formation, e.g. as a binding partner of FasR on the surface of RBCs. This hypothesis was confirmed through adhesion studies of ADP-stimulated platelets which were allowed to adhere to immobilized FasR protein in which two different receptor antagonists were used to block integrin $\alpha_{IIb}\beta_3$, namely tirofiban and abciximab (Fig. 17A, B). Both drugs are categorized as glycoprotein (GP)-IIb/IIIa-receptor-antagonists and are included in clinical trials [187]. The inhibitory effect of each antagonist was comparable to the inhibition of FasL (hDcR3). This suggested an important role of platelet integrin $\alpha_{IIb}\beta_3$ as a binding partner for FasR on the RBC surface. Surprisingly, an additive effect of abciximab and hDcR3 on ADP-stimulated platelets was observed. If saturation of $\alpha_{IIb}\beta_3$ and FasL was achieved by the inhibitors, this observation could be explained by the influence of abciximab on another platelet receptor, the vitronectin receptor ($\alpha_V\beta_3$), which is necessary for platelet adhesion and aggregation [220, 221]. This abciximab induced effect on integrin $\alpha_V\beta_3$ suggests that this integrin could be another binding partner for FasR at the RBC membrane and has to be investigated in near future. The influence of

different receptors on the platelet surface was excluded with additional experiments using CHO cells and A5 CHO cells [222, 223]. In these experiments, A5 CHO cells were able to bind to immobilized FasR (Fig. 17C) but not CHO cells due to the lack of integrin $\alpha_{IIb}\beta_3$ on the surface of these cells, confirming the binding of FasR to integrin $\alpha_{IIb}\beta_3$. Taken together, these results provide the first evidence that FasR on the RBC membrane interacts with integrin $\alpha_{IIb}\beta_3$ at the platelet surface.

Furthermore, this study showed that integrin $\alpha_{IIb}\beta_3$ is not only important for the binding to FasR, but also affects the exposure of PS on platelets under static conditions (Fig. 18A). This impact of integrin $\alpha_{IIb}\beta_3$ on PS exposure of platelets has already been shown. The outside-in integrin $\alpha_{IIb}\beta_3$ signaling enhanced calcium mobilization and PS exposure after strong platelet stimulation [224, 225]. In $\alpha_{IIb}\beta_3$-deficient platelets from patients with Glanzmann's thrombasthenia, PS exposure was dramatically decreased. Furthermore, using different glycoprotein (GP)-IIb/IIIa-receptor-antagonist led to decreased PS exposure on the platelet surface [224]. In contrast to platelets, less is known about the mechanisms of PS exposure on RBCs during platelets-RBC interactions. However, inhibition of integrin $\alpha_{IIb}\beta_3$ (with abciximab) on the platelet surface led to decreased PS exposure on the RBC membrane (Fig. 18B). This is the first indication that integrin $\alpha_{IIb}\beta_3$ not only affects PS exposure of platelets but also of RBCs and further supports a role for integrin $\alpha_{IIb}\beta_3$ in platelet-RBC interactions and procoagulant activity of RBCs. Thus, platelet-RBC interaction via integrin $\alpha_{IIb}\beta_3$/FasR interaction is another mechanism, besides FasL/FasR-mediated interaction, to support procoagulant activity of RBCs after platelet-RBC interaction [63]. Interestingly, the inhibition of both FasL and integrin $\alpha_{IIb}\beta_3$ showed no further decrease in PS exposure of both cell types compared to single blocking experiments (Fig. 18). This could be related to different reasons: first, the saturation of both receptors with specific inhibitors was not fully accomplished, thus allowing still an interaction between RBCs and platelets via this signaling pathway. Second, other yet unknown mechanisms of platelet-RBC interaction play a role in the exposure of PS on both cell types. However, these inhibition studies imply that PS exposure on platelets and RBCs is induced to either FasL/FasR interaction or $\alpha_{IIb}\beta_3$/FasR interaction. In addition, the inhibition of FasL was only successful after platelet activation, which indicated an activation-dependent exposure of FasL on the surface of the platelets. To exclude inefficient blockage of the FasL by hDcR3 and to confirm these inhibitory experiments, additional experiments were performed using platelet-specific FasL KO mice (Figure 18C, D). In these experiments an additive effect on PS exposure of both cell types was observed when FasL-deficient platelets were incubated with an integrin $\alpha_{IIb}\beta_3$ inhibitor. This indicated an additional effect of $\alpha_{IIb}\beta_3$/FasR interaction of RBCs and platelets to induce

PS exposure. However, differences could be due to the use of different species or inefficient blocking of FasL by hDcR3.

Further investigation of integrin $\alpha_{IIb}\beta_3$/FasR interaction, e.g. in thrombus formation and aggregation, is not possible because inhibition of integrin $\alpha_{IIb}\beta_3$ abolishes platelet aggregation because fibrinogen binding of integrin $\alpha_{IIb}\beta_3$ is crucial for these processes [226]. Nevertheless, it would be of great interest to investigate platelets from GT patients and the adhesion of these platelets to immobilized FasR. These experiments will give new insights about the amount of integrin $\alpha_{IIb}\beta_3$ or the binding capacity that is necessary for FasR binding. Furthermore, the results of platelet integrin $\alpha_{IIb}\beta_3$ binding to FasR on the RBC surface, could be strengthened by direct binding studies, such as biolayer interferometry [227] that should be performed in near future.

5.3 Erythroid CD36 and platelet-released TSP-1 support thrombus formation under arterial shear rate through binding of TSP-1 to RBCs

In this study, another possible receptor-ligand interaction of platelets and RBCs via CD36 and TSP-1 was investigated. It is well known that these two proteins play a major role in the pathology of cardiovascular diseases and cancer [101, 108, 228]. Under physiological conditions binding of TSP-1 to CD36 on the surface of ECs is essential for maintaining the normal architecture of the vascular system [108]. Furthermore, recent studies showed that CD36 signaling can lead to a prothrombotic platelet phenotype and is essential for platelet adhesion to immobilized TSP-1 [83, 87, 92, 114]. However, it was controversially discussed whether or not RBCs, especially matured RBCs, express CD36 on their surface. It was commonly accepted for a long time that only erythroid progenitor cells express CD36, which is lost through maturation of the cell [56]. In this study, expression levels of CD36 on the surface of platelets and RBCs was investigated using six different healthy volunteers that showed a constitutive expression of CD36 on the surfaces of both cell types (Fig. 19C) which was also described by the group of van Schravendijk [81]. However, no differentiation of young and matured cells was analyzed. Nevertheless, it is published that CD36 on platelets has a wide range of expression levels in healthy volunteers, from almost 200 to 14,000 copies per cell [229], which is in contrast to the constitutive expression described in this thesis (Fig. 19C). These differences might depend on the experimental setup and the different binding domains of the utilized antibodies. In addition, Western blot analysis of CD36 using platelet lysates revealed four different glycosylation and splicing forms

(Fig. 19A). The most prominent band appears at 88 kDa, which is described as the fully glycosylated functional receptor. The 53 kDa band is at the predicted size of the unglycosylated full length form of the protein [188]. Quantification of both, the 88 kDa and 53 kDa band revealed no significant differences between resting and activated platelets. In addition, Western blot analysis revealed a different glycosylation form of erythroid CD36 compared to platelets. The major CD36 glycosylated form of platelets is the 88 kDa variant; however, the apparent band of CD36 on the surface of RBCs was approximately ~ 65 kDa in size (figure 19A). While it is known that CD36 in erythroblasts appears at a size of ~ 78 kDa [189], the 65 kDa band has not been described yet. It remains currently uncertain whether the CD36 receptor has different functions on platelets or RBCs. The analysis of the platelet supernatant revealed the presence of an unglycosylated form of the soluble CD36 that is independent of platelet stimulation or the presence of RBCs. The release of CD36 may depend on additional copies of CD36 stored in platelet α-granules that could be released upon platelet activation [70]. Another study demonstrated that the soluble CD36 is secreted by platelets exclusively via microparticle (MP) release [230]. Interestingly, no soluble CD36 was observed in the supernatant of RBCs suggesting that RBCs are not able to release CD36.

TSP-1, the native ligand of CD36, is the most abundant protein in platelet α-granules with 101,000 copies per cell [94]. It is released after platelet activation and it is already proven that TSP-1 mediates platelet adhesion by a CD36-dependent pathway [92]. However, RBCs do not express TSP-1, as demonstrated by Western blot analysis (Fig. 23A). TSP-1 expression and fragmentation was analyzed in lysates of resting and activated platelets, where TSP-1 appeared in two different forms. The upper band could represent the monomeric full length form (185 kDa) [99] and was notably decreased in activated platelets compared to resting controls, indicating the secretion of the 185 kDa form after platelet activation (Fig. 23B). As for the full length monomeric form of TSP-1, the amount of the cleaved TSP-1 form (110 kDa) decreased upon platelet activation, indicating the secretion of both forms. In line with that, both TSP-1 forms were detected in the supernatant of activated platelets (Fig. 23A). Surprisingly, the 185 kDa form of TSP-1 could not be detected when platelets were incubated with RBCs, independently of platelet activation. Simultaneously, the cleaved form (110 kDa) was increased in resting platelets that were coincubated with RBCs which may indicate a role of prototypical cleavage of TSP-1 by RBCs. It is known that the cleavage of TSP-1 by the metalloproteinase ADAMTS1 results in a 37 kDa N-terminal and 110 kDa C-terminal monomeric fragment [104]. However, RBCs do not express ADAMTS1, but this result implies somehow the cleavage of TSP-1 by RBC due to an unknown process. But it is described that platelets exhibit an unknown elastase [231] and elastase induces the

full degradation of TSP-1 [104]. For example, it is tempting to speculate that the platelet-RBC interaction or the proximity of RBCs and platelets lead to an increase in the release of elastase from platelets, which might induce the degradation of TSP-1. In contrast to this full degradation of TSP-1, e.g. the proteolytic cleavage of TSP-1 by thrombin results in two fragments with a molecular weight of 25 kDa (N-terminal fragment) and 160 kDa (C-terminal fragment) [103-105].

As mentioned above, results of Klatt *et al.* were able to demonstrate that procoagulant surface is one of the main mechanisms of RBCs to support thrombus growth and formation [63]. Interaction of RBCs and platelets induces the exposure of PS and supports thrombin generation. To investigate if the exposure of PS on RBCs and β_3 integrin on platelets is also regulated by CD36 signaling, Annexin V binding and β_3 integrin externalization was analyzed under static conditions using a CD36 blocking antibody. The inhibition of CD36 affected both, the externalization of β_3 integrin on platelets and the procoagulant activity of platelets and RBCs (Fig. 19D – F). In detail, the inhibition of CD36 on RBCs and the subsequent coincubation with platelets led to reduced externalization of β_3 integrin at the platelet surface, while no effect was observed after CD36 inhibition on platelets alone (Fig. 19D). The PS exposure of platelets and RBCs was decreased as well when CD36 was inhibited only on the RBC membrane (washed RBCs) (Fig. 19E, F). Interestingly, CD36 inhibition of platelets led to decreased PS exposure of RBCs. This was confirmed by either $Cd36^{-/-}$ RBCs or platelets, leading to reduced PS exposure only on the RBC surface (Fig. 22B). However, impaired PS exposure of platelets was not observed (Fig. 22C). Thus, not only erythroid CD36 but platelet CD36 affects procoagulant activity of RBCs. Furthermore, these results show that erythroid CD36 is important for β_3 integrin externalization on the platelet surface.

Different flow chamber experiments were performed to analyze the contribution of CD36 and TSP-1 to thrombus formation and PS exposure under dynamic conditions at high shear rates. In line with the steady state expression of CD36 on the cell surface of platelets and RBCs in flow cytometry experiments under static conditions (Fig. 19C), a constitutive expression of CD36 on the cell surface of platelets and RBCs from flow through was obtained (Fig. 20F). Surprisingly, CD36 expression on RBCs that have been isolated from thrombi, was notably increased compared to RBCs from flow through, while it remained almost unaltered on the platelet surface (Fig. 20F). This result was unexpected, as it is known that platelets and RBCs have only limited abilities to synthesize proteins [232, 233]. In addition, it raises the question of which mechanism is responsible for the upregulation of CD36 on the membrane of RBCs that have been isolated from thrombi. One possible mechanism could be the release of CD36 positive MPs from platelets and/or RBCs. The existence of such CD36 positive MPs has already been described. CD36 positive MPs in the

plasma of healthy human volunteers were of EC origin, but in obese people CD36 positive MPs were primarily derived from RBCs and platelets [234]. Furthermore, CD36 was shown to be a "core protein" of plasma MPs in cardiovascular disease and diabetes [235]. The internalization of MPs into target cells has already been described [236]. This all points to a mechanism by which CD36 positive MPs might be able to increase the exposure of CD36 on RBCs which could lead to increased binding of TSP-1 to RBCs under dynamic conditions. Another explanation could be the binding of CD36 derived from platelet α-granules after platelet activation [70] and this may explain the increased expression of CD36 on RBCs after dynamic conditions. Thus, CD36 exposure of RBCs might be regulated by the fusion of CD36 positive MPs to the RBC membrane or by the binding of platelet derived additional copies of CD36 in the growing thrombus. In addition, TSP-1 on the surface of platelets and RBCs was dramatically increased in cells that have been isolated from thrombi (Fig. 24C). With regard to RBCs, this could be explained by the fusion of CD36 positive MPs or platelet derived CD36 and PS on their surface. In platelets, the exposure of several integrins and PS increases during thrombus formation and mediates TSP-1 binding to platelets [95]. This is the first study that showed an upregulation of CD36 on the surface of RBCs inside the growing thrombus, and suggested that binding of platelet-derived TSP-1 to erythroid CD36 is important for thrombus formation and –stabilization.

However, the significance of platelet-derived TSP-1 and CD36 for thrombus formation on a collagen matrix has been previously demonstrated [114]. Collagen-dependent thrombus formation was caused by binding of CD36 at the surface of platelets to on collagen-immobilized TSP-1, which triggered platelet activation. The potentiation of thrombus formation on a mixed collagen/TSP-1 matrix compared to a collagen matrix was shown [114]. In addition, the secretion of TSP-1 from platelet α-granules and the interaction with CD36 induces an autocrine feed-forward loop that enforces the interaction of platelets in a thrombus [92]. The group of Heemskerk performed all experiments under dynamic conditions with whole blood from humans and mice, but they did not distinguish between CD36 on the surface of platelets and RBCs [92, 114]. Moreover, they performed the experiments only at a shear rate of 1,000 s^{-1}, excluding the possibility of a shear rate dependent role of CD36. This study revealed a reduction of collagen-dependent thrombus formation after antibody-mediated inhibition of TSP-1 (Fig. 23C) and CD36 (Fig. 20A) using human whole blood that was perfused through the chamber under a shear rate of 1,700 s^{-1}. In addition, inhibition of TSP-1 under dynamic conditions led to unaltered PS exposure of platelets and RBCs that have been isolated from thrombi (Fig. 23D, E). Furthermore, the specific inhibition of CD36 on the RBC surface led to unaltered PS exposure of platelets (Fig. 20C); however, PS exposure of RBCs was impaired (Fig. 20B). In contrast to these results, the group of

Heemskerk showed no reduction of collagen-dependent thrombus formation with human whole blood (after CD36 inhibition) and murine whole blood using $Tsp\text{-}1^{-/-}$ and $Cd36^{-/-}$ mice at a shear rate of 1,000 s^{-1} compared to the here presented experiments with a shear rate of 1,700 s^{-1} using human whole blood (Fig. 20A, 23D). This implies that CD36 and TSP-1 have a shear-dependent role in thrombus formation. Thus, it is not surprising that collagen-induced thrombus formation using whole blood from $Cd36^{-/-}$ mice showed unaltered PS exposure of platelets and RBCs at a shear rate of 1,000 s^{-1}. In addition, the analysis of thrombi from $Tsp1^{-/-}$ mice revealed decreased PS exposure under a shear rate of 1,000 s^{-1} on a collagen matrix [92, 114]. These contrary observations in PS exposure might not only depend on the different shear rates but could be due to the differences between species or from differences in the experimental setup. In detail, the group of Heemskerk stained the PS at the cell membrane using Annexin V during flow chamber experiments [92]. Here, thrombi of flow chamber experiments were isolated and Annexin V binding was determined by flow cytometric analysis. Furthermore, the here presented data show that decreased collagen-dependent thrombus formation was mediated by erythroid CD36 rather than CD36 on the surface of platelets in human (Fig. 20A) and mice (Fig. 22A). This was also confirmed with experiments where thrombus formation on a collagen/TSP-1 matrix was analyzed. The effect was more pronounced when CD36 was specifically inhibited on RBCs compared to specific inhibition of platelets (Fig. 21A, B). This in turn suggests that the previously described role of CD36 in thrombus formation on a collagen and on a collagen/TSP-1 matrix depends on RBCs rather than platelets. Additionally, these results showed that erythroid CD36 signaling provides another pathway by which PS exposure is induced and confirmed the results of Klatt *et al.*, showing that PS exposure on RBCs is required for thrombus formation and growth. Apart from this, only $Cd36^{-/-}$ RBCs affected the externalization of FasL on resting platelets (Fig. 22D). This is in line with TSP-1 binding to CD36 of platelets and the feed-forward loop described by the group of Heemskerk, which probably leads to FasL externalization of platelets [92, 114]. Surprisingly, the aggregation of WT platelets was almost abolished in the presence of $Cd36^{-/-}$ RBCs. In contrast, $Cd36^{-/-}$ platelets showed only diminished aggregation when coincubated with WT RBCs (Fig. 22E). This underlines the importance of erythroid CD36 in platelet aggregation and thrombus formation. To further investigate the impact of CD36 on thrombus formation in hemostasis and thrombosis, it is of great interest to analyze CD36 deficiency in humans, especially CD36-deficient RBCs, which will be done in near future.

As mentioned above, previous investigations showed that erythroid CD36 and platelet-derived TSP-1 are essential for thrombus formation under arterial shear rates [92, 114]. However, these experiments were not suited to prove a direct binding between CD36

and TSP-1. A direct binding of TSP-1 to RBCs of healthy individuals has not been described yet. In literature, it is described that TSP-1 is able to bind to several CD36 synthetic peptides [237]. Furthermore, CD36 acts as receptor for the rosetting of *plasmodium falciparum* infected RBCs (infected RBCs, IRBCs) with uninfected RBCs and mediate the cytoadherence of IRBCs to microvascular ECs [85]. Moreover, inhibition of CD36 on either RBCs [238] or platelets [114] decreased the adhesion of both cell types to immobilized TSP-1. In sickle cell disease, PS on the RBC surface binds to immobilized or soluble TSP-1 [190]. Upon vascular injury this could mean that platelets and RBCs adhere to TSP-1 exposed by the ECM, resulting in platelet activation with subsequent platelet degranulation and PS exposure. Platelet degranulation leads to a massive release and accumulation of TSP-1, which is stored in platelet α-granules [239, 240]. The accumulation of TSP-1 is followed by the recruitment of platelets and RBCs to the growing thrombus. By cross linkage of the adherent cells via TSP-1 binding to CD36, PS, CD47 and several integrins, thrombus stabilization is facilitated [95]. Thus, binding of TSP-1 to PS and CD36 might play an important role during thrombus formation and –stabilization. However, the direct binding and interaction of erythroid CD36 or PS with TSP-1 has not been shown yet. To further analyze this hypothesis, binding experiments under static and dynamic conditions were performed. In this study it was demonstrated that under static conditions platelet-released TSP-1 binds to resting or activated platelets and to RBCs using whole blood from healthy human volunteers (Fig. 24A, B). As mentioned above, the binding of TSP-1 was markedly increased on the surface of platelets and RBCs isolated from thrombi (Fig. 24C). This may indicate that RBCs either need a direct cell-cell contact with platelets or the incorporation inside thrombi for efficient TSP-1 binding. Unexpectedly, inhibition of CD36 and PS resulted in unaltered TSP-1 binding to RBCs and platelets under static conditions in human whole blood (Fig. 25A – D). Since the static experiments showed no inhibitory effect for TSP-1 binding, flow chamber experiments were performed in order to investigate if dynamic conditions are important for the interaction (Fig. 25E, F). Surprisingly, the same results were observed under dynamic conditions. Thus, both experiments did not lead to any alterations of TSP-1 binding to platelets and RBCs after inhibition of CD36 and PS. No reduction of TSP-1 binding to resting or activated platelets was observed indicating that platelets can most likely compensate the blocking of CD36 due to multiple integrins on their membrane which can bind TSP-1 [102]. However, it was surprising that no differences in TSP-1 binding to RBCs could be observed when PS exposure and CD36 on the RBC surface were blocked, although studies of RBCs from patients with sickle cell disease showed binding of RBCs to TSP-1 via CD36 and PS [190]. To exclude inefficient blocking of CD36 as a cause of this result, further experiments with whole blood of *Cd36*^{-/-} mice under static and dynamic conditions were performed (Fig. 26). Flow cytometric analysis showed unaltered TSP-1 binding to *Cd36*^{-/-} resting and

CRP-activated platelets compared to WT (Fig. 26A). In addition, no alteration of TSP-1 binding to WT or *Cd36*$^{-/-}$ platelets isolated from the flow through or from thrombi was observed (Fig. 26C). Both experiments further support the hypothesis that platelets can compensate the loss of CD36 by other surface receptors. However, the loss of CD36 on the RBC surface led to a strong decrease of TSP-1 positive RBCs under static conditions and of RBCs incorporated into the thrombus, indicating an important role of erythroid CD36 for TSP-1 binding (Fig. 26B, C). No alterations of TSP-1 binding occurred on RBCs isolated from the flow through, which showed that the effect is not related to shear stress. Most likely the proximity of RBCs to platelets and the accumulation of TSP-1 in the growing thrombus enable strong binding of TSP-1 to the surface of RBCs. Furthermore, the differences between mice and men might be due to differences in the glycosylation of CD36 at the surface of platelets and/or RBCs. The glycosylation of human CD36 was already demonstrated in Western blot analysis but has to be investigated in murine cells in near future. Unexpectedly, TSP-1 binding to platelets and RBCs showed no differences under static and dynamic conditions when PS exposure was blocked by recombinant Annexin V. This could imply that PS is not a binding partner for TSP -1, or that Annexin V treatment does not block all PS binding sites so that TSP-1 is still able to bind to the residual PS. Therefore, complete blockage of exposed PS should be analyzed by flow cytometry. Moreover, titration of the amount of rec. Annexin V needed for sufficient blockage of PS is required.

Nevertheless, these results provide first evidence for TSP-1 binding to erythroid CD36 under both static and dynamic conditions, while platelets presumably have the ability to compensate TSP-1 binding due to different integrins such as $\alpha_{IIb}\beta_3$ and $\alpha_V\beta_3$ [102]. The highest TSP-1 binding was observed when RBCs and platelets were incorporated into a growing thrombus under flow conditions.

To summarize (Fig. 34), this study showed that platelet activation with different agonists reinforces FasL and integrin $\alpha_{IIb}\beta_3$ externalization at the platelet membrane, which results in platelet binding to FasR on the RBC surface. This is followed by PS exposure at the RBC membrane which is induced by FasL and integrin-mediated FasR activation of RBCs that is important to reinforce platelet activation, thrombus formation, fibrin generation, and thrombus stabilization. After platelet activation, platelet-released TSP-1 binds to CD36 on the surface of both, platelets and RBCs.
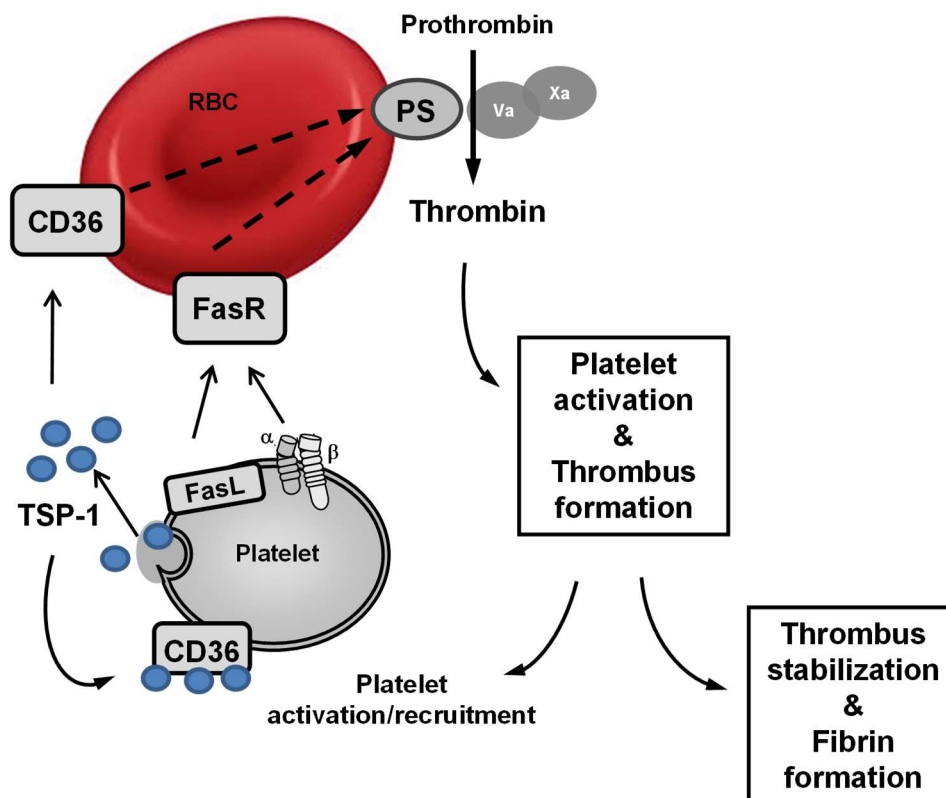
Figure 34: Different mechanisms of platelet-RBC interaction and their impact on thrombus formation. Following platelet activation, FasL and integrin $\alpha_{IIb}\beta_3$ are upregulated at the platelet surface and bind to FasR on RBCs leading to enhanced PS exposure on platelets and RBCs. This is important for local thrombin generation at the RBC and platelet surface and reinforces platelet activation, thrombus formation, fibrin generation and thrombus stabilization. Simultaneously, platelet-released TSP-1 binds to CD36 on the surface of both, platelets and RBCs, leading to PS exposure and FasL externalization of platelets. PS = phosphatidylserine; Va = activated form of Factor V; Xa = activated form of Factor X; FasL = Fas ligand; FasR = Fas receptor; CD36 = glycoprotein IV; TSP-1 = thrombospondin-1 (blue spheres).

5.4 Several surface molecules of platelets and RBCs are essential for the active recruitment of RBCs to collagen-adherent platelets in the growing thrombus

Data from this study and from other members of the research group identified different mechanisms of how platelets and RBCs interact to support thrombus formation in hemostasis and thrombosis. All these mechanisms lead to PS exposure at the RBC and platelet membrane to support local thrombin generation on the platelet and RBC surface important for thrombus growth and stability. However, it is not yet understood how and when RBCs come into contact with activated platelets following vessel injury. Especially, in AAA the recruitment of RBCs and platelets to the interface of the ILT or the aortic vessel wall is not understood. Therefore, it is of great interest to investigate the initial recruitment of RBCs to collagen-adherent platelets. A first study of Goel and colleagues who investigated deep

vein thrombosis (DVT), demonstrated tethering, adherence, and strong binding of RBCs to platelets under depressed venous shear rates [67]. Under depressed shear rates of 25 s^{-1}, approximately 600 events of tethering and residential RBCs were measured. These events inversely correlated to the shear rate, e.g. for a shear rate of 100 s^{-1}, approximately 25 RBCs were counted [67]. So far, nothing was known about the mechanisms of how RBC bind to platelets under arterial shear. Here, 8 to 50 events of tethering RBCs to collagen-adherent platelets at a shear rate of 1,700 s^{-1} were detected (over a 3 min time period). However, under these conditions no stable adhesion of RBCs to collagen-adherent platelets was measured. With regard to the previous findings of platelet-RBC interactions via FasL/FasR, integrin $\alpha_{IIb}\beta_3$/FasR and the importance of TSP-1/CD36 signaling for procoagulant activity and thrombus formation, inhibitory studies were performed to target these interaction partners at the membrane of platelets or RBCs. Surface molecules on either RBCs or collagen-adherent platelets were blocked to investigate if these mechanisms are also important for the initial contact and the recruitment of RBCs to activated platelets (Fig. 27). Interestingly, in experiments under high shear rate as well as in recently published data under depressed venous shear rates [67], inhibition of CD36 on the RBC surface was accompanied by decreased tethering of RBCs to collagen-adherent platelets (Fig. 27H). Furthermore, the inhibition of CD36 on the surface of platelets resulted in decreased tethering of RBCs on collagen-adherent platelets, indicating that not only CD36 on the surface of RBCs is necessary for RBC recruitment, but also CD36 on the surface of platelets (Fig. 27G, H). This suggests that CD36 of RBC and platelet origin is involved in the recruitment of RBCs indepent of the shear rate and may be important under venous and arterial thrombosis. In contrast to the study of Goel *et al.*, decreased RBC recruitment to collagen-adherent platelets was observed when TSP-1 was inhibited (Fig. 27I), indicating a notable role of TSP-1 for RBC recruitment to the growing thrombus under high shear rates. Noteworthy, for their interaction with the endothelium, RBCs with enhanced PS exposure have been identified to establish specific interactions via several receptors including thrombospondin and CD36 [241, 242]. The exposure of PS at the RBC and platelet membrane modulated the recruitment of RBCs (Fig. 27C, D), suggesting a role for PS positive RBCs (under 1%) from the circulation [243] and for different signaling pathway such as FasL/FasR, TSP-1/CD36 and $\alpha_{IIb}\beta_3$/FasR that induce the exposure of PS at the membrane of platelets and RBCs. These results confirmed the hypothesis that PS on RBCs can act as an adhesion molecule for the binding of platelets and that PS exposing RBCs contribute to the development of a thrombus [244, 245].

The data presented here clearly showed a role for FasL and FasR in the active recruitment of RBCs (Fig. 27E, F). These results provided first evidence that the recently identified

mechanism of platelet-RBC interaction via FasL/FasR plays a role not only for PS exposure at the cell membrane but also for the recruitment of RBCs to the growing thrombus. Although it is known that integrins are important for cell-cell attachment and for cell migration [213], the inhibition of integrin $\alpha_{IIb}\beta_3$ did not alter the tethering of RBCs at the surface of activated platelets (Fig. 27J). Thus, integrin $\alpha_{IIb}\beta_3$ is not involved in the initial recruitment of RBCs to the growing thrombus.

Taken together, RBCs from healthy human volunteers showed transient interactions with collagen-adherent platelets at a high shear rate of 1,700 s^{-1}. The results point to an active recruitment of RBCs to activated platelets that is controlled by several surface proteins on the platelet and the RBC membrane including CD36 on both cell types, erythroid FasR, FasL externalization of platelets and the release of TSP-1 from platelets. This initial mechanism might play a prominent role in hemostasis and thrombus formation with CD36 as a major adhesion protein for the recruitment of RBCs under arterial and venous shear rates.

5.5 Preactive state of platelets, procoagulant surface of RBCs and a role for TSP-1/CD36 in AAA pathology

AAA is a life threatening disease with high morbidity and mortality [246]. Makers for blood coagulation in AAA patients are increased during the immediate perioperative period after open surgical and EVAR which may account for the frequent perioperative thrombotic complications [191, 192]. Furthermore, AAA is associated with increased thrombin generation while fibrinolysis remains unaltered [191, 192]. The formation of a procoagulant cell surface followed by thrombin generation is a hallmark of severe vascular diseases such as arterial thrombosis since it may lead to myocardial infarction or stroke. While the impact of platelets in arterial thrombosis has been investigated for years, only small-size preliminary clinical trials have suggested that platelets may affect AAA formation and progression. However, neither antiplatelet nor anticoagulant drugs could be established for clinical use and the treatment of AAA patients. To date, only ASA therapy is recommended for the treatment of AAA patients [8, 247, 248]. Furthermore, platelet activation and aggregation is important for ILT formation and expansion of the aneurysm [160]; however, the underlying mechanisms are not yet understood.

This study demonstrated that platelets from AAA patients are in a preactivated state (Fig. 28). Platelets were activated (activation of integrin $\alpha_{IIb}\beta_3$, PAC-1) already with low doses of different agonists such as CRP [0.01 µg/mL] or PAR4 peptide [70 µM] and ADP [10 µM] compared to age-matched controls (AMCs), suggesting that the threshold for full platelet

activation is decreased in platelets from AAA patients (Fig. 28B). The degranulation (P-selectin externalization) of platelets was severely increased after stimulation with low dose of CRP [0.1 µg/mL], whereby high doses of CRP [5 µg/mL] resulted in decreased platelet degranulation (Fig. 28C). This is probably due to the preactivation status of resting platelets in the circulation of AAA patients that cannot be fully activated anymore. In contrast, the externalization of β_3 integrin was unaltered in AAA platelets (Fig. 28A). The results from Touat and colleagues also suggests an altered activation status of platelets in AAA [160]. They showed that blocking of integrin $\alpha_{IIb}\beta_3$ leads to decreased ILT formation and aneurysmal enlargement in rats. In addition, P-selectin that was associated with the accumulation of platelets, were increased at site of the luminal layer of the ILT [160]. This demonstrates a potential for further development into the orally available antiplatelet therapies in addition to ASA, because ASA therapy is recommended, but ASA therapy has been used in AAA with retrospective analyses showing no improvement in patient outcomes [249]. Antiplatelet drugs, and also anticoagulant therapy, have to be carefully considered because some aneurysms are stabilized through the ILT, then antithrombotic therapy could be disadvantageous. This suggests the use of an antithrombotic therapy in AAA patients on a patient-to-patient basis.

The preactivated status of AAA platelets was also characterized by altered exposure of PS at the surface of platelets and RBCs because increased Annexin V binding to resting platelets and after platelet activation with low doses of CRP was detected (Fig. 29A, B). The increased thrombin plasma levels that have been reported for AAA patients [48] might help explain increased PS exposure of RBCs and platelets from AAA patients as detected in this study. Thus, it is tempting to speculate that platelets and RBCs play an essential role to renew the ILT by incorporation of these PS positive cells into the permanently growing thrombus. This hypothesis is supported by highly expressed PS in the luminal layer of the ILT in AAA patients and the described role of platelet aggregation for the renewal of the mural thrombus [160]. In line with the preactive state of platelets from AAA patients, FasL externalization at the surface of resting platelets was increased (Fig. 29D), giving a first hint that the interaction of platelets and RBCs is altered in AAA patients, including FasL/FasR-mediated signaling. However, FasR exposure on the surface of RBCs was unaltered in AAA patients compared to AMCs and showed a constitutive expression pattern as detected by flow cytometry (Fig. 29C). Thus, the enhanced interaction of RBCs and platelets in AAA is probably due to FasL exposure on the platelet surface. In addition, TSP-1 binding to RBCs was unaltered in AAA patients under resting and stimulated conditions compared to AMCs (Fig. 31D). Taking into consideration that TSP-1 binding to RBCs is probably a shear rate dependent process (Fig. 24C); flow chamber experiments with whole blood from AAA patients have to be

performed to analyze TSP-1 binding to RBCs under arterial shear in near future. Interestingly, TSP-1 binding to platelets was increased following activation of platelets with low doses with either CRP or PAR4 peptide (Fig. 31C). However, it is not known if enhanced TSP-1 binding to platelets is due to an enhanced release of TSP-1 because of the preactivated state of platelets and the high thrombin plasma levels in AAA patients or if the expression of platelet surface receptors is altered in AAA. However, this has to be investigated in further detail in near future.

Western blot analysis of CD36 expression in platelets and RBCs from AAA patients was unaltered compared to AMCs (Fig. 30C, D). As mentioned above, it was observed that platelets and RBCs showed different expression patterns of CD36 (different glycosylated forms) in cell lysates which were unaltered in AAA patients compared to controls (Fig. 30C, D). However, since first results of this study point to CD36 expression on RBCs and platelets to be shear rate dependent it might not be surprising that no change in the expression pattern of AAA patients and AMCs were detected under static conditions in the experiments performed here. Earlier studies suggested that soluble CD36 is a potential biomarker in different diseases including diabetes and atherosclerosis [250, 251]. To analyze if CD36 could serve as biomarker for AAA, further experiments with plasma samples of AAA patients need to be performed in near future.

Western blot analysis of TSP-1 protein expression in platelet lysates and supernatants in the absence or presence of RBCs were analyzed in AAA patients and AMCs (Fig. 30A, B). The monomeric full length TSP-1 form was unaltered compared to AMCs, whereby the ADAMTS1 cleaved TSP-1 form at approximately ~ 110 kDa [103] was increased (Fig. 30A, B). Thus, there might be increased ADAMTS1 activity present in AAA patients. ADAMTS1 are down regulated at mRNA level in AAA, due to unknown mechanisms, at the same time ADAMTS1 protein is induced and protein analysis of ADAMTS1 revealed that ADAMTS1 was present predominantly in areas of SMCs and macrophages in aneurysmal aorta [252]. Therefore, the origin of ADAMTS1 and the impact of ADAMTS1 cleaving TSP-1 in AAA patients have to be investigated in near future, e.g. by the analysis of plasma samples of AAA patients. In addition, this cleaved TSP-1 form (110 kDa) is upregulated under inflammatory conditions as they occur in AAA progression [106]. Thus, one could hypothesize that the increased TSP-1 protein levels under nonstimulated conditions in AAA patients compared to AMCs are due to the release of TSP-1 from preactivated platelets. Furthermore, the cleavage of TSP-1 might be explained by the release of ADAMTS1 by SMCs located in the damaged aortic wall and by macrophages after infiltration in the ILT and the aortic wall in AAA disease. This was further supported by histological staining showing platelets, nuclear positive cells and TSP-1 in near proximity inside the ILT (Fig. 32) and the

aortic wall (Fig. 33) of AAA patients. Interestingly, the thrombi isolated from patients who underwent thrombectomy, showed accumulation of TSP-1 and RBCs in the whole thrombus, whereby the multi-layered ILT of AAA patients has a more unstructured morphology (Fig. 32). This might depend on a continuous network of canaliculi, allowing unrestricted macromolecular penetration [170]. In summary, this work and recently published data from our working group [63] suggests that platelet-RBC interactions with enhanced exposure of PS and the generation of thrombin contributes to arterial thrombosis in vascular diseases such as AAA. However, further studies are needed to clarify the role of platelet-RBC interactions for the pathology of vascular diseases to identify new therapeutic approaches for the treatment of patients with AAA, myocardial infarction or stroke.

5.6 Outlook and conclusion remarks

The results summarized in this thesis shed new light on the potential underlying mechanisms of platelet-RBC interaction, which might influence arterial thrombosis and AAA progression. However, the question remains, if calcium mobilization is important for PS exposure at the RBC membrane. Furthermore, integrin $\alpha_{IIb}\beta_3$ binding to FasR on the surface of RBCs may be a further mechanism of platelet-RBC interaction and could act synergistically with the FasL/FasR signaling pathway. Therefore, adhesion studies with platelets from GT patients and biolayer interferometry of integrin $\alpha_{IIb}\beta_3$ and FasR are indispensable. Here, it was shown that RBCs bind platelet-released TSP-1. However, the pathophysiological consequences of TSP-1 binding to RBCs are not known to date but should be investigated in near future because this pathomechanism could be important in cardiovascular diseases such as AAA. Moreover, the study provides strong evidence for a role of erythroid CD36 in thrombus formation. Since CD36 expression was increased on RBCs isolated from thrombi, leading to increased TSP-1 binding, it is of utmost interest to identify the consequences of enhanced CD36 exposure on RBCs, especially because RBCs are only limited in their ability to synthesis proteins. Therefore, experiments that investigate how CD36 exposure at the RBC membrane is enhanced are of great interest. In detail, MPs might be responsible for upregulated CD36 on RBCs because the presence of CD36 in MPs and their impact for the pathology of cardiovascular diseases and diabetes has been shown before [235]. Thus, the investigation of those MPs in AAA patients may help to understand the pathology of AAA. The analysis of CD36 deficiency (type I and type II) in humans in hemostasis and thrombosis and the underlying mechanisms of CD36-TSP-1 interactions has to be investigated by the fact that CD36 deficiency in humans and mice does not lead to thrombotic or major bleeding

complications. In addition, it is not yet known if the lack of CD36 (type I and type II deficiency) in humans affects RBCs as well.

To date, there is no antiplatelet or anticoagulant therapy available for AAA patients, although ASA therapy is recommended [8]. According to the presented results, which indicate a preactivated state of platelets there is an urge need for an antithrombotic therapy in AAA. However, different experiments and clinical trials are needed to identify possible target for an antithrombotic therapy in AAA. E.g. flow chamber experiments with whole blood from AAA patients should be performed using different arterial shear rates (1,700 s^{-1} or higher) and different matrices to add knowledge about the process of ILT formation in AAA pathology. Furthermore, the expression levels of different glycoproteins such as GPVI or GPIb on the surface of platelets should be analyzed using platelets from AAA patients.

Antiplatelet therapy is the first line treatment for cardiovascular diseases, but limitations of the current therapies include weak inhibition of platelet function and bleeding complications. For example, anti-GPVI antibody treatment of patients with AAA could be a possibility to limit the progression of the ILT, because GPVI blocking provides protection from pathological thrombus formation without causing major bleeding complications [253]. However, further studies are needed to clarify if AAA patients benefit from an antithrombotic therapy. Furthermore, there is a need to identify new antithrombotic targets that avoid arterial thrombosis but preserve hemostasis that might be also beneficial in AAA pathology to limit ILT progression and platelet activation.

6. References

1.	Bessis, M., *Living Blood Cells and Their Ultrastructure*. 1973, New York/Heidelberg/Berlin: Springer.
2.	Hartenstein, V., *Blood cells and blood cell development in the animal kingdom.* Annu Rev Cell Dev Biol, 2006. **22**: p. 677-712.
3.	Jurk, K. and B.E. Kehrel, *[Pathophysiology and biochemistry of platelets].* Internist (Berl), 2010. **51**(9): p. 1086, 1088-92, 1094.
4.	Gawaz, M., H. Langer, and A.E. May, *Platelets in inflammation and atherogenesis.* J Clin Invest, 2005. **115**(12): p. 3378-84.
5.	Ruggeri, Z.M., *Platelets in atherothrombosis.* Nat Med, 2002. **8**(11): p. 1227-34.
6.	Smyth, S.S., et al., *Platelet functions beyond hemostasis.* Journal of Thrombosis and Haemostasis, 2009. **7**(11): p. 1759-1766.
7.	Milne, A.A., et al., *Effects of Asymptomatic Abdominal Aortic Aneurysm on the Soluble Coagulation System, Platelet Count and Platelet Activation.* European Journal of Vascular and Endovascular Surgery, 1999. **17**(5): p. 434-437.
8.	Cameron, S.J., H.M. Russell, and A.P. Owens, 3rd, *Antithrombotic therapy in abdominal aortic aneurysm: beneficial or detrimental?* Blood, 2018. **132**(25): p. 2619-2628.
9.	Kehrel, B.E., *[Blood platelets: biochemistry and physiology].* Hamostaseologie, 2003. **23**(4): p. 149-58.
10.	Schmitt, A., et al., *Of mice and men: comparison of the ultrastructure of megakaryocytes and platelets.* Exp Hematol, 2001. **29**(11): p. 1295-302.
11.	Kaushansky, K., et al., *Thrombopoietin, the Mp1 ligand, is essential for full megakaryocyte development.* Proc Natl Acad Sci U S A, 1995. **92**(8): p. 3234-8.
12.	Lefrancais, E., et al., *The lung is a site of platelet biogenesis and a reservoir for haematopoietic progenitors.* Nature, 2017. **544**(7648): p. 105-109.
13.	Odell, T.T. and T.P. McDonald, *Life Span of Mouse Blood Platelets.* Proceedings of the Society for Experimental Biology and Medicine, 1961. **106**(1): p. 107-108.
14.	George, J.N., *Platelets.* Lancet, 2000. **355**(9214): p. 1531-9.
15.	Jirouskova, M., A.S. Shet, and G.J. Johnson, *A guide to murine platelet structure, function, assays, and genetic alterations.* J Thromb Haemost, 2007. **5**(4): p. 661-9.
16.	Selvadurai, M.V. and J.R. Hamilton, *Structure and function of the open canalicular system - the platelet's specialized internal membrane network.* Platelets, 2018. **29**(4): p. 319-325.
17.	Angenieux, C., et al., *Time-Dependent Decay of mRNA and Ribosomal RNA during Platelet Aging and Its Correlation with Translation Activity.* PLoS One, 2016. **11**(1): p. e0148064.
18.	Wu, K.K. and J.Y. Liou, *Cellular and molecular biology of prostacyclin synthase.* Biochem Biophys Res Commun, 2005. **338**(1): p. 45-52.
19.	Radziwon-Balicka, A., et al., *Differential eNOS-signalling by platelet subpopulations regulates adhesion and aggregation.* Cardiovasc Res, 2017. **113**(14): p. 1719-1731.
20.	Cox, D., *Platelet Function Studies*, in *Platelet Function*. 2005. p. 201-222.
21.	Jackson, S.P., *Arterial thrombosis--insidious, unpredictable and deadly.* Nat Med, 2011. **17**(11): p. 1423-36.
22.	Baker-Groberg, S.M., et al., *Development of a method to quantify platelet adhesion and aggregation under static conditions.* Cellular and molecular bioengineering, 2014. **7**(2): p. 285-290.
23.	Mccarty, O.J.T., et al., *Evaluation of the role of platelet integrins in fibronectin-dependent spreading and adhesion.* Journal of Thrombosis and Haemostasis, 2004. **2**(10): p. 1823-1833.
24.	Varga-Szabo, D., I. Pleines, and B. Nieswandt, *Cell adhesion mechanisms in platelets.* Arterioscler Thromb Vasc Biol, 2008. **28**(3): p. 403-12.

25. Ruggeri, Z.M. and G.L. Mendolicchio, *Adhesion mechanisms in platelet function.* Circ Res, 2007. **100**(12): p. 1673-85.

26. Shattil, S.J., M.H. Ginsberg, and J.S. Brugge, *Adhesive signaling in platelets.* Curr Opin Cell Biol, 1994. **6**(5): p. 695-704.

27. Hechler, B. and C. Gachet, *Purinergic Receptors in Thrombosis and Inflammation.* Arterioscler Thromb Vasc Biol, 2015. **35**(11): p. 2307-15.

28. Fabre, J.E., et al., *Decreased platelet aggregation, increased bleeding time and resistance to thromboembolism in P2Y1-deficient mice.* Nat Med, 1999. **5**(10): p. 1199-202.

29. Maayani, S., et al., *Agonist concentration-dependent differential responsivity of a human platelet purinergic receptor: pharmacological and kinetic studies of aggregation, deaggregation and shape change responses mediated by the purinergic P2Y1 receptor in vitro.* Platelets, 2003. **14**(7-8): p. 445-62.

30. Offermanns, S., *Activation of platelet function through G protein-coupled receptors.* Circ Res, 2006. **99**(12): p. 1293-304.

31. Jones, R.L., N.H. Wilson, and R.A. Armstrong, *Characterization of thromboxane receptors in human platelets.* Adv Exp Med Biol, 1985. **192**: p. 67-81.

32. Estevez, B., B. Shen, and X. Du, *Targeting integrin and integrin signaling in treating thrombosis.* Arterioscler Thromb Vasc Biol, 2015. **35**(1): p. 24-9.

33. Jurk, K. and B.E. Kehrel, *Platelets: physiology and biochemistry.* Semin Thromb Hemost, 2005. **31**(4): p. 381-92.

34. Riddel, J.P., Jr., et al., *Theories of blood coagulation.* J Pediatr Oncol Nurs, 2007. **24**(3): p. 123-31.

35. Coller, B.S. and S.J. Shattil, *The GPIIb/IIIa (integrin αIIbβ3) odyssey: a technology-driven saga of a receptor with twists, turns, and even a bend.* Blood, 2008. **112**(8): p. 3011-3025.

36. Gale, A.J., *Continuing education course #2: current understanding of hemostasis.* Toxicol Pathol, 2011. **39**(1): p. 273-80.

37. Reddy, E.C. and M.L. Rand, *Procoagulant Phosphatidylserine-Exposing Platelets in vitro and in vivo.* Front Cardiovasc Med, 2020. **7**: p. 15.

38. Dale, G.L., et al., *Stimulated platelets use serotonin to enhance their retention of procoagulant proteins on the cell surface.* Nature, 2002. **415**(6868): p. 175-9.

39. Kruithof, E.K. and S. Dunoyer-Geindre, *Human tissue-type plasminogen activator.* Thromb Haemost, 2014. **112**(2): p. 243-54.

40. Hynes, R.O., *Integrins: bidirectional, allosteric signaling machines.* Cell, 2002. **110**(6): p. 673-87.

41. Shattil, S.J. and P.J. Newman, *Integrins: dynamic scaffolds for adhesion and signaling in platelets.* Blood, 2004. **104**(6): p. 1606-15.

42. Wagner, C.L., et al., *Analysis of GPIIb/IIIa receptor number by quantification of 7E3 binding to human platelets.* Blood, 1996. **88 3**: p. 907-14.

43. Hynes, R.O., *Integrins: A family of cell surface receptors.* Cell, 1987. **48**(4): p. 549-554.

44. Moser, M., et al., *The Tail of Integrins, Talin, and Kindlins.* Science, 2009. **324**(5929): p. 895-899.

45. Larjava, H., E.F. Plow, and C. Wu, *Kindlins: essential regulators of integrin signalling and cell-matrix adhesion.* EMBO Rep, 2008. **9**(12): p. 1203-8.

46. Kahner, B.N., et al., *Kindlins, integrin activation and the regulation of talin recruitment to αIIbβ3.* PLoS one, 2012. **7**(3): p. e34056.

47. Martin Pfaff, K.T., Beate Muller, Marion Gurrathn, Gerhard Miiller, and R.T. Horst Kessler, and Jurgen Engel, *Selective Recognition of Cyclic RGD Peptides of NRIR Defined Conformation by aIIbp3, aVP3, and a5pl Integrins.* The Journal of Biological Chemistry, 1994. **269**.

48. Sánchez-Cortés, J. and M. Mrksich, *The platelet integrin alphaIIbbeta3 binds to the RGD and AGD motifs in fibrinogen.* Chemistry & biology, 2009. **16**(9): p. 990-1000.

49. Nieswandt, B., D. Varga-Szabo, and M. Elvers, *Integrins in platelet activation.* J Thromb Haemost, 2009. **7 Suppl 1**: p. 206-9.

50. Obergfell, A., et al., *Coordinate interactions of Csk, Src, and Syk kinases with [alpha]IIb[beta]3 initiate integrin signaling to the cytoskeleton.* J Cell Biol, 2002. **157**(2): p. 265-75.

51. Mazharian, A., et al., *Megakaryocyte-specific deletion of the protein-tyrosine phosphatases Shp1 and Shp2 causes abnormal megakaryocyte development, platelet production, and function.* Blood, 2013. **121**(20): p. 4205-4220.

52. Nurden, A.T., *Should studies on Glanzmann thrombasthenia not be telling us more about cardiovascular disease and other major illnesses?* Blood Rev, 2017. **31**(5): p. 287-299.

53. Dixon, L.R., *The Complete Blood Count: Physiologic Basis and Clinical Usage.* J Perinat Neonat Nurs, 1997.

54. Moras, M., S.D. Lefevre, and M.A. Ostuni, *From Erythroblasts to Mature Red Blood Cells: Organelle Clearance in Mammals.* Frontiers in physiology, 2017. **8**: p. 1076-1076.

55. Patel, H.H., H.R. Patel, and J.M. Higgins, *Modulation of red blood cell population dynamics is a fundamental homeostatic response to disease.* American journal of hematology, 2015. **90**(5): p. 422-428.

56. Pretini, V., et al., *Red Blood Cells: Chasing Interactions.* Front Physiol, 2019. **10**: p. 945.

57. Andrews, D.A. and P.S. Low, *Role of red blood cells in thrombosis.* Current Opinion in Hematology, 1999. **6**(2).

58. Duke, W.W., *The relation of blood platelets to haemorrhagic disease: Description of a method for determining the bleeding time and coagulation time and report of three cases of haemorrhagic diease relieved by transfusion.* Journal of the American Medical Association, 1910. **55**(14): p. 1185-1192.

59. Kroll, M.H., L.C. Michaelis, and S. Verstovsek, *Mechanisms of thrombogenesis in polycythemia vera.* Blood Reviews, 2015. **29**(4): p. 215-221.

60. Tokish, J.M., M.S. Kocher, and R.J. Hawkins, *Ergogenic aids: a review of basic science, performance, side effects, and status in sports.* Am J Sports Med, 2004. **32**(6): p. 1543-53.

61. Flamm, M.H. and S.L. Diamond, *Multiscale Systems Biology and Physics of Thrombosis Under Flow.* Annals of Biomedical Engineering, 2012. **40**(11): p. 2355-2364.

62. R. I. Litvinov, J.W.W., *Role of red blood cells in haemostasis and thrombosis.* International Society of Blood Transfusion, 2017.

63. Klatt, C., et al., *Platelet-RBC interaction mediated by FasL/FasR induces procoagulant activity important for thrombosis.* J Clin Invest, 2018. **128**(9): p. 3906-3925.

64. Walker, B., et al., *Dynamic adhesion of eryptotic erythrocytes to immobilized platelets via platelet phosphatidylserine receptors.* Am J Physiol Cell Physiol, 2014. **306**(3): p. C291-7.

65. Whelihan, M.F. and K.G. Mann, *The role of the red cell membrane in thrombin generation.* Thromb Res, 2013. **131**(5): p. 377-82.

66. Wautier, J.L. and M.P. Wautier, *Molecular basis of erythrocyte adhesion to endothelial cells in diseases.* Clin Hemorheol Microcirc, 2013. **53**(1-2): p. 11-21.

67. Goel, M.S. and S.L. Diamond, *Adhesion of normal erythrocytes at depressed venous shear rates to activated neutrophils, activated platelets, and fibrin polymerized from plasma.* Blood, 2002. **100**(10): p. 3797-803.

68. Gersh, K., C. Nagaswami, and J. Weisel, *Fibrin network structure and clot mechanical properties are altered by incorporation of erythrocytes.* Thrombosis and Haemostasis, 2009. **102**(12): p. 1169-1175.

69. Wohner, N., et al., *Lytic Resistance of Fibrin Containing Red Blood Cells.* 2011. **31**(10): p. 2306-2313.

70. Berger, G., et al., *Ultrastructural demonstration of CD36 in the alpha-granule membrane of human platelets and megakaryocytes.* Blood, 1993. **82**(10): p. 3034-44.

71. Glatz, J.F., J.J. Luiken, and A. Bonen, *Membrane fatty acid transporters as regulators of lipid metabolism: implications for metabolic disease.* Physiol Rev, 2010. **90**(1): p. 367-417.

72. Silverstein, R.L. and M. Febbraio, *CD36, a scavenger receptor involved in immunity, metabolism, angiogenesis, and behavior.* Sci Signal, 2009. **2**(72): p. re3.

73. Deitch, E.A., et al., *Trauma-hemorrhagic shock induces a CD36-dependent RBC endothelial-adhesive phenotype.* Crit Care Med, 2014. **42**(3): p. e200-10.

74. Park, Y.M., *CD36, a scavenger receptor implicated in atherosclerosis.* Exp Mol Med, 2014. **46**: p. e99.

75. Tandon, N.N., U. Kralisz, and G.A. Jamieson, *Identification of glycoprotein IV (CD36) as a primary receptor for platelet-collagen adhesion.* J Biol Chem, 1989. **264**(13): p. 7576-83.

76. Daniel, J.L., et al., *Collagen induces normal signal transduction in platelets deficient in CD36 (platelet glycoprotein IV).* 1994(0340-6245).

77. Kehrel, B., et al., *Glycoprotein VI is a major collagen receptor for platelet activation: it recognizes the platelet-activating quaternary structure of collagen, whereas CD36, glycoprotein IIb/IIIa, and von Willebrand factor do not.* Blood, 1998. **91**(2): p. 491-9.

78. Yamamoto, N., et al., *Platelet glycoprotein IV (CD36) deficiency is associated with the absence (type I) or the presence (type II) of glycoprotein IV on monocytes.* Blood, 1994. **83**(0006-4971): p. 392-397.

79. Madan, N., et al., *Functionalization of CD36 cardiovascular disease and expression associated variants by interdisciplinary high throughput analysis.* PLoS Genet, 2019. **15**(7): p. e1008287.

80. Hirano, K.-i., et al., *Pathophysiology of Human Genetic CD36 Deficiency.* Trends in Cardiovascular Medicine, 2003. **13**(4): p. 136-141.

81. van Schravendijk, M.R., et al., *Normal human erythrocytes express CD36, an adhesion molecule of monocytes, platelets, and endothelial cells.* Blood, 1992. **80**(8): p. 2105-14.

82. Brock, T. *Inflammation in Atherosclerosis: Macrophage Functions*. 2008 [cited 2020 08.07]; Available from: https://www.caymanchem.com/news/inflammation-in-atherosclerosis-macrophage-functions.

83. Silverstein, R.L., *Inflammation, atherosclerosis, and arterial thrombosis: role of the scavenger receptor CD36.* Cleve Clin J Med, 2009. **76 Suppl 2**: p. S27-30.

84. Philips, J.A., E.J. Rubin, and N. Perrimon, *Drosophila RNAi screen reveals CD36 family member required for mycobacterial infection.* Science, 2005. **309**(5738): p. 1251-3.

85. Smith, T.G., et al., *CD36-mediated nonopsonic phagocytosis of erythrocytes infected with stage I and IIA gametocytes of Plasmodium falciparum.* Infection and immunity, 2003. **71**(1): p. 393-400.

86. Glenister, F.K., et al., *Functional alteration of red blood cells by a megadalton protein of Plasmodium falciparum.* Blood, 2009. **113**(4): p. 919-928.

87. Chen, K., et al., *A Specific CD36-Dependent Signaling Pathway Is Required for Platelet Activation by Oxidized Low-Density Lipoprotein.* Circulation Research, 2008. **102**(12): p. 1512-1519.

88. Wraith, K.S., et al., *Oxidized low-density lipoproteins induce rapid platelet activation and shape change through tyrosine kinase and Rho kinase-signaling pathways.* Blood, 2013. **122**(4): p. 580-9.

89. Maschberger, P., et al., *Mildly oxidized low density lipoprotein rapidly stimulates via activation of the lysophosphatidic acid receptor Src family and Syk tyrosine kinases and Ca2+ influx in human platelets.* J Biol Chem, 2000. **275**(25): p. 19159-66.

90. Yang, M., et al., *Platelet CD36 signaling through ERK5 promotes caspase-dependent procoagulant activity and fibrin deposition in vivo.* Blood Adv, 2018. **2**(21): p. 2848-2861.

91. Yang, M., et al., *Platelet CD36 promotes thrombosis by activating redox sensor ERK5 in hyperlipidemic conditions.* Blood, 2017: p. blood-2016-11-75.

92. Kuijpers, M.J., et al., *Supporting roles of platelet thrombospondin-1 and CD36 in thrombus formation on collagen.* Arterioscler Thromb Vasc Biol, 2014. **34**(6): p. 1187-92.

93. Nancy Lewis Baenziger, G.N.B., and Philip W. Majerus, *A Thrombin-Sensitive Protein of Human Platelet Membranes.* Proceedings of the National Academy of Sciences, 1971. **68**(1): p. 240-243.

94. Bornstein, P., *Thrombospondins as matricellular modulators of cell function.* The Journal of Clinical Investigation, 2001. **107**(8).

95. Bonnefoy, A., et al., *A Model of Platelet Aggregation Involving Multiple Interactions of Thrombospondin-1, Fibrinogen, and GPIIbIIIa Receptor.* 2001. **276**(8): p. 5605-5612.

96. Wight, T.N., et al., *Light microscopic immunolocation of thrombospondin in human tissues.* J Histochem Cytochem, 1985. **33**(4): p. 295-302.

97. Lawler, J.W., F.C. Chao, and P.H. Fang, *Observation of a high molecular weight platelet protein released by thrombin.* Thromb Haemost, 1977. **37**(2): p. 355-7.

98. Maloney, J.P., et al., *Loss-of-function thrombospondin-1 mutations in familial pulmonary hypertension.* American journal of physiology. Lung cellular and molecular physiology, 2012. **302**(6): p. L541-L554.

99. Seif, K., et al., *Neutrophil-Mediated Proteolysis of Thrombospondin-1 Promotes Platelet Adhesion and String Formation.* Thromb Haemost, 2018. **118**(12): p. 2074-2085.

100. Patrick Starlinger, L.A., Dominic Schauer, Philipp Brugger, Silvia Sommerfeldt, Irene Kuehrer, Sebastian F. Schoppmann, Michael Gnant and Christine Brostjan, *Platelet-stored angiogenesis factors: Clinical monitoring is prone to artifacts.* Disease Markers, 2011. **31**.

101. Krishna, S.M. and J. Golledge, *The role of thrombospondin-1 in cardiovascular health and pathology.* Int J Cardiol, 2013. **168**(2): p. 692-706.

102. Florence de Fraipont, A.C.N., Jean-Jacques Feige and Erwin G.Van Meir, *Thrombospondins and tumor angiogenesis.* TRENDS in Molecular Medicine, 2001. **7**(9).

103. Lee, N.V., et al., *ADAMTS1 mediates the release of antiangiogenic polypeptides from TSP1 and 2.* The EMBO Journal, 2006. **25**(22): p. 5270-5283.

104. Iruela-Arispe, M.L., *Regulation of TSP1 by extracellular proteases.* Curr Drug Targets, 2008. **9**: p. 863-868.

105. Lawler, J., et al., *Thrombin and chymotrypsin interactions with thrombospondin.* Ann N Y Acad Sci, 1986. **485**: p. 273-87.

106. Lee, N.V., et al., *ADAMTS1 mediates the release of antiangiogenic polypeptides from TSP1 and 2.* EMBO J, 2006. **25**(22): p. 5270-83.

107. Legrand, A.B.a.C., *Proteolysis of Subendothelial Adhesive Glycoproteins (Fibronectin, Thrombospondin, and von Willebrand Factor) by Plasmin, Leukocyte Cathepsin G, and Elastase.* Thrombosis Research, 2000. **98**.

108. Nör, J.E., et al., *Thrombospondin-1 Induces Endothelial Cell Apoptosis and Inhibits Angiogenesis by Activating the Caspase Death Pathway.* Journa of Vascular Research, 2000. **37**(3): p. 209-218.

109. Bornstein, P., *Thrombospondins function as regulators of angiogenesis.* Journal of Cell Communication and Signaling, 2009. **3**(3-4): p. 189-200.

110. Isenberg, J.S., et al., *Thrombospondin-1 limits ischemic tissue survival by inhibiting nitric oxide-mediated vascular smooth muscle relaxation.* Blood, 2007. **109**(5): p. 1945-52.

111. Chandrasekaran, L., et al., *Cell contact-dependent activation of alpha3beta1 integrin modulates endothelial cell responses to thrombospondin-1.* Mol Biol Cell, 2000. **11**(9): p. 2885-900.

112. Young, G.D. and J.E. Murphy-Ullrich, *Molecular interactions that confer latency to transforming growth factor-beta.* J Biol Chem, 2004. **279**(36): p. 38032-9.

113. Yamauchi, Y., et al., *Opposite effects of thrombospondin-1 via CD36 and CD47 on homotypic aggregation of monocytic cells.* Matrix Biology, 2002. **21**(5): p. 441-448.

114. Nergiz-Unal, R., et al., *Signaling role of CD36 in platelet activation and thrombus formation on immobilized thrombospondin or oxidized low-density lipoprotein.* J Thromb Haemost, 2011. **9**(9): p. 1835-46.

115. Pimanda, J.E., et al., *Role of thrombospondin-1 in control of von Willebrand factor multimer size in mice.* J Biol Chem, 2004. **279**(20): p. 21439-48.

116. Bonnefoy, A., *Thrombospondin-1 controls vascular platelet recruitment and thrombus adherence in mice by protecting (sub)endothelial VWF from cleavage by ADAMTS13.* 2005. **107**(3): p. 955-964.

117. Jurk, K., et al., *Thrombospondin-1 mediates platelet adhesion at high shear via glycoprotein Ib (GPIb): an alternative/backup mechanism to von Willebrand factor.* Faseb j, 2003. **17**(11): p. 1490-2.

118. Bonnefoy, A., et al., *A model of platelet aggregation involving multiple interactions of thrombospondin-1, fibrinogen, and GPIIbIIIa receptor.* J Biol Chem, 2001. **276**(8): p. 5605-12.

119. Asch, A.S., et al., *Platelet membrane topography: colocalization of thrombospondin and fibrinogen with the glycoprotein IIb-IIIa complex.* Blood, 1985. **66**(4): p. 926-34.

120. McGregor, J.C., J.G. Pollock, and H.C. Anton, *The value of ultrasonography in the diagnosis of abdominal aortic aneurysm.* Scott Med J, 1975. **20**(3): p. 133-7.

121. Alcorn, H.G., et al., *Risk factors for abdominal aortic aneurysms in older adults enrolled in the Cardiovascular Health Study.* Arteriosclerosis, Thrombosis, and Vascular Biology, 1996. **16**(8): p. 963-970.

122. Sakalihasan, N., et al., *Abdominal aortic aneurysms.* Nat Rev Dis Primers, 2018. **4**(1): p. 34.

123. Grondal, N., R. Sogaard, and J.S. Lindholt, *Baseline prevalence of abdominal aortic aneurysm, peripheral arterial disease and hypertension in men aged 65-74 years from a population screening study (VIVA trial).* Br J Surg, 2015. **102**(8): p. 902-6.

124. Sampson, U.K., et al., *Estimation of global and regional incidence and prevalence of abdominal aortic aneurysms 1990 to 2010.* Glob Heart, 2014. **9**(1): p. 159-70.

125. Henderson, E.L., et al., *Death of Smooth Muscle Cells and Expression of Mediators of Apoptosis by T Lymphocytes in Human Abdominal Aortic Aneurysms.* Circulation, 1999. **99**(1): p. 96-104.

126. Defawe, O.D., et al., *TIMP-2 and PAI-1 mRNA levels are lower in aneurysmal as compared to athero-occlusive abdominal aortas.* Cardiovascular Research, 2003. **60**(1): p. 205-213.

127. Vardulaki, K.A., et al., *Quantifying the risks of hypertension, age, sex and smoking in patients with abdominal aortic aneurysm.* Br J Surg, 2000. **87**(2): p. 195-200.

128. Brady, A.R., et al., *Abdominal aortic aneurysm expansion: risk factors and time intervals for surveillance.* Circulation, 2004. **110**(1): p. 16-21.

129. Lindholt, J.S., et al., *Systemic Levels of Cotinine and Elastase, but not Pulmonary Function, are Associated with the Progression of Small Abdominal Aortic Aneurysms.* European Journal of Vascular and Endovascular Surgery, 2003. **26**(4): p. 418-422.

130. Hay, N., et al., *Endovascular stent-grafts for the treatment of abdominal aortic aneurysms: NICE technology appraisal guidance.* Heart, 2009. **95**(21): p. 1798.

131. Juvonen, J., et al., *Elevated circulating levels of inflammatory cytokines in patients with abdominal aortic aneurysm.* Arterioscler Thromb Vasc Biol, 1997. **17**(11): p. 2843-7.

132. Hellenthal, F.A.M.V.I., et al., *Biomarkers of abdominal aortic aneurysm progression. Part 2: inflammation.* Nature Reviews Cardiology, 2009. **6**(8): p. 543-552.

133. Michel, J.B., et al., *Novel aspects of the pathogenesis of aneurysms of the abdominal aorta in humans.* Cardiovasc Res, 2011. **90**(1): p. 18-27.

134. Sakalihasan, N., R. Limet, and O.D. Defawe, *Abdominal aortic aneurysm.* The Lancet, 2005. **365**(9470): p. 1577-1589.

135. Houard, X., et al., *Differential inflammatory activity across human abdominal aortic aneurysms reveals neutrophil-derived leukotriene B4 as a major chemotactic factor released from the intraluminal thrombus.* The FASEB Journal, 2009. **23**(5): p. 1376-1383.

136. Lum, H. and K.A. Roebuck, *Oxidant stress and endothelial cell dysfunction.* Am J Physiol Cell Physiol, 2001. **280**(4): p. C719-41.

137. Lakshminarayanan, V., et al., *Differential regulation of interleukin-8 and intercellular adhesion molecule-1 by H2O2 and tumor necrosis factor-alpha in endothelial and epithelial cells.* J Biol Chem, 1997. **272**(52): p. 32910-8.

138. Marumo, T., et al., *Platelet-derived growth factor-stimulated superoxide anion production modulates activation of transcription factor NF-kappaB and expression of monocyte chemoattractant protein 1 in human aortic smooth muscle cells.* Circulation, 1997. **96**(7): p. 2361-7.

139. Patel, K.D., et al., *Oxygen radicals induce human endothelial cells to express GMP-140 and bind neutrophils.* J Cell Biol, 1991. **112**(4): p. 749-59.

140. Grote, K., et al., *Mechanical stretch enhances mRNA expression and proenzyme release of matrix metalloproteinase-2 (MMP-2) via NAD(P)H oxidase-derived reactive oxygen species.* Circ Res, 2003. **92**(11): p. e80-6.

141. Rajagopalan, S., et al., *Reactive oxygen species produced by macrophage-derived foam cells regulate the activity of vascular matrix metalloproteinases in vitro. Implications for atherosclerotic plaque stability.* J Clin Invest, 1996. **98**(11): p. 2572-9.

142. López-Candales, A., et al., *Decreased vascular smooth muscle cell density in medial degeneration of human abdominal aortic aneurysms.* The American journal of pathology, 1997. **150**(3): p. 993-1007.

143. Davis, V., et al., *Matrix metalloproteinase-2 production and its binding to the matrix are increased in abdominal aortic aneurysms.* Arterioscler Thromb Vasc Biol, 1998. **18**(10): p. 1625-33.

144. Thompson, R.W., et al., *Production and localization of 92-kilodalton gelatinase in abdominal aortic aneurysms. An elastolytic metalloproteinase expressed by aneurysm-infiltrating macrophages.* J Clin Invest, 1995. **96**(1): p. 318-26.

145. Curci, J.A., et al., *Expression and localization of macrophage elastase (matrix metalloproteinase-12) in abdominal aortic aneurysms.* J Clin Invest, 1998. **102**(11): p. 1900-10.

146. Airhart, N., et al., *Smooth muscle cells from abdominal aortic aneurysms are unique and can independently and synergistically degrade insoluble elastin.* Journal of Vascular Surgery, 2014. **60**(4): p. 1033-1042.e5.

147. Knox, J.B., et al., *Evidence for altered balance between matrix metalloproteinases and their inhibitors in human aortic diseases.* Circulation, 1997. **95**(1): p. 205-12.

148. Tamarina, N.A., et al., *Expression of matrix metalloproteinases and their inhibitors in aneurysms and normal aorta.* Surgery, 1997. **122**(2): p. 264-71; discussion 271-2.

149. McMillan, W.D. and W.H. Pearce, *Increased plasma levels of metalloproteinase-9 are associated with abdominal aortic aneurysms.* J Vasc Surg, 1999. **29**(1): p. 122-7; discussion 127-9.

150. Satta, J., et al., *Increased turnover of collagen in abdominal aortic aneurysms, demonstrated by measuring the concentration of the aminoterminal propeptide of type III procollagen in peripheral and aortal blood samples.* Journal of Vascular Surgery, 1995. **22**(2): p. 155-160.

151. Dobrin, P.B., W.H. Baker, and W.C. Gley, *Elastolytic and Collagenolytic Studies of Arteries: Implications for the Mechanical Properties of Aneurysms.* Archives of Surgery, 1984. **119**(4): p. 405-409.

152. Meilhac, O., et al., *Pericellular plasmin induces smooth muscle cell anoikis.* The FASEB Journal, 2003. **17**(10): p. 1301-1303.

153. Michel, J.B., *Anoikis in the cardiovascular system: known and unknown extracellular mediators.* Arterioscler Thromb Vasc Biol, 2003. **23**(12): p. 2146-54.

154. Yamanouchi, D., et al., *Effects of Caspase Inhibitor on Angiotensin II-Induced Abdominal Aortic Aneurysm in Apolipoprotein E–Deficient Mice.* Arteriosclerosis, Thrombosis, and Vascular Biology, 2010. **30**(4): p. 702-707.

155. Ross, R. and S.J. Klebanoff, *The smooth muscle cell. I. In vivo synthesis of connective tissue proteins.* J Cell Biol, 1971. **50**(1): p. 159-71.

156. Rasmussen, L.M., Y.G. Wolf, and E. Ruoslahti, *Vascular smooth muscle cells from injured rat aortas display elevated matrix production associated with transforming growth factor-beta activity.* Am J Pathol, 1995. **147**(4): p. 1041-8.

157. Michel, J.-B., et al., *Novel aspects of the pathogenesis of aneurysms of the abdominal aorta in humans.* Cardiovascular research, 2011. **90**(1): p. 18-27.

158. Martinez-Pinna, R., et al., *From tissue iron retention to low systemic haemoglobin levels, new pathophysiological biomarkers of human abdominal aortic aneurysm.* Thromb Haemost, 2014. **112**(07): p. 87-95.

159. Martinez-Pinna, R., et al., *Label-free proteomic analysis of red blood cell membrane fractions from abdominal aortic aneurysm patients.* PROTEOMICS – Clinical Applications, 2014. **8**(7-8): p. 626-630.

160. Touat, Z., et al., *Renewal of Mural Thrombus Releases Plasma Markers and Is Involved in Aortic Abdominal Aneurysm Evolution.* The American Journal of Pathology, 2006. **168**(3): p. 1022-1030.

161. Bruemmer, D., et al., *Angiotensin II-accelerated atherosclerosis and aneurysm formation is attenuated in osteopontin-deficient mice.* J Clin Invest, 2003. **112**(9): p. 1318-31.

162. Krishna, S.M., et al., *High serum thrombospondin-1 concentration is associated with slower abdominal aortic aneurysm growth and deficiency of thrombospondin-1 promotes angiotensin II induced aortic aneurysm in mice.* Clin Sci (Lond), 2017. **131**(12): p. 1261-1281.

163. Liu, O., et al., *Clopidogrel, a platelet P2Y12 receptor inhibitor, reduces vascular inflammation and angiotensin II induced-abdominal aortic aneurysm progression.* PloS one, 2012. **7**(12): p. e51707-e51707.

164. Liu, Z., et al., *Thrombospondin-1 (TSP1) contributes to the development of vascular inflammation by regulating monocytic cell motility in mouse models of abdominal aortic aneurysm.* Circ Res, 2015. **117**(2): p. 129-41.

165. Toghill, B.J., A. Saratzis, and M.J. Bown, *Abdominal aortic aneurysm-an independent disease to atherosclerosis?* Cardiovasc Pathol, 2017. **27**: p. 71-75.

166. Moura, R., et al., *Thrombospondin-1 deficiency accelerates atherosclerotic plaque maturation in ApoE-/- mice.* Circ Res, 2008. **103**(10): p. 1181-9.

167. Giulia Taraboletti, L.M., Sandra Donnini, Astrid Parenti, Harris J. Granger, Raffaella Giavazzi, and Marina Ziche, *The heparin binding 25 kDa fragment of thrombospondin-1 promotes angiogenesis and modulates gelatinase and TIMP2 production in endothelial cells.* The FASEB Journal, 2000. **10**.

168. Harter, L.P., et al., *Ultrasonic evaluation of abdominal aortic thrombus.* J Ultrasound Med, 1982. **1**(8): p. 315-8.

169. O'Leary, S.A., et al., *The biaxial mechanical behaviour of abdominal aortic aneurysm intraluminal thrombus: Classification of morphology and the determination of layer and region specific properties.* Journal of Biomechanics, 2014. **47**(6): p. 1430-1437.

170. Adolph, R., et al., *Cellular content and permeability of intraluminal thrombus in abdominal aortic aneurysm.* Journal of Vascular Surgery, 1997. **25**(5): p. 916-926.

171. Wolf, Y.G., et al., *Computed tomography scanning findings associated with rapid expansion of abdominal aortic aneurysms.* J Vasc Surg, 1994. **20**(4): p. 529-35; discussion 535-8.

172. von Kodolitsch, Y., et al., *Intramural hematoma of the aorta: predictors of progression to dissection and rupture.* Circulation, 2003. **107**(8): p. 1158-63.

173. Frösen, J., et al., *Remodeling of saccular cerebral artery aneurysm wall is associated with rupture: histological analysis of 24 unruptured and 42 ruptured cases.* Stroke, 2004. **35**(10): p. 2287-93.

174. Kazi, M., et al., *Influence of intraluminal thrombus on structural and cellular composition of abdominal aortic aneurysm wall.* J Vasc Surg, 2003. **38**(6): p. 1283-92.

175. Khan, J.A., et al., *Intraluminal thrombus has a selective influence on matrix metalloproteinases and their inhibitors (tissue inhibitors of matrix metalloproteinases) in the wall of abdominal aortic aneurysms.* Ann Vasc Surg, 2012. **26**(3): p. 322-9.

176. Fontaine, V., et al., *Involvement of the mural thrombus as a site of protease release and activation in human aortic aneurysms.* The American journal of pathology, 2002. **161**(5): p. 1701-1710.

177. Sakalihasan, N., et al., *Activated forms of MMP2 and MMP9 in abdominal aortic aneurysms.* Journal of Vascular Surgery, 1996. **24**(1): p. 127-133.

178. Vorp, D.A., et al., *Association of intraluminal thrombus in abdominal aortic aneurysm with local hypoxia and wall weakening.* J Vasc Surg, 2001. **34**(2): p. 291-9.

179. Thubrikar, M.J., et al., *Effect of thrombus on abdominal aortic aneurysm wall dilation and stress.* J Cardiovasc Surg (Torino), 2003. **44**(1): p. 67-77.

180. Bergfeld, G.R. and T. Forrester, *Release of ATP from human erythrocytes in response to a brief period of hypoxia and hypercapnia.* Cardiovasc Res, 1992. **26**(1): p. 40-7.

181. Gaarder, A., et al., *Adenosine diphosphate in red cells as a factor in the adhesiveness of human blood platelets.* Nature, 1961. **192**: p. 531-2.

182. Munnix, I.C., et al., *Segregation of platelet aggregatory and procoagulant microdomains in thrombus formation: regulation by transient integrin activation.* Arterioscler Thromb Vasc Biol, 2007. **27**(11): p. 2484-90.

183. Peter, M.E., et al., *The role of CD95 and CD95 ligand in cancer.* Cell Death Differ, 2015. **22**(4): p. 549-59.

184. Strasser, A., P.J. Jost, and S. Nagata, *The many roles of FAS receptor signaling in the immune system.* Immunity, 2009. **30**(2): p. 180-192.

185. Mandal, D., et al., *Fas-, caspase 8-, and caspase 3-dependent signaling regulates the activity of the aminophospholipid translocase and phosphatidylserine externalization in human erythrocytes.* J Biol Chem, 2005. **280**(47): p. 39460-7.

186. Berg, C.P., et al., *Human mature red blood cells express caspase-3 and caspase-8, but are devoid of mitochondrial regulators of apoptosis.* Cell Death & Differentiation, 2001. **8**(12): p. 1197-1206.

187. Coller, B.S., *Platelet GPIIb/IIIa antagonists: the first anti-integrin receptor therapeutics.* The Journal of clinical investigation, 1997. **99**(7): p. 1467-1471.

188. Febbraio, M. and R.L. Silverstein, *CD36: implications in cardiovascular disease.* The international journal of biochemistry & cell biology, 2007. **39**(11): p. 2012-2030.

189. Dale E. Greenwalt, R.H.L., Christian F. Ockenhouse, Hisami Ikeda, Narendra N. Tandon, and G.A. Jamieson, *Membrane Glycoprotein CD36: A Review of Its Roles in Adherence, Signal Transduction, and Transfusion Medicine.* The Journal of The American Society of Hematology, 1992.

190. Gayen Betal, S. and B.N.Y. Setty, *Phosphatidylserine-positive erythrocytes bind to immobilized and soluble thrombospondin-1 via its heparin-binding domain.* Translational research : the journal of laboratory and clinical medicine, 2008. **152**(4): p. 165-177.

191. Abdelhamid, M.F., et al., *Changes in thrombin generation, fibrinolysis, platelet and endothelial cell activity, and inflammation following endovascular abdominal aortic aneurysm repair.* J Vasc Surg, 2012. **55**(1): p. 41-6.

192. Abdelhamid, M.F., et al., *Effect of endovascular and open abdominal aortic aneurysm repair on thrombin generation and fibrinolysis.* J Vasc Surg, 2013. **57**(1): p. 103-7.

193. Davies, R.S., et al., *Coagulation, fibrinolysis, and platelet activation in patients undergoing open and endovascular repair of abdominal aortic aneurysm.* J Vasc Surg, 2011. **54**(3): p. 865-78.

194. Rao, J., et al., *Distinct macrophage phenotype and collagen organization within the intraluminal thrombus of abdominal aortic aneurysm.* Journal of Vascular Surgery, 2015. **62**(3): p. 585-593.

195. Wautier, M.P., et al., *Increased adhesion to endothelial cells of erythrocytes from patients with polycythemia vera is mediated by laminin alpha5 chain and Lu/BCAM.* (0006-4971 (Print)).

196. White, J., et al., *Increased erythrocyte adhesion to VCAM-1 during pulsatile flow: Application of a microfluidic flow adhesion bioassay.* (1875-8622 (Electronic)).

197. Reimers, R.C., S.P. Sutera, and J.H. Joist, *Potentiation by red blood cells of shear-induced platelet aggregation: relative importance of chemical and physical mechanisms.* Blood, 1984. **64**(6): p. 1200-1206.

198. Ott, C., et al., *The influence of erythrocyte aggregation on induced platelet aggregation.* Clin Hemorheol Microcirc, 2010. **45**(2-4): p. 375-82.

199. Constance, C.F.M.J.B., et al., *Impaired mitochondrial activity explains platelet dysfunction in thrombocytopenic cancer patients undergoing chemotherapy.* Haematologica, 2018. **103**(9): p. 1557-1567.

200. Brzoska, T., et al., *Binding of Thrombin-Activated Platelets to a Fibrin Scaffold through αIIbβ3 Evokes Phosphatidylserine Exposure on Their Cell Surface.* PLOS ONE, 2013. **8**(2): p. e55466.

201. Tutwiler, V., et al., *Kinetics and mechanics of clot contraction are governed by the molecular and cellular composition of the blood.* Blood, 2016. **127**(1): p. 149-159.

202. Nagata, S., *Apoptosis by Death Factor.* Cell, 1997. **88**(3): p. 355-365.

203. Strand, S., et al., *Lymphocyte apoptosis induced by CD95 (APO–1/Fas) ligand–expressing tumor cells — A mechanism of immune evasion?* Nature Medicine, 1996. **2**(12): p. 1361-1366.

204. Scaffidi, C., et al., *Two CD95 (APO-1/Fas) signaling pathways.* Embo j, 1998. **17**(6): p. 1675-87.

205. Li-Weber, M. and P.H. Krammer, *Function and regulation of the CD95 (APO-1/Fas) ligand in the immune system.* Semin Immunol, 2003. **15**(3): p. 145-57.

206. O'Brien, D.I., et al., *Targeting the Fas/Fas ligand pathway in cancer.* Expert Opin Ther Targets, 2005. **9**(5): p. 1031-44.

207. Ahmad, R., et al., *Activated human platelets express Fas-L and induce apoptosis in Fas-positive tumor cells.* J Leukoc Biol, 2001. **69**(1): p. 123-8.

208. Schleicher, R.I., et al., *Platelets induce apoptosis via membrane-bound FasL.* Blood, 2015. **126**(12): p. 1483-93.

209. Berg, C.P., et al., *Human mature red blood cells express caspase-3 and caspase-8, but are devoid of mitochondrial regulators of apoptosis.* Cell death and differentiation, 2001. **8**(12): p. 1197-1206.

210. Bratosin, D., et al., *Programmed cell death in mature erythrocytes: a model for investigating death effector pathways operating in the absence of mitochondria.* Cell Death Differ, 2001. **8**(12): p. 1143-56.

211. Nagata, S., et al., *Exposure of phosphatidylserine on the cell surface.* Cell death and differentiation, 2016. **23**(6): p. 952-961.

212. Cifone, M.G., et al., *Apoptotic signaling through CD95 (Fas/Apo-1) activates an acidic sphingomyelinase.* J Exp Med, 1994. **180**(4): p. 1547-52.

213. Russell, A.J., et al., *Alpha 6 beta 4 integrin regulates keratinocyte chemotaxis through differential GTPase activation and antagonism of alpha 3 beta 1 integrin.* J Cell Sci, 2003. **116**(Pt 17): p. 3543-56.

214. Hermand, P., et al., *Red cell ICAM-4 is a novel ligand for platelet-activated alpha IIbbeta 3 integrin.* J Biol Chem, 2003. **278**(7): p. 4892-8.

215. Hermand, P., et al., *Integrin receptor specificity for human red cell ICAM-4 ligand. Critical residues for alphaIIbeta3 binding.* Eur J Biochem, 2004. **271**(18): p. 3729-40.

216. Du, V.X., et al., *New insights into the role of erythrocytes in thrombus formation.* Semin Thromb Hemost, 2014. **40**(1): p. 72-80.

217. Vallés, J., et al., *Platelet-erythrocyte interactions enhance alpha(IIb)beta(3) integrin receptor activation and P-selectin expression during platelet recruitment: down-regulation by aspirin ex vivo.* Blood, 2002. **99**(11): p. 3978-84.

218. Santos, M.T., et al., *Role of red blood cells in the early stages of platelet activation by collagen.* Thromb Haemost, 1986. **56**(3): p. 376-81.

219. Valles, J., et al., *Erythrocytes metabolically enhance collagen-induced platelet responsiveness via increased thromboxane production, adenosine diphosphate release, and recruitment.* Blood, 1991. **78**(1): p. 154-62.

220. Asch, E. and E. Podack, *Vitronectin binds to activated human platelets and plays a role in platelet aggregation.* The Journal of clinical investigation, 1990. **85**(5): p. 1372-1378.

221. Gawaz, M., et al., *Vitronectin Receptor (αvβ3) Mediates Platelet Adhesion to the Luminal Aspect of Endothelial Cells.* Circulation, 1997. **96**(6): p. 1809-1818.

222. Buensuceso, C.S., et al., *Regulation of outside-in signaling in platelets by integrin-associated protein kinase C beta.* J Biol Chem, 2005. **280**(1): p. 644-53.

223. Bunch, T.A., *Integrin alphaIIbbeta3 activation in Chinese hamster ovary cells and platelets increases clustering rather than affinity.* The Journal of biological chemistry, 2010. **285**(3): p. 1841-1849.

224. van der Meijden, P.E.J., et al., *Key role of integrin αIIbβ3 signaling to Syk kinase in tissue factor-induced thrombin generation.* Cellular and Molecular Life Sciences, 2012. **69**(20): p. 3481-3492.

225. Heinzmann, A.C.A., et al., *Complementary roles of platelet αIIbβ3 integrin, phosphatidylserine exposure and cytoskeletal rearrangement in the release of extracellular vesicles.* Atherosclerosis, 2020.

226. Jobe, S.M. and J. Di Paola, *9 - Congenital and Acquired Disorders of Platelet Function and Number*, in *Consultative Hemostasis and Thrombosis (Fourth Edition)*, C.S. Kitchens, et al., Editors. 2019, Content Repository Only!: Philadelphia. p. 145-166.

227. Thomaier, M., et al., *High-Affinity Binding of Monomeric but Not Oligomeric Amyloid-β to Ganglioside GM1 Containing Nanodiscs.* Biochemistry, 2016. **55**(48): p. 6662-6672.

228. Streit, M., et al., *Overexpression of thrombospondin-1 decreases angiogenesis and inhibits the growth of human cutaneous squamous cell carcinomas.* The American journal of pathology, 1999. **155**(2): p. 441-452.

229. Ghosh, A., et al., *Platelet CD36 surface expression levels affect functional responses to oxidized LDL and are associated with inheritance of specific genetic polymorphisms.* Blood, 2011. **117**(23): p. 6355-6366.

230. Alkhatatbeh, M.J., et al., *The putative diabetic plasma marker, soluble CD36, is non-cleaved, non-soluble and entirely associated with microparticles.* J Thromb Haemost, 2011. **9**(4): p. 844-51.

231. James, H.L., et al., *A unique elastase in human blood platelets.* J Clin Invest, 1985. **76**(6): p. 2330-7.

232. Kabanova, S., et al., *Gene expression analysis of human red blood cells.* Int J Med Sci, 2009. **6**(4): p. 156-9.

233. Weyrich, A.S., et al., *Protein synthesis by platelets: historical and new perspectives.* J Thromb Haemost, 2009. **7**(2): p. 241-6.

234. Alkhatatbeh, M.J., et al., *The origin of circulating CD36 in type 2 diabetes.* Nutrition & diabetes, 2013. **3**(2): p. e59-e59.

235. Little, K.M., et al., *The Plasma Microparticle Proteome.* Semin Thromb Hemost, 2010. **36**(08): p. 845-856.

236. Barteneva, N.S., et al., *Circulating microparticles: square the circle.* BMC Cell Biology, 2013. **14**(1): p. 23.

237. Leung, L.L., et al., *CD36 peptides enhance or inhibit CD36-thrombospondin binding. A two-step process of ligand-receptor interaction.* J Biol Chem, 1992. **267**(25): p. 18244-50.

238. Asch, A., et al., *Analysis of CD36 binding domains: ligand specificity controlled by dephosphorylation of an ectodomain.* Science, 1993. **262**(5138): p. 1436-1440.

239. Burkhart, J.M., et al., *The first comprehensive and quantitative analysis of human platelet protein composition allows the comparative analysis of structural and functional pathways.* Blood, 2012. **120**(15): p. e73-82.

240. Nancy Lewis Baenziger, G.N.B., and Philip W. Majerus, *Isolation and Properites of a Thombin-sensitive Protein of Human Platelets.* The Journal of Biological Chemistry, 1972. **247**.

241. Manodori, A.B., et al., *Adherence of phosphatidylserine-exposing erythrocytes to endothelial matrix thrombospondin.* Blood, 2000. **95**(4): p. 1293-300.

242. Setty, B.N.Y. and S.G. Betal, *Microvascular endothelial cells express a phosphatidylserine receptor: a functionally active receptor for phosphatidylserine-positive erythrocytes.* Blood, 2008. **111**(2): p. 905-914.

243. Wautier, M.P., et al., *Red blood cell phosphatidylserine exposure is responsible for increased erythrocyte adhesion to endothelium in central retinal vein occlusion.* J Thromb Haemost, 2011. **9**(5): p. 1049-55.

244. Walker, B., et al., *Dynamic adhesion of eryptotic erythrocytes to immobilized platelets via platelet phosphatidylserine receptors.* Am J Physiol Cell Physiol, 2014. **306**(3): p. C291-7.

245. Noh, J.-Y., et al., *Procoagulant and prothrombotic activation of human erythrocytes by phosphatidic acid.* American Journal of Physiology-Heart and Circulatory Physiology, 2010. **299**(2): p. H347-H355.

246. Kuhnl, A., et al., *Incidence, Treatment and Mortality in Patients with Abdominal Aortic Aneurysms.* Dtsch Arztebl Int, 2017. **114**(22-23): p. 391-398.

247. Kamp, T.J., et al., *Myocardial infarction, aortic dissection, and thrombolytic therapy.* Am Heart J, 1994. **128**(6 Pt 1): p. 1234-7.

248. Kantelhardt, S.R., et al., *Recurrent aortic dissection in Marfan's syndrome: possible effects of anticoagulation.* Cardiol Rev, 2003. **11**(4): p. 240-3.

249. Thompson, A., et al., *An analysis of drug modulation of abdominal aortic aneurysm growth through 25 years of surveillance.* Journal of Vascular Surgery, 2010. **52**(1): p. 55-61.e2.

250. Handberg, A., et al., *Soluble CD36 in plasma is increased in patients with symptomatic atherosclerotic carotid plaques and is related to plaque instability.* Stroke, 2008. **39**(11): p. 3092-5.

251. Handberg, A., et al., *Identification of the oxidized low-density lipoprotein scavenger receptor CD36 in plasma: a novel marker of insulin resistance.* Circulation, 2006. **114**(11): p. 1169-76.

252. Vorkapic, E., et al., *ADAMTS-1 in abdominal aortic aneurysm.* PLOS ONE, 2017. **12**(6): p. e0178729.

253. Andrews, R.K., J.F. Arthur, and E.E. Gardiner, *Targeting GPVI as a novel antithrombotic strategy.* Journal of blood medicine, 2014. **5**: p. 59-68.

7. Appendix

7.1 Immunofluorescence straining
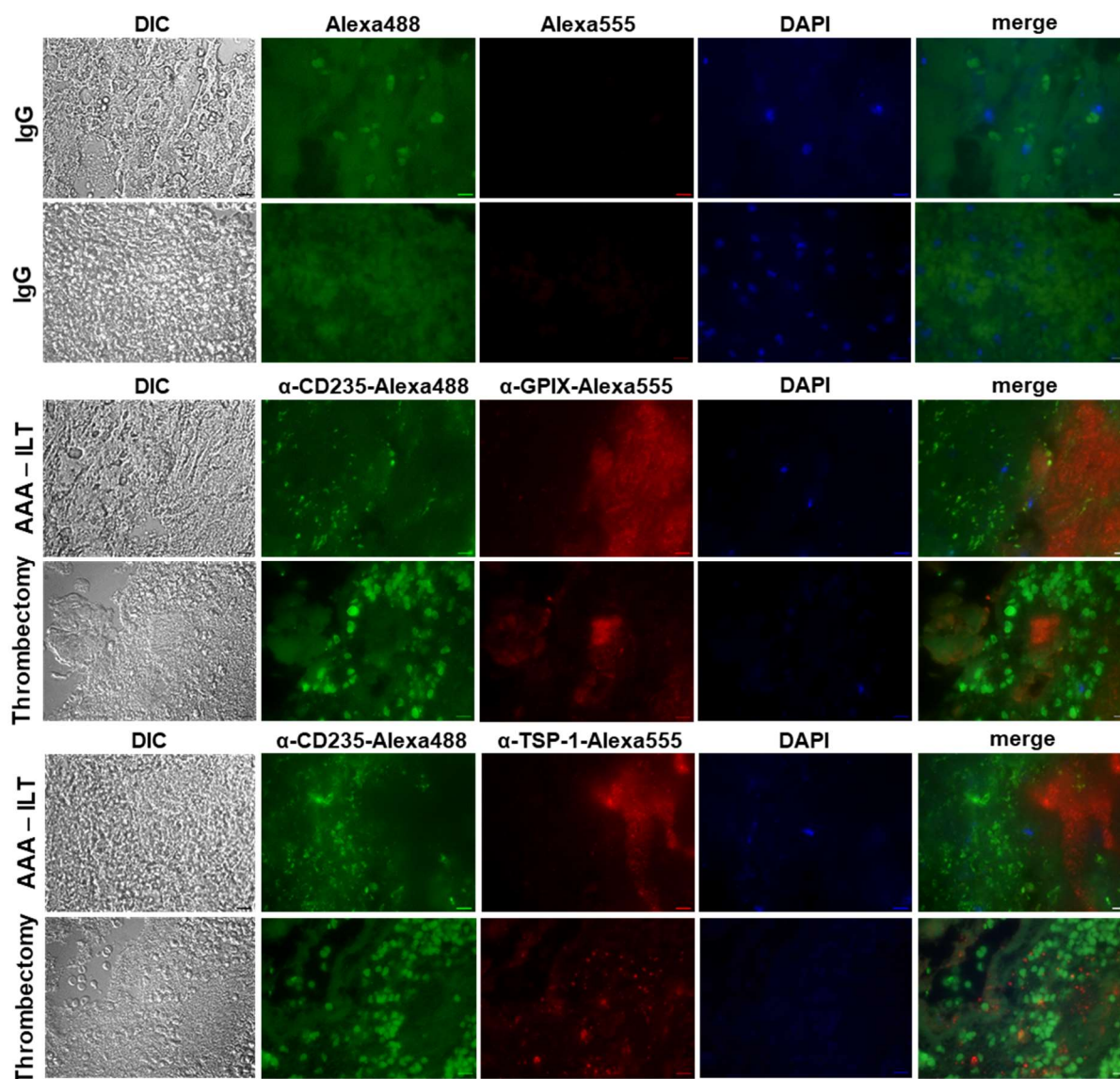
Figure 35: Immunofluorescence straining of platelets, RBCs and TSP-1 in the ILT of AAA patients as well as thrombi isolated from patients after thrombectomy. Paraffin-embedded sections (5 micron) of intraluminal thrombi (ILT) of AAA patients and of thrombi from patients who underwent thrombectomy (thrombi from peripheral vessels) were stained with a GPIX antibody [20 µg/mL] to detect platelets, with a CD235 antibody [0.5 µg/mL] to detect RBCs and with a TSP-1 mAb [20 µg/mL] (n = 4). IgG served as controls (same concentration as respective primary antibody were used) (n = 4). Additionally, fluorescence emission at 488 nm showed autofluorescence of red blood cells in IgG controls. 4',6-diamidino-2-phenylindole (DAPI) was used as nucleus staining. Representative DIC and fluorescent images with 1000-fold magnification are shown. Scale bar: 10 µm. AAA = abdominal aortic aneurysm; ILT = intraluminal thrombus; DIC = differential interference contrast.
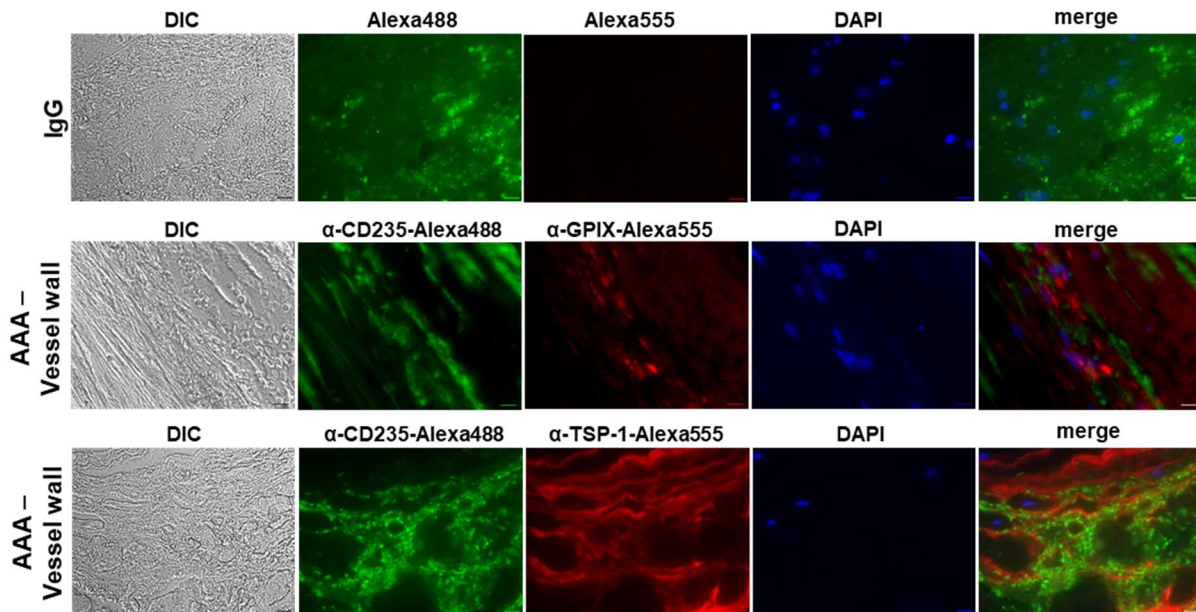
Figure 36: Immunofluorescence straining of platelets, RBCs and TSP-1 in the aortic wall of AAA patients. Paraffin-embedded sections (5 micron) of the aortic wall of AAA patients were stained with a GPIX antibody [20 µg/mL] to detect platelet, with a CD235 antibody [0.5 µg/mL] to detect RBCs and with a TSP-1 mAb [20 µg/mL] (n = 4). IgG served as control (same concentration as respective primary antibody) (n = 4). Additionally, fluorescence emission at 488 nm showed autofluorescence of red blood cells in IgG controls and autofluorescence of elastic lamina in vessel wall samples. 4',6-diamidino-2-phenylindole (DAPI) was used as nucleus staining. Representative DIC and fluorescent images with 1000-fold magnification are shown. Scale bar: 10 µm. AAA = abdominal aortic aneurysm; DIC = differential interference contrast.

7.2 Acknowledgements

The work presented here was accomplished at the Department of Vascular and Endovascular Surgery, University Hospital of Düsseldorf in the working group Experimental Vascular Medicine of Prof. Dr. Elvers. During the period of my PhD project (November 2016 – December 2020) many people helped and supported me and without this help this thesis would not have been possible. Therefore, I would like to express my thanks to the following people:

• My supervisor, Prof. Dr. Margitta Elvers, for giving me the opportunity to work in her laboratory, for her constant support and outstanding scientific ideas. Especially, I would like to thank her for allowing me to travel to and/or participate in several international conferences and meetings.

• My mentor and the spokesmen of the IRTG 1902, Prof. Dr. Axel Gödecke for reviewing my thesis and allowing me to travel to and/or participate in several international conferences and meetings.

• Beate Kehrel for her support and the outstanding scientific discussions.

• My colleagues: Friedrich, Lili, Alicia, Laura, Lisa and Beate for their encouragement in lab, for listening to me and for spending their time on carefully proofreading my thesis.

• Prof. Dr. Hadi Al-Hasani and Dr. Alexandra Chadt for sharing their CD36 knockout mice with me.

• Our technical assistant Martina, for her everyday support. You are fantastic!

• All past and present members of the Elvers group that have not been mentioned here by name for the great working atmosphere, the numerous help in lab and the fun at work.

• Thank you Jackie and Phil for carefully proofreading my thesis.

• The most important person in my life, my wife Lea who encouraged and constantly supported me all my life. I love you!

• And last, but most importantly, I wish to thank my parents Christine and Jürgen Krott who have always supported me in my professional and private life. Thank you!

7.3 Reuse of figures from own publications

Klatt, C., Krüger, I., Zey, S., **Krott, K.J.**, Spelleken, M., Gowert, N.S., Oberhuber, A., Pfaff, L., Lückstädt, W., Jurk, K., Schaller, M., Al-Hasani, H., Schrader, J., Massberg, S., Stark, K., Schelzig, H., Kelm, M., Elvers, M., *Platelet-RBC interaction mediated by FasL/FasR induces procoagulant activity important for thrombosis*. J Clin Invest. 2018 Aug 31; **128**(9):3906-3925. doi: 10.1172/JCI92077.

Figures of this thesis are already published in the publication above as mentioned in the respective figure legends. A permission and license are received from JCI for the reuse of figure 8C, E-G and figure 9A-D.

7.4 Curriculum vitae

PERSONAL DETAILS

Name:	Kim Jürgen Krott
Occupation:	PhD student
Date of birth:	09 December 1987, in Leverkusen
Nationality:	German
Place of residence:	████████████████████████████
Family status:	██████

RESEARCH AND PROFESSIONAL EXPERIENCE

11/2016 – 12/2020   PhD student in the group of Prof. Dr. Margitta Elvers at the Research Group Experimental Vascular Medicine, University Hospital of Düsseldorf, Germany

02/2015 – 06/2016   Master thesis, Institute of Bio- and Geoscience IBG-1:Biotechnology at the Research Center Jülich, Germany "Hfq-mediated regulation of target gene expression by synthetic small RNAs for application in *Corynebacterium glutamicum*" in the laboratory of Prof. Dr. Bott

05/2009 – 09/2012   Bachelor thesis, Institute for Microbiology at the Heinrich-Heine-University Düsseldorf, Germany. "Biosynthesis of the *Candida albicans* Msb2 sensor protein by heterologous gene expression" in the laboratory of Prof. Dr. J. Ernst

EDUCATION

10/2012 – 06/2016   Studies in biology, Heinrich-Heine-University, Düsseldorf, Germany, in cooperation with the Research Center in Jülich.

Majors: Molecular and Microbiology
Degree: Master of Science (M.Sc.)

10/2009 – 09/2012   Studies in biology, Heinrich-Heine-University, Düsseldorf, Germany
Degree: Bachelor of Science (B.Sc.)

08/1998 – 06/2008   A level (Abitur) Lise-Meitner-Gymnasium, Leverkusen, Germany. Majors: Biology and chemistry

Düsseldorf, December 2020 _____

7.5 Publications

1. Klatt, C., Krüger, I., Zey, S., **Krott, K.J.**, Spelleken, M., Gowert, N.S., Oberhuber, A., Pfaff, L., Lückstädt, W., Jurk, K., Schaller, M., Al-Hasani, H., Schrader, J., Massberg, S., Stark, K., Schelzig, H., Kelm, M., Elvers, M., *Platelet-RBC interaction mediated by FasL/FasR induces procoagulant activity important for thrombosis*. J Clin Invest. 2018 Aug 31; **128**(9):3906-3925. doi: 10.1172/JCI92077.

7.6 International conferences

1. Krott, J.K., Klatt C., Zey, S., Gowert, N.S., Oberhuber, A., Schaller, M., Kelm, M., Schelzig H. and Elvers, M., Platelet-mediated activation of FasR and subsequent phosphatidylserine exposure of red blood cells is substantial for thrombus formation and hemostasis. **Oral communication**. **International Society on Thrombosis and Haemostasis (ISTH) 2017**. Berlin, Germany.
2. Krott, J.K., Klatt C., Zey, S., Gowert, N.S., Oberhuber, A., Schaller, M., Kelm, M., Schelzig H. and Elvers, M., Platelet-mediated activation of FasR and subsequent phosphatidylserine exposure of red blood cells is substantial for thrombus formation and hemostasis. **Oral communication. 62nd Annual Meeting of the Society of Thrombosis and Haemostasis Research 2018**. Vienna, Austria.
3. Krott, J.K. and Elvers, M., The active recruitment of red blood cells to activated platelets during hemostasis and arterial thrombus formation. **Oral communication. 64nd Annual Meeting of the Society of Thrombosis and Haemostasis Research 2020**. Bremen, Germany.
4. Krott, J.K., Klatt C., Zey, S., Gowert, N.S., Oberhuber, A., Schaller, M., Kelm, M., Schelzig H. and Elvers, M., Platelet-mediated activation of FasR and subsequent phosphatidylserine exposure of red blood cells is substantial for thrombus formation and hemostasis. **Poster**. **Platelets 2018 International Symposium.** Ramat Gan, Israel.
5. Krott, J.K., Klier, M., and Elvers, M., The active recruitment of red blood cells to activated platelets during hemostasis and arterial thrombus formation. **Poster and Top Poster Price Winner**. **International Society on Thrombosis and Haemostasis (ISTH) 2019**. Melbourne, Australia.

7.7 Affidavit

I affirm in lieu of oath that the dissertation was written by me independently and without unauthorized outside help, in accordance with the "Quality principles of good scientific practice at the Heinrich-Heine-University Düsseldorf". Furthermore, I confirm that this thesis has not yet been submitted as part of another examination process neither in identical nor in similar.

Düsseldorf, December 2020 _____

7.8 Eidesstattliche Erklärung

Ich versichere an Eides Statt, dass die Dissertation von mir selbständig und ohne unzulässige fremde Hilfe unter Beachtung der „Grundsätze zur Sicherung guter wissenschaftlicher Praxis an der Heinrich-Heine-Universität Düsseldorf" erstellt worden ist. Ich erkläre außerdem, dass die Dissertation weder in gleicher noch in ähnlicher Form bereits in einem anderen Prüfungsverfahren vorgelegen hat.

Düsseldorf, Dezember 2020 _____